AFCRL-70-0366

AD 711405

A METHOD OF COMPUTING
WINDS, DENSITY, TEMPERATURE, PRESSURE,
AND THEIR ASSOCIATED ERRORS
FROM THE HIGH ALTITUDE ROBIN SPHERE
USING AN OPTIMUM FILTER

James K. Luers

Final Report
Period Covered: January 1967 thru December 1969

July 1970

Contract Monitor: John B. Wright
Aerospace Instrumentation Laboratory

Prepared for:

Air Force Cambridge Research Laboratories
United States Air Force
Bedford, Massachusetts 01730

D D C
SEP 10 1970
RECEIVED

C. — 104

Qualified requestors may obtain additional copies from the Defense
Documentation Center.   All others should apply to the Clearinghouse
for Federal Scientific and Technical Information.

AFCRL-70-0366

A METHOD OF COMPUTING WINDS, DENSITY,

TEMPERATURE, PRESSURE, AND THEIR ASSOCIATED ERRORS

FROM THE HIGH ALTITUDE ROBIN SPHERE

USING AN OPTIMUM FILTER

James K. Luers

Contract No. F19628-67-C-0102
Project No. 6682, 6670
Task No. 668202, 667003
Work Unit No. 66820201, 66700301

University of Dayton
Research Institute
Dayton, Ohio 45409

Final Report

Period Covered: January 1967 thru December 1969

July 1970

Contract Monitor: John B. Wright
Aerospace Instrumentation Laboratory

Prepared for

Air Force Cambridge Research Laboratories
United States Air Force
Bedford, Massachusetts 01730

ACKNOWLEDGEMENTS

ABSTRACT

Optimum reduction techniques have been determined and a computer program written to measure density, winds, temperature and pressure from the passive ROBIN Sphere in the 30-100 km region of atmosphere. The program extends the altitude range of the 1965 ROBIN Program from 70 to 100 km. Output from the computer program also includes the estimated noise errors in density, winds, temperature, and pressure, the frequency response of density and winds as a function of altitude, and Cal-comp plots of the meteorological parameters.

The smoothing techniques used in the program were determined so as to minimize the sum of the random and bias errors in density and winds. A separate smoothing function was determined for density and for wind calculations. The density smoothing function expands below 60 km in order to maintain a constant 2% noise error in density.

All possible sources of error in the meteorological parameters are discussed. For the first time error equations have been derived for temperature and pressure errors. Error estimates are made for random errors, bias errors, and errors resulting from the initial estimate of temperature.

TABLE OF CONTENTS

LIST OF FIGURES

LIST OF TABLES

LIST OF SYMBOLS

LIST OF SYMBOLS (CON'T)

1. INTRODUCTION

1.1 Arcas ROBIN System

The ROBIN system consists of a ROBIN sphere, an Arcas rocket motor and an AN/FPS-16 tracking radar. The ROBIN sphere is made of one half mil Mylar inflatable to a diameter of one meter containing an internally-supported corner reflector. Packaged in a collapsed condition within the nosecone of a meteorological rocket, it is ejected at the apogee of the rocket and inflated by vaporization of isopentane, to a super pressure of approximately ten millibars. Thus inflated, the ROBIN sphere is tracked from apogee to approximately 30 kilometers by an AN/FPS-16 high precision tracking radar. The Arcas rocket motor is a 4.5 inch diameter solid pro-pellant, end burning rocket capable of carrying the sphere payload to an altitude of 75 kilometers. The FPS-16 tracking radar generates spherical space-time coordinates at digitized increments of 1/10 of a second. From the space-time coordinates, the meteorological parameters of density, wind, temperature and pressure are deduced. A complete discussion of the Arcas ROBIN system, its advantages and shortcomings is contained in the report by Engler, "Development of Methods to Determine Winds, Density, Pressure and Temperature from the ROBIN Falling Balloon, 1965". (Ref. 1).

1.2 Viper Dart ROBIN System

In recent years the Air Force has extended the concept of the falling sphere experiment to measurements at altitudes from 70 to 100 km. To implement this concept, the capability of the rocket vehicle had to be increased to permit sphere apogees in excess of 120 km. Boosted-Arcas vehicles have been utilized but, because of their high cost, have generally been superceded by a lower cost vehicle, the Viper Dart, developed especially for the small light-weight ROBIN payload. The Viper Dart rocket (Ref. 11) was developed successfully and has been employed to carry the sphere to its required apogee. Although the March 1965 ROBIN Computer Program gave highly accurate measurements below 70 km, it was not satisfactory for measurement above 70 km. (see Ref. 2). Hence, a new high altitude ROBIN program was required for measurements extending to 100 km. The problems encountered with the 1965 program which had to be dealt with in designing a high altitude program were:

i) The smoothing used in the March 1965 ROBIN program introduced a significant bias in density above 70 km.

ii) Above 80 km, wind accuracy decreased rapidly with increasing altitude.

iii) An examination of the adequacy of the Lambda (λ) check below 40 km was in order. A high altitude collapse check also had to be deter-mined.

1

It is the purpose of this report to discuss the new high altitude data
reduction program which is titled, "The May-1970 AFCRL ROBIN Program",
explain the rationale and methodology used to design the program, and to discuss
the errors in the winds and thermodynamic data that results with the use of this
program.

1.2.1   Program Specifications

The preliminary specifications for the May-1970 AFCRL ROBIN Program
consisted of the following items: a) the program should be optimum for measuring
density and wind in the 70 to 100 kilometer region of the atmosphere, assuming a
sphere apogee of 125 kilometers; b) the program should also give accurate and
reliable density measurements from 30 to 70 kilometers; c) even though the data
reduction technique need not be optimum for sphere apogees other than 125 kilo-
meters, other sphere apogees between 75 and 140 kilometers should not result
in a serious degradation of the accuracy of the meteorological parameters;
d) temperature and pressure accuracies should be commensurate with density
accuracy; e) the program should accurately determine the altitude of sphere
collapse.

1.2.2   Discussion of Coordinate System

The coordinate system chosen is a left-handed system in which the
two horizontal directions are X (down-range) and Y (cross-range). Looking
down-range, the positive cross-range direction is to the right. The positive
clockwise angle from geographical north to the positive X-axis of the range
coordinate system is called Z_b (see Figure 1). The azimuth angle (A) is the
angle clockwise from the positive X-axis. The vertical direction is Z, and
its negative direction is toward the center of the earth at the origin of the
coordinate system. Hence, the horizontal X-Y plane (assuming a spherical
earth) is tangent to the earth at the launch site. The altitude (h) is defined
as the perpendicular distance from the sphere to the earth.
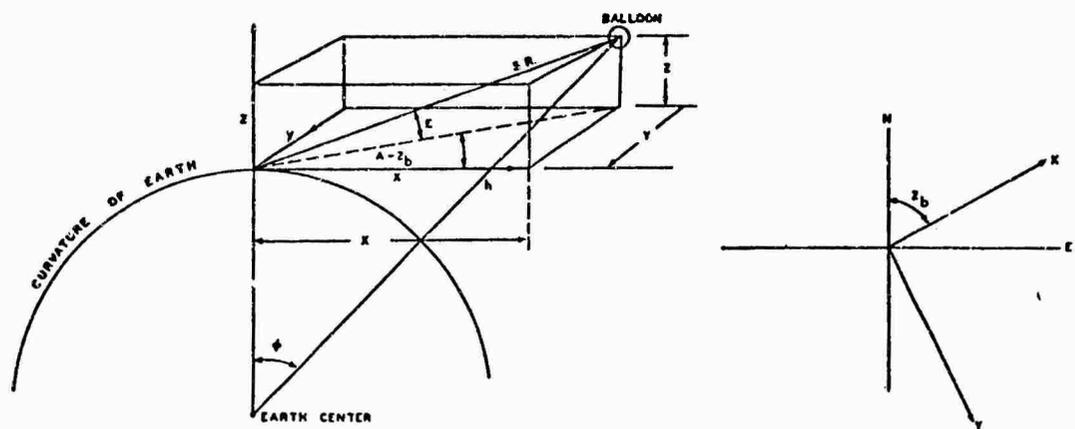
Figure 1:   Three-dimensional Coordinate System used in Defining Equations
of Motion.

2

In contrast to the coordinate system defined above, the meteorologist desires wind velocities with respect to the coordinate system with "h" defined as the vertical axis. To determine the practical effect of the differences between the two coordinate systems, winds were computed from several flights using each coordinate system. The largest difference in component wind velocity between the two systems was 0.2 m/sec. Winds are initially computed in the original coordinate system (with Z as vertical axis) and later transformed to the coordinate system with "h" defined as the vertical axis.

1.2.3   Density and Wind Measurement

To obtain density, the drag force that the atmosphere exerts upon the sphere must be measured. In the 70 to 100 kilometer region, the vertical velocities and accelerations are much larger than the horizontal velocities and accelerations. For this reason the drag acceleration is primarily in the vertical direction. Accurate density calculations are thus largely a result of the accuracy to which vertical velocities and accelerations can be measured.

Horizontal winds influence the sphere's trajectory by inducing horizontal excursions in its path in three dimensional space. These horizontal excursions are used to reconstruct the wind profile. At altitudes above 85 km, the vertical acceleration also plays an important role in reconstructing the horizontal wind profile. Thus, for measuring wind, the horizontal velocity and acceleration components, as well as the vertical acceleration, must be determined accurately.

Since density is derived primarily upon vertical measurements and winds depend on vertical as well as horizontal measurements, two separate smoothing functions have been introduced into the program. The first smoothing function is defined so as to optimize density measurements. This smoothing is applied only to vertical position coordinates to obtain vertical velocities and accelerations. A second smoothing function is defined so as to optimize wind measurements. This smoothing is applied to horizontal position coordinates to obtain horizontal velocities and accelerations as well as reapplying it to vertical position to obtain a second estimate of vertical velocity and acceleration to be used in the wind equation. The determination of these two smoothing functions is the critical problem in devising a reduction program. The rationale and methodology used to define these smoothing functions is set forth in the following sections.

2.   DENSITY

Density, ρ, is computed by

$$\rho = \frac{m(g_z - \ddot{Z} - C_z)}{1/2 \, C_D \, A \, V(\dot{Z} - W_z) + V_b g_z} \qquad (1)$$

(See Ref. 1)

3

where

m	=	Mass of sphere
g_z	=	Gravitational acceleration in vertical direction
$\ddot{Z}$	=	Vertical acceleration of sphere
C_z	=	Coriolis acceleration in vertical direction
C_D	=	Drag coefficient
A	=	Cross section area of sphere
V	=	Velocity of the sphere relative to the air
$\dot{Z}$	=	Vertical velocity of sphere
W_z	=	Vertical wind velocity
V_b	=	Volume of sphere

The computed density error is a result of the errors present in the parameters on the right side of Equation 1. The error present in many of the variables of Equation 1 makes a negligible contribution to the error in density.

2.1   Variables Not Producing Significant Density Errors

The vertical component of the acceleration due to gravity (g_z) is computed by the equation

$$g_z = \frac{g_s \ (Z+r)}{(1+\frac{h}{r})^2 \ (h+r)}$$ (2)

where

g_s	=	Sea level gravitational constant
r	=	Radius of the earth
h	=	Altitude of sphere
Z	=	Vertical position of sphere

The accuracy of Equation 2 is sensitive only to the accuracy of the radius of the earth, or more precisely, the determination of the center of mass of earth. Even if the radius to the center of mass of the earth were in error by 10 kilometers, the resultant error in density would be less than 1/2% at an altitude of 100 kilometers and much less at lower altitudes.

The mass of the sphere (m) is determined for each sphere individually by the manufacturer. The accuracy of the mass thus obtained should be to at least 1/2 gram. For a nominal sphere mass of 120 grams this would result in less than 1/2% density error.

4

Manufacturer's specifications for the ROBIN sphere demand that it should deviate less than 1% from a perfect sphere. A 1% error in diameter produces a 2% error in A and thus a 2% bias in density. An error in either diameter or mass would not effect the shape of the density profile but only translate it in some direction. This results because the error in diameter or mass is constant for the entire flight. Thus, to a first order approximation, a constant bias results. However, if mass should vary due to a gas leak, the bias error would not be constant.

From 30 to 100 kilometers the bouyancy ($V_b g_z$) and coriolis (C_z) terms make only minor contributions to the determination of density. Hence, any error present in these terms gives negligible contribution to density error.

The remaining variables which could make a significant contribution to density error are C_D, $\dot{Z}$, $\ddot{Z}$, W_z, and V.

2.2 Density Error Equation

For the purpose of deriving an error equation for density, the density equation can be simplified to Equation 3

$$\rho = \frac{m(g_z - \ddot{Z})}{1/2 \, C_D \, A \, V \, (\dot{Z} - W_z)} \tag{3}$$

where both the bouyancy and coriolis forces have been neglected.

Considering the error in density to be a function of the errors in C_D, W_z, $\dot{Z}$, $\ddot{Z}$, and V. The error increment in density due to errors in the five parameters is given by the differential approximation formula as

$$\Delta\rho = \frac{\partial \rho}{\partial C_D} \, \Delta C_D + \frac{\partial \rho}{\partial V} \, \Delta V + \frac{\partial \rho}{\partial \dot{Z}} \, \Delta \dot{Z} + \frac{\partial \rho}{\partial \ddot{Z}} \, \Delta \ddot{Z} + \frac{\partial \rho}{\partial W_z} \, \Delta W_z. \tag{4}$$

Each of these six terms can be analyzed to determine the magnitude of its contribution to the error in density. Since C_D, W_z and errors in V (primarily a result of horizontal wind errors) are essentially independent, they can be analyzed individually. Errors in $\dot{Z}$ and $\ddot{Z}$ are not independent due to the smoothing process. Thus, the terms containing $\dot{Z}$ and $\ddot{Z}$ must be considered together. The following sections describe the error terms and provide means of estimating their effect on density accuracy.

2.2.1 Drag Coefficient Error Term

The percent error in density in terms of the percent error in C_D is given by the error variance formula $\left(\dfrac{\sigma_\rho}{\rho}\right)^2 = \left(\dfrac{\sigma_{C_D}}{C_D}\right)^2$ (See Appendix A)

5

a) Error due to Drag Table

Since the accuracy of the drag coefficients cannot be determined precisely, it is impossible to give an exact error variance value for the resulting per cent error in density. The accuracy of any individual drag table in the literature today is suspect. There are several experimenters, Aroesty (Ref. 3), Ashkanes (Ref. 4), Heinrich et. al. (Ref. 5 and 6), and Goin and Lawrence (AEDC) (Ref. 7) who have measured drag coefficients for a passive sphere. The inconsistencies of results obtained by these experimenters have been pointed out by Luers (Ref. 8) and others. Until further concentrated effort is supported by interested parties, the accuracy cf any drag coefficient presently in use is not known, and probably varies for different sections of the tables. As a result, the density error due to drag coefficient error cannot be determined directly and will probably vary over different segments of the flight.

The drag table to be used in the High Altitude ROBIN Program appears as figure 2 and is basically the work of Heinrich (Ref. 5 and 6) in the supersonic section, and of Arnold Engineering Development Center (Ref. 7) in the subsonic region. The low Reynolds number (< 50) high Mach number drag coefficients were taken from Potter and Miller (Ref. 9). The impressive aspect of this drag table is the similar shapes of the C_D curves given as a function of Mach and Reynolds number even though the drag table was the result of two independent researchers using two different techniques for calculating drag. (Heinrich used a stationary sphere in a wind tunnel; Lawrence and Goin used a ballistic range). However, even though this drag table shows smooth, consistent drag curves, it is impossible to quote specific accuracies of the drag table because of the interpolated section of the table. The stated accuracies by the experimenters are as follows: Lawrence and Goin subsonic, approximately 2%; Heinrich supersonic; maximum possible error ranges from ±2.37% to ±27.9% depending on Reynolds number. However, actual errors are usually not the maximum possible. By interpreting Heinrich's maximum possible error as a 3σ error and by extrapolating Heinrich's and AEDC error values in the interpolated section of the drag table a crude approximation to C_D error as a function of sphere altitude was derived for a sphere with apogee of 125 km. The results are as presented in Table 1.

As of this writing a very comprehensive sphere drag determination program is being undertaken at AEDC for AFCRL which will cover broad areas of interest for both the ROBIN and accelerometer equipped spheres. When the tests are completed, it is expected that further analysis will indicate the need to modify the values of C_D used herein.

6
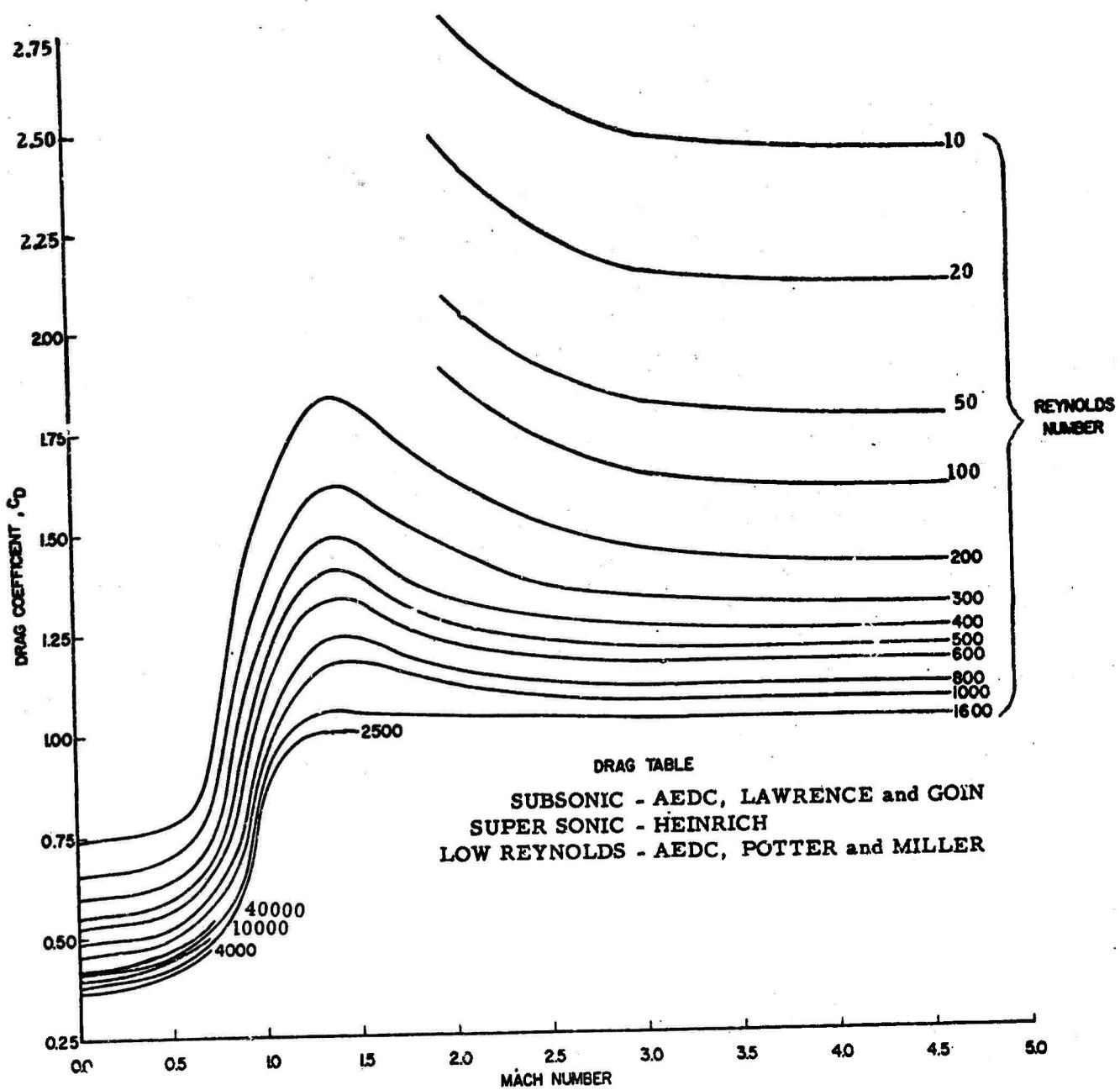
Figure 2: Drag Curves used in High Altitude ROBIN Program.

7

Figure 2:(Continued)

8

If so a new table of C_D will be incorporated into the High Altitude Program. At that time the error in density due to the error in C_D will be re-evaluated.

TABLE 1

Approximation to Percent Error in C_D -vs- Altitude
for a Sphere with Apogee 125 Km

Sphere Altitude ~ Km	% Error in C_D
100	10
95	8
90	6
85	3
80	1
75	2
70	6
65	4
60	3
55 and below	2

b) Error due to Initial Estimate of Temperature

In addition to the error in density due to the inaccuracies of the drag table, a density error also results from the error in the initial estimate of temperature.

At the first point of density computation an initial estimate of temperature (or pressure) is required (see Ref. 1). The error in the initial temperature produces errors in succeeding temperatures that decrease in magnitude. These temperature errors produce errors in Mach number and Reynold's number since both are functions of temperature. Consequently, an error in C_D and density results. The magnitude of the resultant density error depends upon the magnitude of the initial error in temperature and the shape of the drag curves. The shape of the drag curves is important since this determines the change in C_D resulting from a given error in Mach and Reynold's numbers.

The density error profile due to a 10% error in the initial estimate of temperature is presented in Table 2. Table 2 was derived by first determining the trajectory of the ROBIN Sphere assuming it fell in the 1962 Standard Atmosphere (i. e., Standard Atmosphere density $(\rho_{"62"})$ and temperature $(T_{"62"})$ from a 125 km

9

apogee. Using this trajectory as if it represented a radar track, temperature, density and pressure were computed using the 1965 ROBIN Program. A $\pm 10\%$ error in the initial estimate of temperature was introduced by taking $T_0 = 1.1 T_{"62"}$ and $T_0 = .9 T_{"62"}$ at the initial point of computation. As seen from Table 2, the resultant error in density becomes less than 1% after approximately 4 km of flight.

Table 2:

Percent Error in Density
Resulting from a 10% Error in the Initial Temperature

	ALTITUDE ~KM				
	100	95	90	85	< 85
$\frac{\Delta\rho}{\rho}(100)$	4.0	.8	.3	.1	Less than 0.1%

2.2.2 Relative Velocity (V) Error Terms

The percent error variance of density as a function of the error in relative velocity $V = [(\dot{X} - W_x)^2 + (\dot{Y} - W_y)^2 + (\dot{Z} - W_z)^2]^{1/2}$ is

$$\left(\frac{\sigma_\rho}{\rho}\right)^2 = \left(\frac{\dot{X} - W_x}{V^2}\right)^2 \sigma_{w_x}^2 + \left(\frac{\dot{Y} - W_y}{V^2}\right)^2 \sigma_{w_y}^2 \,. \qquad (5)$$

(See Appendix A)

The variables $\dot{X}$, $\dot{Y}$, W_x, W_y and V are basically dependent upon a) the sphere apogee, b) the horizontal velocity imparted to the sphere by the rocket, and c) the wind field experienced by the sphere. Since these variables change from flight to flight, Equation 5 was evaluated using the values of these variables from a representative flight with sphere apogee 125 km. σ_{w_x} and σ_{w_y} were each taken to be 10 m/sec above 70 km and less at lower altitudes. Later in this report it will be shown that the mean wind profile can be measured to an accuracy in excess of that used in deriving Table 3.* Table 3 shows the percent error in ρ resulting from horizontal wind errors. The table indicates that the

*If a high frequency (wavelength < 5 km) large amplitude (in excess of 10 m/sec) wind structure exists above 70 km, then the smoothing filter used for determining winds will not see these waves and actual wind errors may exceed 10 m/sec for these high frequency waves. However, such large wind errors will not result in the density errors that would be predicted by Equation 5, since the density filter will compensate by not allowing the resulting ficticious density waves derived from the wind error to pass.

10

maximum error in density is only 1.1% and occurs at 70km. Actually, the
1.1% estimate at 70 km is undoubtedly too large since the horizontal wind errors
at 70 km are generally much less than 10 m/sec. Hence it can safely be
stated that for the entire altitude range from 30 - 100 km, the error in density
resulting from the inaccuracies of the horizontal wind measurements is less
than 1%.

      Equation 5 also shows the need for computing horizontal winds at all
altitudes at which density is computed (i.e. Density calculations should
commence at the same altitude as horizontal winds or higher). For if hori-
zontal winds are not computed and taken to be zero, a 100 m/sec horizontal
wind could induce a 10% error in density.

TABLE 3

Density Error Resulting from Horizontal Wind Errors of 10, 5, and 2 m/sec

Altitude km	$\dot{X}$	From VIPER DART 13 W_x	$\dot{Y}$	W_y	$\dot{Z}$	Wind Error σ_{W_x}	σ_{W_y}	% Density Error $(\sigma_\rho/\rho)(100)$
100	279	-56	-98	-71	-510	10	10	.89
90	252	-43	-89	-18	-626	10	10	.6
80	172	- 3	-64	- 1	-559	10	10	.5
70	11	-68	-29	-40	-262	10	10	1.1
60	-83	-80	-38	-37	-156	5	5	.05
50	-71	-70	-29	-34	-100	5	5	.25
40	-46	-46	-32	-31	- 41	2	2	.1
30	-39	-39	-21	-22	- 14	2	2	1.1

2.2.3 Vertical Velocity and Acceleration Error Terms

      Two types of errors are present in velocity and acceleration
measurements when a smoothing process is employed to obtain these
measurements: noise error and bias error. The noise error is the error
resulting from the noise present in the radar coordinates. A bias error
results when the smoothing function does not adequately represent the true
path of the sphere. The error in density due to the noise and bias errors in
velocity and acceleration is given by the terms

11

$$\left(\frac{\sigma_\rho}{\rho}\right)^2 = \left(\frac{2\sigma_{\dot{z}}}{\dot{z}}\right)^2 + \left(\frac{\sigma_{\ddot{z}}}{\ddot{z}-g_z}\right)^2 + \left[\frac{2\Delta\dot{z}}{\dot{z}} + \frac{\Delta\ddot{z}}{\ddot{z}-g_z}\right]^2 \qquad (6)$$

(See Appendix A)

where $\Delta\dot{z}$, $\Delta\ddot{z}$ represent the bias errors in vertical velocity and acceleration. The first two terms of Equation 6 are the noise error terms and the third term, the bias error term.

a) Discussion of Variables in Equation 6

The noise error in vertical velocity $(\sigma_{\dot{z}})$ and acceleration $(\sigma_{\ddot{z}})$ depend upon the noise present in the radar coordinates (σ_z), the type of smoothing technique used (polynomial of degree P), the number of data points used in the smoothing process (N), and the time spacing between consecutive data points (Δt). Of these four variables, two are dependent upon the radar being used. For example, for an FPS 16 radar, σ_z varies between 10 and 15 meters, depending upon slant range and tracking conditions, and Δt is generally fixed at 1/10 of a second. The other two variables, the degree polynomial and the number of data points are arbitrary and will be chosen in such a way so as to minimize Equation 6. The values of $\dot{z}$ and $\ddot{z}$ in Equation 6 depend primarily upon the sphere apogee, but are also affected to a much lesser degree by atmospheric density. If a balloon flight in the 1962 Standard Atmosphere from a given apogee is assumed, then the $\dot{z}$ and $\ddot{z}$ computed from this theoretical flight will be very nearly the same as that of an operational flight having the same apogee, since deviations of the ac.   :tmospheric profile from the 1962 standard wiil have a negligible effect on sphere velocity and acceleration. (the notation $\rho_{"62"}$ will refer to the density profile of the 1962 Standard Atmosphere).

The bias errors in velocity and acceleration $(\Delta\dot{z}, \Delta\ddot{z})$ depend upon N, Δt, the degree polynomial, and the true position Z vs t of the sphere. The true position path is primarily a function of sphere apogee, and only secondarily dependent upon the deviations of density from a standard atmos. Since the true position field of a passive sphere is never known, some assumption must be made so that the bias error term can be evaluated. A representative position field can be obtained for the sphere assuming that the sphere fell in the 1962 Standard Atmosphere from a given apogee. Using this assumption, the next section will describe the technique for evaluating the bias error in density.

b) Estimation of Noise and Bias Error Terms

Equation 6 has been determined to be a function of N, Δt, degree polynomial, and apogee. The problem to be solved is: determine the N, degree, and apogee that will minimize Equation 6 in the 70-100 km region, assuming a

12

known radar error and a known sample rate (Δt). For the passive sphere system, an FPS 16 tracking radar is assumed, with RMS error of 15 meters in the Z component, and a sample rate of 2 per second ($\Delta t = 1/2$ second). In actuality, FPS 16 data is generally digitized in 1/10 second intervals. However, to obtain independent measurements and to minimize the data handling problem, five 1/10 second data points are averaged, producing independent 1/2 second data points.

Estimation of Noise Error Terms

There are two methods of estimating the noise error terms: a) examining an actual flight of a passive sphere tracked by two identical FPS 16 radars and b) using equations which directly relate $\sigma_{\dot{z}}$ and $\sigma_{\ddot{z}}$ to N, Δt, σ_z, and the smoothing function. In method a, densities are calculated from each set of radar data using the same number of points (N), and degree of smoothing polynomial (P). Since the same bias appears in the density computations from each of the two radar tracks, calculation of the RMS difference between the densities as obtained by the first radar and those from the second radar determines the noise error terms. The equations of method b are presented in Figure 3 and derived in Appendix B. As seen in Figure 3, the form of the noise error expression is determined by the degree (P) of the smoothing polynomials used. Linear polynomial smoothing is defined as fitting a linear polynomial over N data points and assigning the slope of the fit to be the velocity at the midpoint $\left(\frac{N+1}{2}\right)$ of the

interval. Linear-linear smoothing to obtain acceleration is described as fitting N position points to a linear polynomial to obtain velocities and fitting M of these velocities by a linear polynomial to obtain acceleration (see Ref. 1). A cubic-linear fit is described as fitting N position points to a cubic polynomial, taking the slope at the midpoint as the velocity, and fitting M of these velocities by a linear polynomial to obtain acceleration. The method is similar for cubic-cubic and linear-cubic smoothing techniques. (Second and fourth degree polynomial smoothing result in the same slope at the midpoint of the interval as does the first and third degree smoothing, respectively.) Quadratic smoothing is defined as fitting a second degree polynomial to position points, and evaluating the first and second derivatives of the polynomial (at the midpoint) as the velocity and acceleration, respectively. The validity of these formulas has been established by comparisons with RMS errors which were obtained by method a.

Estimation of Bias Errors

For a given apogee, bias errors can be determined by the following technique (see Figure 4). Given a drag table and sphere apogee, the equations of motion can be integrated to obtain the theoretical path of the sphere, assuming 1962 Standard Atmosphere. The vertical position Z, velocity $\dot{Z}$, and acceleration $\ddot{Z}$ are determined by the theoretical trajectory program. The Z position coordinates (Z, t) are now treated as radar data and the smoothing routine is

13

VELOCITY

Linear fit
$$\sigma_{\dot{z}_1}^2 = \frac{12}{N(N^2-1)} \cdot \frac{\sigma_z^2}{\Delta t^2}$$

Cubic fit
$$\sigma_{\dot{z}_3}^2 = \left[\frac{12}{N(N^2-1)} + \frac{7(3N^2-7)^2(N-4)!}{(N+3)!}\right]\frac{\sigma_z^2}{\Delta t^2}$$

Quadratic fit   Same as linear fit $\sigma_{\dot{z}_2}^2 = \sigma_{\dot{z}_1}^2$

Quartic fit   Same as cubic fit $\sigma_{\dot{z}_4}^2 = \sigma_{\dot{z}_3}^2$

ACCELERATION

Linear-linear fit
$$\sigma_{\ddot{z}_{11}}^2 = \frac{12}{M(M^2-1)} \cdot \frac{\sigma_{\dot{z}_1}^2}{\Delta t_2}$$

Cubic-linear fit
$$\sigma_{\ddot{z}_{31}}^2 = \frac{12}{M(M^2-1)} \cdot \frac{\sigma_{\dot{z}_3}^2}{\Delta t_1^2}$$

Cubic-cubic fit
$$\sigma_{\ddot{z}_{33}}^2 = \left[\frac{12}{M(M^2-1)} + \frac{7(3M^2-7)^2(M-4)!}{(M+3)!}\right]\frac{\sigma_{\dot{z}_3}^2}{\Delta t_1^2}$$

Linear-cubic fit
$$\sigma_{\ddot{z}_{13}}^2 = \left[\frac{12}{M(M^2-1)} + \frac{7(3M^2-7)^2(M-4)!}{(M+3)!}\right]\frac{\sigma_{\dot{z}_1}^2}{\Delta t_1^2}$$

Quadratic (second derivative)
$$\sigma_{\ddot{z}_2}^2 = \left[\frac{720}{N^5-5N^3+4N}\right] \cdot \frac{\sigma_z^2}{\Delta t^4}$$

Quartic (second derivative)
$$\sigma_{\ddot{z}_4}^2 = \left[\frac{720}{N^5-5N^3+4N} + \frac{44100(3N^2-13)^2}{49N(N^2-1)(N^6-29N^4+244N^2-576)}\right]\frac{\sigma_z^2}{\Delta t^4}$$

Figure 3: Noise Error Formulas for Polynomial Smoothing. (Derivations Given in Appendix B)

14
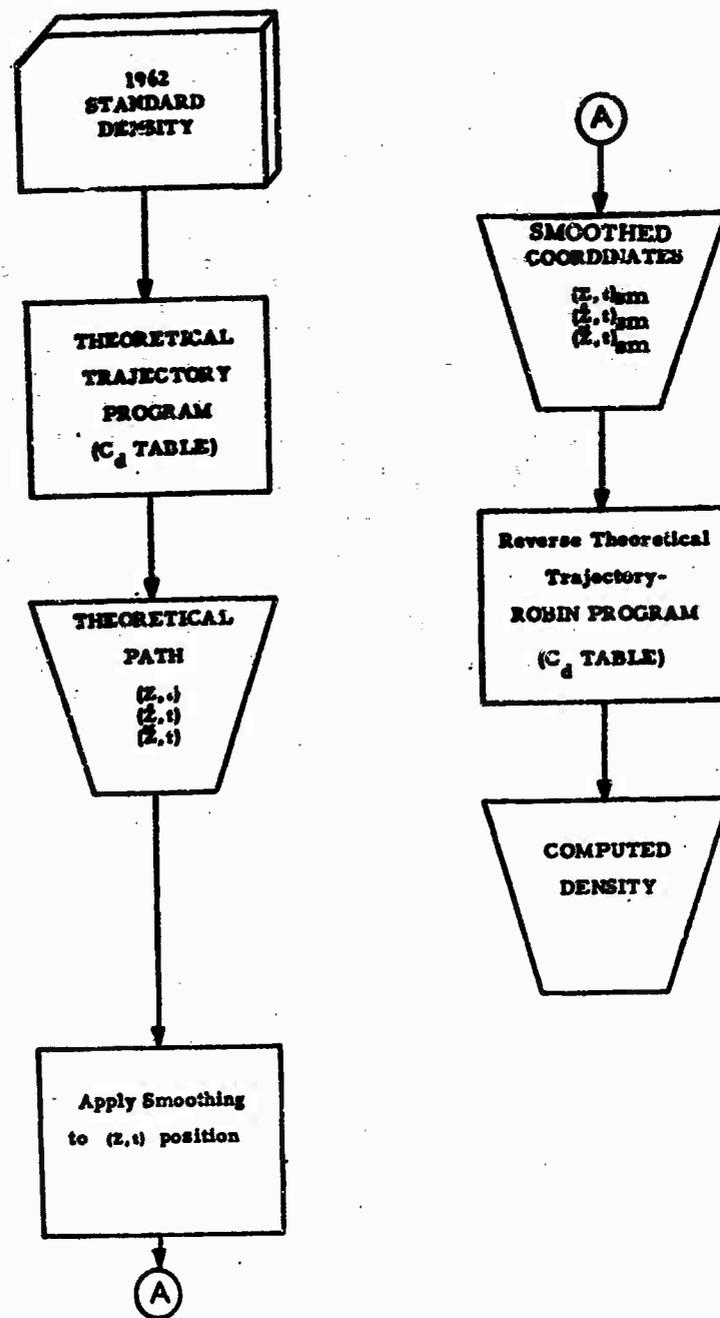
Figure 4: Schematic for Determining Density Bias Error

applied using N data points and the degree polynomial F. The smoothed Z, Ż, and Z̈ coordinates differ from the theoretical Z, Ż, and Z̈ coordinates only because of the bias error resulting from the smoothing technique. (No noise has been introduced into the data.) The smoothed coordinates are then re-substituted into the equation of motion, using the same drag table, and density is computed. The only difference between this computed density and the original input density (1962 Standard Atmosphere Density) is due to the bias error induced by the smoothing function. The percent bias error in density is then determined as the ratio of the computed minus the standard density to the standard density.

c)   Determination of Optimum Smoothing Technique

        The optimum smoothing for determining density is defined to be that smoothing of vertical coordinates that minimizes the sum of the noise and bias error variances in density (i. e. minimizes Equation 6). The determination of the polynomial and interval that minimizes Equation 6 in the 70-100 km region was derived by employing the above techniques. Initially, an escape altitude of 125 km was chosen. For each type double smoothing (linear-linear, cubic-linear, linear-cubic, cubic-cubic), the total error in density due to velocity and acceleration errors (Equation 6) was computed for all possible combinations of N and M. The noise error was calculated by method b (the formulas), as given in Figure 3, using Δt = 1/2 second and σ_z = 15 meters. The bias error was computed as described by Figure 4. Figures 5-8 are examples of the total error plots that were generated. The plots indicate the percent bias error (the deviation of density ratio from 1) and the 1σ confidence bands of the noise error about the bias. Careful analysis of total error plots for all combinations of degree polynomial (double smoothing) and N and M resulted in the choice of the 19-21 linear-cubic combination as optimum.

        Total error plots were then generated in the same fashion, using a quadratic polynomial fit and its first and second derivatives for velocity and acceleration. The best smoothing interval for using a quadratic was determined to be 31 data points (Figure 9). In comparing the optimum quadratic and the optimum linear-cubic smoothing techniques, it is easily seen that the 19-21 linear-cubic produced significantly better results in the 70-100 km region. The probable explanation for this is the following. By fitting two different functions, one to get velocity and the other to get acceleration, it is possible to partially compensate for, say, a positive bias in density due to a velocity error, by using a different degree polynomial or different interval to generate accelerations which will produce a negative density bias. This advantage is not present when using a single function for smoothing.

        The decreased density accuracy below 60 km for the 19-21 linear-cubic is due to the slower vertical velocity of the sphere which results in the constant time smoothing technique applied   over a shallower layer of altitude.

16
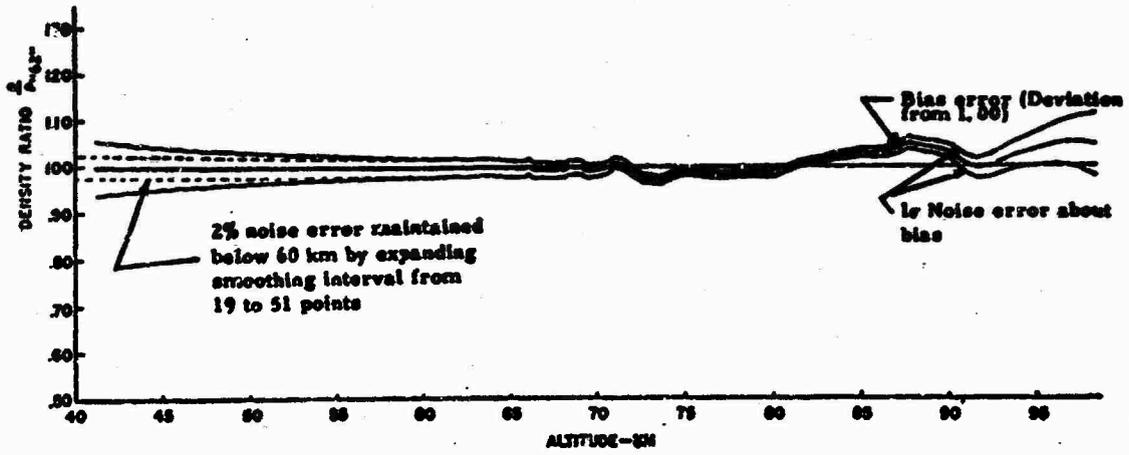
Figure 5: Bias and Noise Errors in Density for 19-21 Linear-Cubic Smoothing
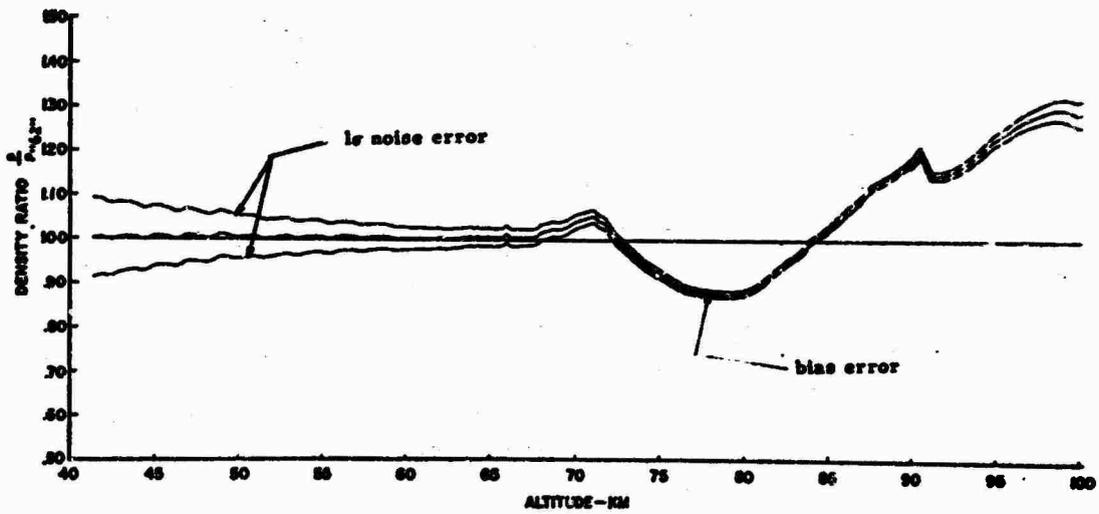
Figure 6: Bias and Noise Errors in Density for 29-25 Cubic-Linear Smoothing
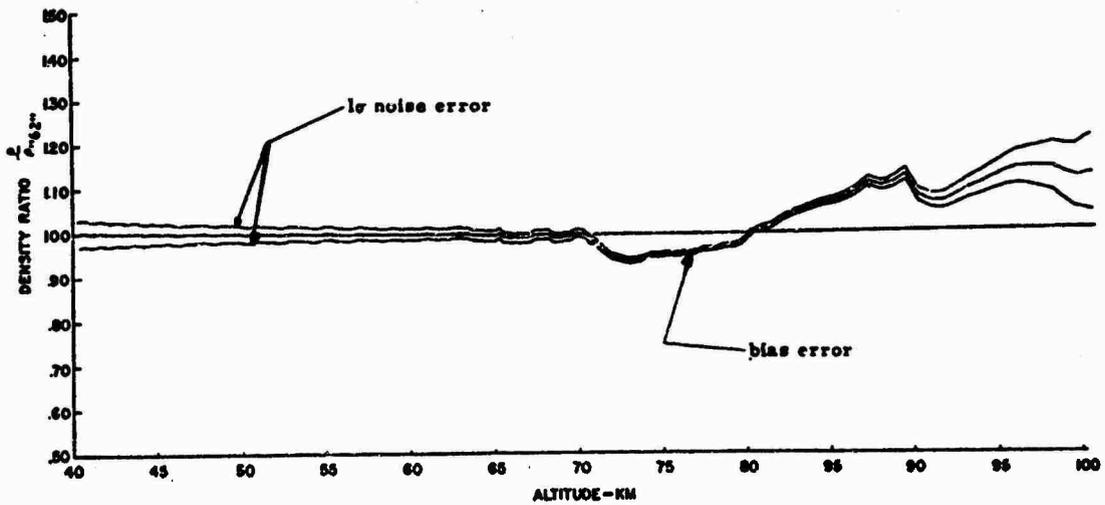
Figure 7: Bias and Noise Errors in Density for 31-7 Linear-Linear Smoothing

17
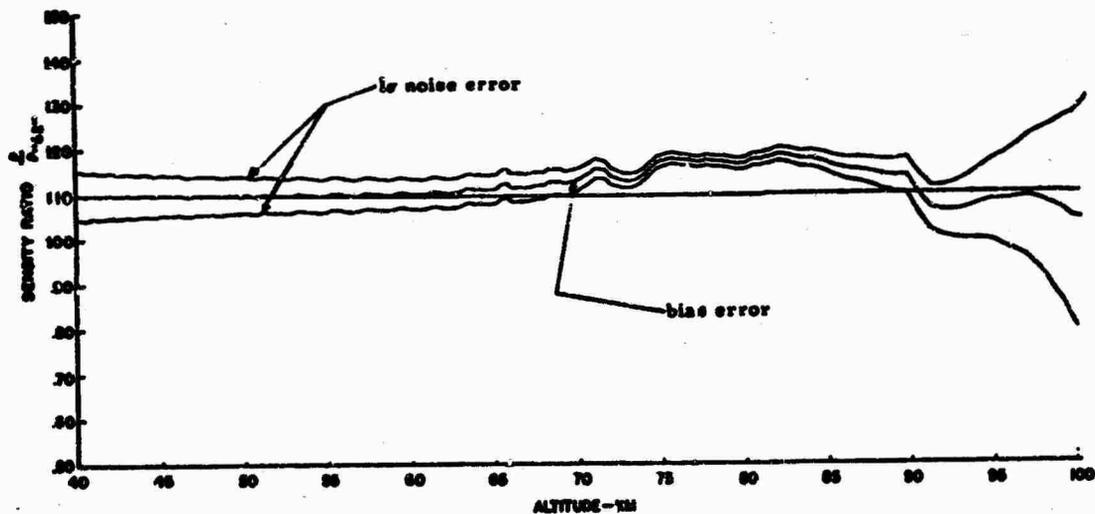
Figure 8: Bias and Noise Errors in Density for 49-11 Cubic-Cubic Smoothing
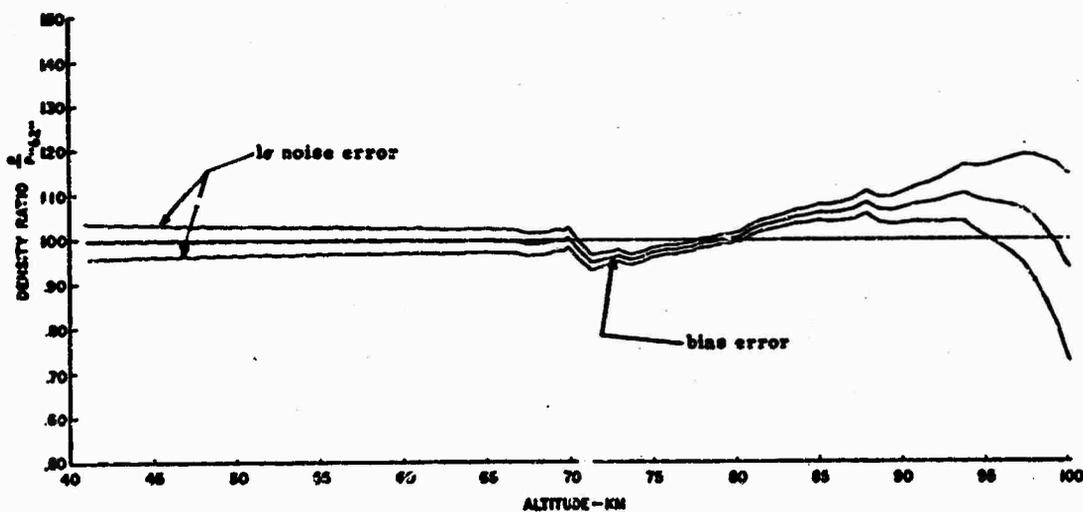
Figure 9: Bias and Noise Errors in Density for 31 Point Quadratic Smoothing

This situation was alleviated by expanding the position smoothing interval from 19 points at all altitudes above 60 km to a maximum of 51 points at approximately 35 km in such a fashion as to maintain a 2% noise error in density.

The 19-21 linear-cubic smoothing interval was next evaluated for other sphere apogees from 70 to 150 km, and the noise and bias plots were generated. As anticipated, an increase in sphere apogee resulted in higher velocities and accelerations experienced by the sphere at a given altitude, which increased the bias error in a measured density. Conversely, from observing the noise error terms, it is seen that an increase in velocity and acceleration results in a decrease of the noise error. In calculating the total error in the 70 to 100 km region for the various apogees, it was determined that the 125 km apogee is

18

most practical (See Table 4). Not only is the total error one of the smallest at every altitude, but from the logistic standpoint, the 125 km apogee is more easily obtained by available rocket hardware systems than higher apogees. The actual noise and bias errors in density for the various apogees are found in Table 4. This data verifies the requirement that serious degradation of density accuracy does not result for other apogees.

Table 4

Percent Noise, Bias, and Total Error in Density for Sphere Apogees from 70 to 150 Km.

ALTITUDE ~KM

Sphere Apogee ~Km	100 Noise Bias	100 Total	95 Noise Bias	95 Total	90 Noise Bias	90 Total	85 Noise Bias	85 Total	80 Noise Bias	80 Total	75 Noise Bias	75 Total	70 Noise Bias	70 Total	<70 Noise Bias	<70 Total
150	5 / +7	8.5	2 / +2.5	4	1 / +8	8	.5 / +4.5	4.5	.5 / -3	3	.5 / -1	1	1 / +1	1.5	2 / 0	2
140	6 / +6	8.5	3 / +4	5	1.5 / +8	8	.5 / +5	5	.5 / -1.5	2	.5 / +.5	1	1 / +1.5	2	2 / 0	2
125	8 / +2	8.5	4 / +3.5	5	1.5 / +4	4.5	1 / +3	3	.5 / -1.5	2	1 / -1	1.5	1.5 / -1	1.5	2 / 0	2
115	14 / +3	14	5 / +4	6.5	2 / +3	3.5	1 / +3	3	1 / -.5	1	1 / -1	1.5	1.5 / +.5	1.5	2 / 0	2
100			18 / +2	18	4 / +1	4	2 / +2	2.5	1 / -2	2	1 / -1	1.5	1.5 / -.5	1.5	2 / 0	2
90							8 / +2	8	4 / +2	4.5	1.5 / -.5	1.5	1.5 / +.5	1.5	2 / 0	2
80											2 / +1	2.5	1.5 / +.5	1.5	2 / 0	2
70															2 / 0	2

Total Error = $\left[\text{Noise}^2 + \text{Bias}^2 \right]^{1/2}$

2.2.4 Vertical Wind Error Term

The density error variance resulting from vertical winds is given by the expression

$$\left(\frac{\Delta\rho}{\rho} \right)^2 = \left(\frac{2\Delta W_z}{\dot{Z}} \right)^2 \qquad \text{(See Appendix A)} \qquad (7)$$

To a falling sphere, a vertical wind appears identical to a change in density. As a result, a data reduction program cannot distinguish density perturbations from vertical wind oscillations. In order to compute densities, an assumption must be made concerning either vertical winds or density perturbations in the atmosphere.

19

Assumption A

Assuming no vertical motions in the atmosphere, Equation 1 can be solved by substituting $W_z = 0$ on the right side of Equation 1 and evaluating all other terms by conventional means. Under this assumption, any vertical winds present in the atmosphere will appear as density perturbations. The relationship between vertical winds (amplitude and wavelength) and density perturbations is exhibited in Figure 10 for a sphere apogee of 125 km. Figure 10 also contains the effect of the 19-21 (expanding to 51-21) linear-cubic smoothing filter on the vertical wind. An example will clarify this effect. If a sinusoidal vertical wind of wavelength 2 km with amplitude of 1 m/sec is present at 50 km, then this vertical wind would be damped by the smoothing and appear as having amplitude 0.52 m/sec (obtained from Figure 11). Since the program attributed the 0.52 m/sec. vertical motion as a density perturbation, the result of the actual 1 m/sec. vertical wind would be, using Equation 7, a 1.3% density perturbation as shown in Figure 10. The density error introduced by a vertical wind of amplitude X m/sec. is obtained by multiplying the error introduced by a 1 m/sec. vertical wind by X.
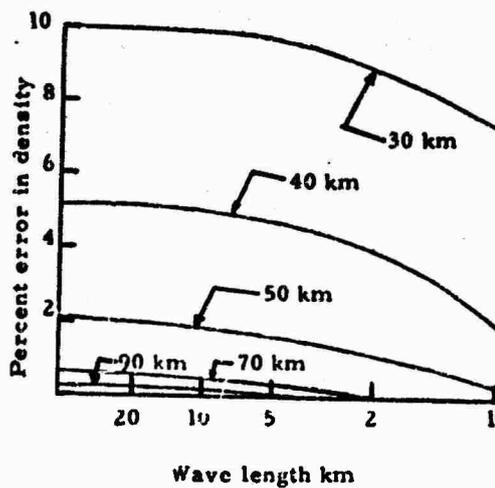
Figure 10: Density Error Produced by a Vertical Wind of 1 m/sec - 125 km Apogee

Assumption B

If density is assumed to follow some mean path, then perturbations from this path can be attributed to vertical winds. Since density varies exponentially with altitude, a mean exponential path is appropriate.

20

Using this assumption, vertical winds can be computed by the equation

$$W_z = \frac{\ddot{Z}_{mean} - \ddot{Z}}{2K\dot{Z}\rho_o e^{\alpha z}} .$$

A description of the variables in this equation and its application is given in Reference 1.

Since, according to present knowledge, meteorologists accept density perturbations at least as much as they accept vertical winds, Assumption A, that is $W_z = 0$, has been incorporated into this program. The magnitude of vertical winds in the upper atmosphere is not yet well substantiated. Consequently, significant density errors may result when using this assumption if the vertical winds exceed a few m/sec (See Figure 10).

2.3 Summary of Density Errors Using Optimum Smoothing

The total percent error in density resulting from a computation using the High Altitude ROBIN program with optimum smoothing cannot be precisely determined because of the unknown accuracy of the drag table and the occurrence of unknown vertical winds. The drag table has been taken from the work of Heinrich in the supersonic mach number regime, and from Lawrence and Goin in the subsonic, with values interpolated and extrapolated between these two drag tables when necessary. The accuracies specified by the experimenters are: Subsonic, ±2% RMS error; and supersonic maximum possible error, from ±2.3% to ±27.9%, depending on Reynolds number.

The vertical wind error depends upon the magnitude of the vertical wind and the altitude at which it appears. A 2 m/sec., 10 km vertical wind will result in a density error less than 2% above 70 km; however, at an altitude of 40 km, the same 2 m/sec. vertical wind will result in a 9% error in density.

The error in density due to errors in horizontal winds and velocity is less than 1% at all altitudes.

The error in density due to a 10% error in the initial estimate of temperature becomes less than 1% after 4 km of flight data.

The other contributing terms to density errors have been accurately determined for the 19-21 linear-cubic (which expands to a maximum 51-21 at 35 km) smoothing. The noise error in density is less than 2% to 90 km and less than 8% to 100 km, and the bias error is less than 1% to 70 km and a varying bias from 1 to 5% from 70 to 100 km. The amount of detail in the density

that passes through the linear-cubic filter is determined by the frequency
response curves (Figure 11). For a given wavelength of a density oscillation,
Figure 11 can be used to determine the percent of the amplitude of the oscillation
that will filter through the reduced data as a function of altitude. As seen
in   Figure 11, wavelengths less than 10 km are largely damped by the smooth-
ing at altitudes exceeding 70 km, whereas below 70 km wavelengths of the order
of 5 km are easily observed.
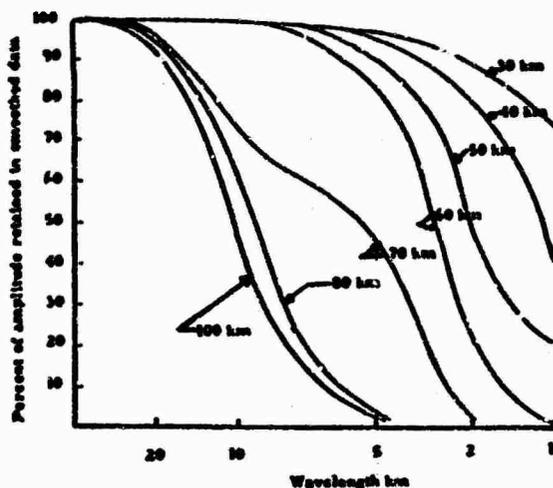
Figure 11: Density Frequency Response for Expanding 19-21 Linear-Cubic Smoothing

2.4   Density Validity: Sphere Collapse Checks

Density data is defined to be valid if the sensing sphere is properly
inflated. A collapsed or elongated sphere will result in highly ficticious density
measurements. Two checks are used to determine proper sphere inflation:
A time of fall check and a density gradient check (λcheck).

2.4.1   Time of Fall Check

Experience with the Arcas ROBIN System has shown that a collapsed
sphere falls with a noticeably slower vertical velocity than does an inflated sphere.
As a result, it is generally possible to determine sphere collapse by comparing
the fall velocity of an actual sphere to the estimated fall velocity for an inflated
sphere. Estimated fall velocities for the ROBIN sphere have been obtained
from computer simulated flights assuming the 1962 Standard Atmosphere and
±20% deviations in density from the 1962 Standard Atmosphere. The times of
fall for sphere apogees between 150 and 70 km is given in Table 5. Above 80 km
the time of fall is strongly dependent upon the sphere apogee. In certain cases
an error of a few km in determining sphere apogee could change the estimated
time of fall more than 20% deviation in density from the 1962 Standard Atmosphere.
For this reason, the time of fall test is not used above 80 km. The altitudes
where the time of fall test is used for each sphere apogee is indicated by the
heavy lines of Table 5. If the time of fall of an actual sphere does not lie

22

between that estimated for a sphere falling through an atmosphere whose density is 0.8 $\rho_{"62"}$ and a density of 1.2 $\rho_{"62"}$ sphere collapse is indicated.

The performance of the time of fall test has been evaluated for numerous flights with varied apogees. In Figure 12 a comparison is made between collapse as indicated by the time of fall test, the λ check (discussed in section 2.4.2), and observations of the density ratio. Experience has shown that a sharp increase in the density ratio over a few kilometers is associated with sphere collapse. Of the 14 flights that were investigated, the time of fall test accurately determined collapse on 12 flights. On the other two flights the time of fall test was apparently 5 to 10 km premature. The time of fall test can only pinpoint collapse to within 5 km. If collapse occurs near the bottom of the test layer it may not vary the time of fall sufficiently to detect collapse until the next 5 km test layer. For this reason the time tolerances which indicate collapse are quite restrictive. For spheres that never inflated or spheres whose collapses is obvious (by the three tests), the time of fall greatly exceeds the allowed tolerances for inflated spheres.

TABLE 5

Time of Fall in Seconds Through Standard Atmosphere
and ±20% Deviation from Standard for Sphere Apogees Between 70 and 150 Km

Apogee Altitude	ALTITUDE BANDS ~ Km									
	100-90	90-80	80-70	70-60	60-55	55-50	50-45	45-40	40-35	35-30
.8ρ	10	10	18	43	32	44	59	84	124	198
150km ρ	10	11	21	49	37	51	69	96	142	218
1.2ρ	16	12	24	52	39	56	74	106	156	232
.8ρ	11	11	19							
140km ρ	11	12	22	Incremental time of fall for all apogees from 70 km through 150 km is the same as that given for 150 km.						
1.2ρ	11	13	25							
.8ρ	14	14	21							
125km ρ	14	15	25							
1.2ρ	14	16	27							
.8ρ	16	14	22							
115km ρ	17	16	26							
1.2ρ	18	17	28							
.8ρ	-	21	26							
100km ρ	-	23	30							
1.2ρ	-	24	32							
.8ρ	-	-	-	43						
80km ρ	-	-	-	49						
1.2ρ	-	-	-	52						
.8ρ	-	-	-	-	32	44	59	84	124	198
70km ρ	-	-	-	-	37	51	69	96	142	218
1.2ρ	-	-	-	-	35	54	74	106	156	232

Figure 12: Evaluation of Sphere Collapse Checks-- Time of Fall Test and λ Check

Time of Fall Through Altitude Layers

Flight I.D.	Apogee	80-70	70-60	60-55	55-50	50-45	45-40	40-35	35-30	Time of fall Performance	λ Check collapse	λ Check performance	Density ratio $(\frac{c}{c_{th}})$ observation	Comments
Viper Dart 11	121	26	49	37	49	66	98	141	2;6*	good	36.5 Km	fair	Ratio 1.07 at 33 Km, 1.50 at 31 Km.	λ check a little premature
Viper Dart 12	124	25	49	36	50	70	100	166	300*	good	37.4 Km	good	Ratio 1.11 at 38.2 Km, 2.16 at 34.0 Km	all checks agree on collapse
Viper Dart 13	115	27	50	37	51	69	97	145	236*	good	34.0 Km	good	Ratio 0.91 at 34.6, 1.4 at 32.5 Km	all checks agree on collapse
Viper Dart 6	-	-	-	39	52	69	102	201	312*	good	57.1 Km	fair	Ratio 1.18 at 40.0 Km, 1.6 35.5 Km	ρ inversion trips λ check at 57 Km
Patrick 45	137	26*	64*	56*	84*	117*	170*	245*	360*	good	58.2 Km	good	Ratio 1.10 at 68 Km, 2.1 at 55 Km	probably no inflation
Patrick 8231	129	25	51	40*	53	98*	150*	221*	331*	fair	49.0 Km	good	Ratio 1.3 at 49.6 Km, 1.8 at 40.6, 1.19 at 44.3	time of fall test premature
Patrick 7780	123	25	49	38	51	69	98	147	227	good	40.1 Km	bad	Ratio between 0.9 and 1.1 entire flight	vertical wind probable cause of λ failure
Patrick 6362	142	22	51	38	53	75*	107*	215*	335*	fair	40.8 Km	good	Ratio 1.15 at 41 Km, 1.89 at 39 Km	time of fall test a little premature
Patrick 4	132	28*	54*	55*	79*	79*	109*	171*	-	good	57.8 Km	good	Ratio 1.25 at 80 Km, 1.90 at 65 Km, 2.35 at 58 Km	all checks indicate no inflation
Patrick 9137	132	30*	63*	56*	82*	117*	154*	188*	326*	good	57.8 Km	good	Ratio high entire flight, 1.33 at 66 Km, 2.08 at 64 Km	all checks indicate no inflation
Holloman 21930	-	-	-	68*	79*	87*	121*	176*	262*	good	53.5 Km	fair	Ratio greater than 2.0 entire flight	λ check a little late
Holloman 21749	85	-	75*	65*	90*	146*	179*	-	-	good	57.8 Km	good	Ratio greater than 2.0 entire flight	all checks indicate no inflation
Holloman 23933	-	-	-	30	53	73	105	-	-	good	51.4 Km	bad	Ratio 1.17 at 43.3 Km, 2.0 at 40.0	vertical wind probable cause of λ failure
Holloman 22751	-	-	-	38	53	88*	142*	193*	283*	good	48.6 Km	good	Ratio 1.22 at 49.4 Km, 1.95 at 48.0 Km	all checks agree
Tolerance		see Table 5	44-52	33-39	44-54	59-74	84-106	124-56	198-232					

* Indicates collapse by time of fall test.

Holloman Flights are ARCAS ROBINS

24

From Figure 12 this is apparent at all altitudes and is a strong arguement to support the validity of the sphere collapse check. A debatable point is whether the tolerances should be increased slightly at the expense of occasionally determining collapse 5 km too late.

2.4.2   Density Gradient Check (λ check)

Engler (Ref. 1) has shown that below 60 km the density gradient can be estimated by λ defined as:

$$\lambda = \frac{2}{Z_2 - Z_1} \left(\text{Log} (\dot{Z}_2) - \text{Log} (\dot{Z}_1) \right) = \frac{1}{\rho} \frac{d\rho}{dz} \tag{8}$$

An estimate of the value of λ one would anticipate for an inflated sphere is determined by observing the density gradient $\frac{1}{\rho} \frac{d\rho}{dz}$ of the 1962 Standard Atmosphere. If the sphere is properly inflated, then the calculated λ should approximate this density gradient. A collapsed balloon will result in incorrect density data and consequently λ will deviate considerably from its anticipated value. To allow for real changes in the density gradient of the atmosphere from the 1962 Standard, the change in $\frac{1}{\rho} \frac{d\rho}{dz}$ due to a 15% perturbation in the density ratio $\left(\frac{\rho}{\rho_{"62"}}\right)$ over a 5 km layer (Figure 13) has been calculated and is presented in Table 6.
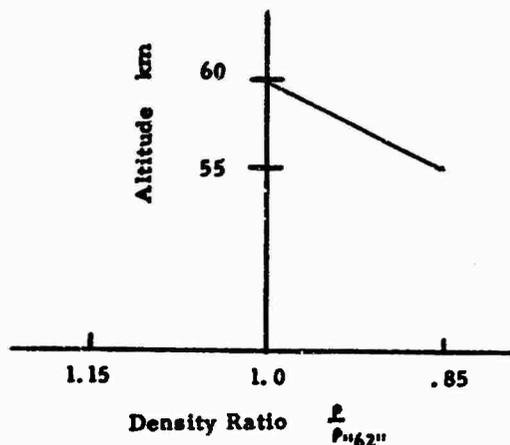
Figure 13: Density Profile of 15% Decrease in Density Ratio per 5 km

25

Table 6 shows the density gradient of the 1962 Standard and the change occuring in the gradient due to a ± 15% perturbation per 5 km.

TABLE 6

Density Gradient of "62" Standard Atmosphere
and Changes Produced by ±15% Density Perturbation Per 5 KM

$\left(\frac{1}{\rho}\frac{d\rho}{dz}\right)$ 62 Std. Atm.	gradient for -15% Perturbation in density	gradient for +15% perturbation in density	difference
60-55	.00012	.00009	.00015	±.00003
55-50	.00013	.00010	.00016	±.00003
50-45	.00014	.00011	.00017	±.00003
45-40	.00015	.00012	.00018	±.00003
40-35	.00016	.00013	.00019	±.00003
35-30	.00015	.00012	.00018	±.00003

From observation of Table 6 an anticipated value of $\lambda = .00014$ was chosen and a tolerance of ±.00005 allowed for density perturbations in the real atmosphere.

In addition to allowing a tolerance in λ for real density perturbations a tolerance must also be allowed for the inaccuracies of the parameters used to compute λ.

It can be shown that errors in a calculation of λ are primarily a result of errors in the velocity measurements ($\dot{Z}_2$ and $\dot{Z}_1$) rather than the position measurements (Z_2 and Z_1).*

Considering errors in λ as a function of velocity errors, the error variance formula for λ is derived as follows

$$\Delta\lambda = \frac{\partial\lambda}{\partial\dot{Z}_2}\Delta\dot{z}_2 + \frac{\partial\lambda}{\partial\dot{Z}_1}\Delta\dot{z}_1$$

(9)

$$\Delta\lambda = \frac{2}{Z_2 - Z_1}\left(\frac{\Delta\dot{z}_2}{\dot{Z}_2} - \frac{\Delta\dot{z}_1}{\dot{Z}_1}\right)$$

Since the program is designed to maintain a constant percent density error ($\frac{\sigma\rho}{\rho}$) of .02 below 60 km, it is desirable to transform Equation 9 into terms of $\frac{\Delta\rho}{\rho}$.

* Z_1 and Z_2 are the respective first and last points of the position smoothing interval.

26

Assuming $\rho = ce^{\lambda z}$ an approximate solution to the equations of motion yields

$$\dot{Z} = \left(\frac{g}{kc}\right)^{1/2} e^{\lambda z/2} = \left(\frac{g}{kc^2}\right)^{1/2} \rho^{1/2} \quad \text{(See Ref. 1)}$$

where g, k, and c are constants defined in Reference 1.

The error increment in $\dot{Z}$ is approximated as

$$\Delta\dot{z} = \frac{\partial\dot{Z}}{\partial\rho} \Delta\rho = \left(\frac{g}{kc^2}\right)^{1/2} \frac{\Delta\rho}{2\rho^{1/2}}$$

Thus

$$\frac{\Delta\dot{z}}{\dot{Z}} = 1/2 \frac{\Delta\rho}{\rho}. \tag{10}$$

Substituting (10) into Equation 9 yields

$$\Delta\lambda = \frac{1}{Z_2 - Z_1} \left(\frac{\Delta\rho_2}{\rho_2} - \frac{\Delta\rho_1}{\rho_1}\right). \tag{11}$$

Taking the variance of both sides of Equation 11 and recalling that $\frac{\Delta\rho}{\rho}$ is maintained constant below 60 km, gives

$$\sigma_\lambda^2 = \frac{1}{(Z_2 - Z_1)^2} 2\left(\frac{\sigma\rho}{\rho}\right)^2.$$

Thus

$$\sigma_\lambda = \frac{\sqrt{2}}{\Delta z} \left(\frac{\sigma\rho}{\rho}\right) \tag{12}$$

where

$$\Delta z = Z_2 - Z_1.$$

For a $\frac{\sigma_\rho}{\rho} = .02$ the noise error in λ becomes

$$\sigma_\lambda = \frac{.02\sqrt{2}}{\Delta z} = \frac{.02828}{\Delta z}$$

27

The 3σ noise error tolerance for λ is

$$3\sigma_\lambda = \frac{.08484}{\Delta z} .$$

The λ check is summarized as follows:

Expected value of $\lambda = .00014$
Tolerance for variations in density $\pm .00005$
3σ noise tolerance $\pm \dfrac{.08484}{\Delta z}$.

A sphere is considered inflated if

$$.00014 - \sqrt{(.0005)^2 + \left(\frac{.08484}{\Delta z}\right)^2} \leq \lambda \leq .00014 + \sqrt{(.00005)^2 + \left(\frac{.08484}{\Delta z}\right)^2} .$$

The performance of the λ check is evaluated in Figure 12. For 9 of the 14 flights the collapse altitude as determined by the λ check is in excellent agreement with the collapse altitude as indicated by time of fall and the density ratio. For these cases the λ check appears to determine the collapse altitude to within 1 km accuracy. For the other flights the λ check generally indicates collapse several kilometers before the time of fall check. This is not caused by radar noise but is undoubtedly the result of an interesting meteorological observation; either a vertical wind or density perturbation. For this reason the λ check should be interepreted in conjunction with results of time of fall test. The time of fall test is the primary determination of collapse. The λ check serves to verify the performance of the time of fall test as well as pointing out interesting meteorological phenomena.

3.   WINDS

The equation used for computing wind with the falling sphere method is given as

$$W_x = \dot{X} - \frac{(\dot{Z} - W_z)(\ddot{X} + C_x - g_x - \dfrac{g_x V_b \rho}{m})}{\ddot{Z} + C_z - g_z - \dfrac{g_z V_b \rho}{m}} . \tag{13}$$

28

The error present in a wind computation is a result of the inaccuracies of parameters in Equation 13. The inaccuracies of several of these parameters have a negligible effect upon the wind accuracy.

3.1 Variables Not Producing Significant Wind Errors

The errors in computing g_z, the gravitational acceleration in the direction perpendicular to the tangent plane, is less than .0004 m/sec^2. This error is negligible when compared to the larger error in measuring $\ddot{Z}$. The error in g_x is approximately 1/10 the magnitude of the error in g_z, and for the same reason can be ignored.

The Z component buoyancy term, $\rho V_b g_z /m$ is very small (approximately .006 m/sec^2). The error in computing this term is many times smaller than the term itself and is negligible when compared to other larger error terms. The error in the X-component buoyancy term $\rho V_b g_x /m$, is approximately 1/10 the magnitude of the error in the term $\rho V_b g_z /m$, and similarly can be ignored when investigating wind accuracy.

For a ROBIN sphere with apogee 125 km, the coriolis acceleration component C_x has approximate magnitude. 09 m/sec^2 at 100 km, .11 at 95 km, and .11 at 90 km. Depending upon the magnitude of the denominator of Equation 13, C_x can make a large contribution to wind measurement. If ignored, the coriolis acceleration at 100 km would result in a ficticious horizontal wind of magnitude 40 m/sec; at 95 km, a ficticious horizontal wind of 19 meters per second; and at 90 km, a wind of 10 m/sec. Hence, the accuracy of C_x must be investigated. C_x is computed by equation

$$C_x = 2 W \left(\dot{Z} \cos \theta + \dot{Y} \sin \theta \right) \tag{14}$$

where
$$W = \text{rotation rate of earth} = 7.29 \times 10^{-5} \text{ radians per sec.}$$
$$\theta = \text{latitude}$$

The error in C_x is a result of the error in $\dot{Z}$. For example, if $\dot{Z}$ were in error by 10 m/sec, the resulting error in C_x would be only .0014. Since this is at least an order of magnitude less than the error in $\ddot{X}$, it is not a significant source of error in wind calculation. The error in the vertical coriolis component C_z is approximately 1/10 the error in C_x. Consequently, errors in both coriolis components of acceleration are not significant sources of wind measurement error.

The effect of vertical winds on horizontal wind measurements depends upon the altitude of the sphere. Table 7 shows the magnitude of errors that will

result from a 5 m/sec and 1 m/sec vertical wind as a function of altitude. The errors may get as large as a couple of m/sec at 100 km. The remaining variables in Equation 13 which may contribute significantly to wind errors are the horizontal and vertical components of velocity and acceleration.

<div align="center">

TABLE 7

Representative Values of Horizontal Wind Error
Resulting from 1 and 5 m/sec Vertical Winds

$W_z = 5$ m/sec
</div>

Altitude km	$\dot{z}$	W_z	$1 - \dfrac{\dot{z} - W_z}{\dot{z}}$	Representative Value of $\langle \rangle$ see below	Error in W_x
100	-500	5	.01	250	2.5 m/sec
90	-625	5	.008	200	1.6
80	-550	5	.01	160	1.6
70	-250	5	.02	100	2.0
60	-160	5	.03	5	.15
50	-100	5	.05	1	.05
40	- 41	5	.12	.05	.007
30	- 14	5	.36	.04	.014

<div align="center">

$W_z = 1$ m/sec
</div>

Altitude km	$\dot{z}$	W_z	$1 - \dfrac{\dot{z} - W_z}{\dot{z}}$	Representative Value of $\langle \rangle$ see below	Error in W_x
100	-500	1	.002	250	.5
90	-625	1	.0016	200	.32
80	-550	1	.0018	160	.288
70	-250	1	.004	100	.4
60	-160	1	.0062	5	.03
50	-100	1	.01	1	.01
40	- 41	1	.024	.06	.002
30	- 14	1	.071	.04	.003

$\langle \rangle$ refers to the term $\dfrac{(\dot{z} - W_z)\,(\ddot{x} + C_x - g_x - \frac{g_x V_B}{m})}{\ddot{z} + C_z - g_z - \frac{\rho V_B g_z}{m}}$. $1 - \dfrac{\dot{z} - W_z}{\dot{z}}$ is the percent error

in $\langle \rangle$ resulting by assuming $W_z = 0$.

<div align="center">30</div>

3.2   Wind Error Equation

Having retained only those error components which are the predominant source of error in a computed wind, the wind equation simplifies to

$$W_x = \dot{X} - \frac{\ddot{X}\dot{Z}}{\ddot{Z}-g}$$

The first order of approximation to an error in W_x resulting from the errors in the parameters is given by Equation 15

$$dw_x = d\dot{x} - \frac{\dot{Z}}{\ddot{Z}-g}\, d\ddot{x} - \frac{\ddot{X}}{\ddot{Z}-g}\, d\dot{z} + \frac{\ddot{X}\dot{Z}}{(\ddot{Z}-g)^2}\, d\ddot{z} \qquad (15)$$

If the differential error components are considered as random noise error with normal distribution, then by taking the variance of Equation 15, the noise error in a wind calculation is given by Equation 16 where $\sigma_{\dot{x}}$, $\sigma_{\ddot{x}}$, etc. are the noise errors in velocity and acceleration due to the noise in the radar data

$$\sigma_{w_x}^2 = \sigma_{\dot{x}}^2 + \left(\frac{\dot{Z}}{\ddot{Z}-g}\right)^2 \sigma_{\ddot{x}}^2 + \left(\frac{\ddot{X}}{\ddot{Z}-g}\right)^2 \sigma_{\dot{z}}^2 + \left(\frac{\ddot{X}\dot{Z}}{(\ddot{Z}-g)^2}\right)^2 \sigma_{\ddot{z}}^2 . \qquad (16)$$

To determine the bias in a wind measurement resulting from the biased (over-smoothing) velocity and acceleration measurements, Equation 15 is again applied. Considering the component differentials as the bias error, the square of the bias wind error is given by Equation 17.

$$\Delta w_x^2 = \left[\Delta \dot{x} - \frac{\dot{Z}}{\ddot{Z}-g}\, \Delta \ddot{x} - \frac{\ddot{X}}{\ddot{Z}-g}\, \Delta \dot{z} + \frac{\ddot{X}\dot{Z}}{(\ddot{Z}-g)^2}\, \Delta \ddot{z}\right]^2 \qquad (17)$$

where the $\Delta \dot{x}$, etc, refer to the bias error in the X component. The total wind error (σ_{w_x} total) is defined as the square root of the sum of the noise error variance plus the bias square error and is given by Equation 18

$$\sigma_{w_x \text{ total}} = \left[\sigma_{w_x}^2 + \Delta w_x^2\right]^{1/2} \qquad (18)$$

31

The optimization problem for wind determination is to find that type smoothing and smoothing intervals for horizontal and vertical coordinates that minimize Equation 18. As in the case of the density smoothing, the noise error will decrease as the smoothing interval increases and the bias error increases as the smoothing interval increases, so that a minimum does exist for Equation 18.

3.3 Minimization of Total Wind Error

3.3.1 Discussion of Variables in Noise Error Term

The noise error variance (Equation 16) is a function of the vertical velocity and acceleration, the horizontal velocity and acceleration, and the errors in measuring the horizontal and vertical velocities and accelerations. As shown previously (Figure 3), the noise error in a velocity or acceleration measurement is a function of the degree of smoothing, smoothing interval, time spacing between data points, and the error in the radar coordinates. The types of smoothing considered were linear-linear, cubic-linear, cubic-cubic, quadratic and quartic (quadratic and quartic smoothing consists of fitting a second and fourth degree polynomial respectively to the position coordinates and evaluating the first and second derivatives of the fits as velocity and acceleration). The noise error formulas for the various degrees of smoothing for velocity and acceleration are given in Figure 3. For any actual sphere flight, and for any of the smoothing techniques considered for measuring velocity and acceleration, the noise error in winds (Equation 16) can be calculated by knowing the radar accuracy (σ_x, σ_y, σ_z)(time spacing between data points (1/2 second for the independence requirements), and the velocity and acceleration experienced by the sphere (these can be taken merely as the smoothed velocity and acceleration measurements). Therefore, by taking a particular ROBIN flight and knowing the radar accuracies, the noise error variance can be calculated for any length velocity and acceleration smoothing intervals, as well as for linear, cubic, quadratic, and quartic velocity and acceleration smoothing procedures.

3.3.2 Discussion of Variables in Bias Error Term

The bias error term has been given by Equation 17. To evaluate this expression, equations must be derived for the bias error in the velocity and acceleration measurements ($\Delta\dot{x}$, $\Delta\ddot{x}$, $\Delta\dot{z}$, $\Delta\ddot{z}$). The rest of the variables in Equation 17 are immediately available from the smoothed velocity and acceleration values. The bias velocity and acceleration measurements can be written as a function of the degree, interval, Δt, and the true position field of the sensor versus time. If one assumes the true position field of the sensor to be a polynomial of degree 3, and assuming a linear polynomial smoothing to evaluate the derivative, then $\Delta\dot{x}$ defined

*A σ of 10 to 15 meters in each component is a representative estimate of FPS-16 radar accuracy obtained over a period of years from numerous dual-tracked flights flown at various ranges.

32

as $\dot{X}_{true} - \dot{X}_{smoothed}$ is given by $A_3 \Delta t^2 (3N^2-7)/20$ where A_2 is the coefficient of the third degree term. (See Appendix C). If cubic smoothing is used, then there will be no bias error for position fields up to and including fourth degree polynomials. That is, $\dot{X}_{smoothed}$ will equal $\dot{X}_{true}$ (assuming noise free data). The bias error formulas for single and double fit smoothing are presented as Figure 14 and derived in Appendix C. To apply the bias error formulas one must be able to substantiate the degree position field and determine the value of A_3, the cubic coefficient. For quadratic and quartic smoothing, the coefficient A_4 must be determined. The next section will show how the position field and A_3 can be estimated for linear-linear, cubic-linear, and cubic-cubic smoothing. A similar approach has been employed for single fit smoothing (quadratic and quartic).

3.3.3 Procedure for Evaluating $\sigma_{\dot{x}\,total}^w$

The total wind error (Equation 18) was evaluated for linear-linear, cubic-linear, and cubic-cubic smoothing with N (velocity smoothing interval) and M (acceleration smoothing interval) varying over a wide range of values to determine the optimum combination of degrees smoothing and smoothing interval that minimizes Equation 18. Linear-cubic smoothing was not considered for the following reason. Assuming position to be an kth degree polynomial, then velocity is an k-1st degree polynomial and acceleration k-2nd degree polynomial. Since acceleration is of one degree less than velocity, one does not anticipate that the degree smoothing on acceleration should exceed the degree smoothing on velocity, thus, linear-cubic is not considered.

This logic is not applicable for the case of smoothing for density. For that case, linear-cubic was considered because the problem there was to determine two degrees for double smoothing that would effectively cancel the bias error in density.

Figure 15 shows the steps in logic used in evaluating the total error equation for winds. The discussion will be restricted to the X coordinate only, However the same procedure holds for the Y and Z coordinates. Step 1 is to determine the radar noise σ_x, and the time spacing (Δt) for independent data points. These two quantities will permit the evaluation of the noise error formulas for linear and cubic smoothing and for any N and M. σ_x is most easily determined from dual tracked flights by calculating the standard deviation of the differences in the X position values from the two tracks. If, however, the flight being analyzed is tracked by only one FPS-16 radar, then theoretical radar position errors of perhaps a tenth of a mil in azimuth and elevation angles and 4.5 yards in slant range may be assumed, and these values can be converted to rectangular coordinate errors. The remaining steps of Figure 15 basically exhibit the logic and procedures required to evaluate the bias error components, Δx $\Delta \dot{x}$, for each type double smoothing. In order to evaluate the bias errors an assumption must

33

DOUBLE SMOOTHING

Position assumption for $N \leq N^*$ data points

$$X = A_0 + A_1 t + A_2 t^2 + A_3 t^3$$

Velocity Bias

Linear fit
$$\Delta \dot{x}_1 = \frac{A_3 \Delta t^2 (3N^2 - 7)}{20}$$

Cubic fit
$$\Delta \dot{x}_3 = 0$$

Position assumption Quintic for M data points where $2M + N - 2 \leqslant N$

$$\dot{X} = B_0 + B_1 t + B_2 t^2 + B_3 t^3 + B_4 t^4 \text{ (velocity)}$$

Acceleration Bias

Linear-linear fit
$$\Delta \ddot{x}_{11} = \ddot{x}_{33} - \ddot{x}_{11}$$

Cubic-linear fit
$$\Delta \ddot{x}_{31} = \frac{B_3 \Delta t_1^2 (3M^2 - 7)}{20}$$

Cubic-cubic fit
$$\Delta \ddot{x}_{33} = 0$$

SINGLE SMOOTHING

Position assumption for N data points

$$X = A_0 + A_1 + A_2 t^2 + A_3 t^3 + A_4 t^4$$

Velocity Bias

Quadratic fit
$$\Delta \dot{x}_2 = \frac{A_3 \Delta t^2 (3N^2 - 7)}{20}$$

Quartic fit
$$\Delta \dot{x}_4 = 0$$

Acceleration Bias

Quadratic fit
$$\Delta \ddot{x}_2 = A_4 \Delta t^2 \frac{(3N^2 - 13)}{7}$$

Quartic fit
$$\Delta \ddot{x}_4 = 0$$

Figure 14: Bias Error Formulas for Polynomial Smoothing

34

NOT REPRODUCIBLE
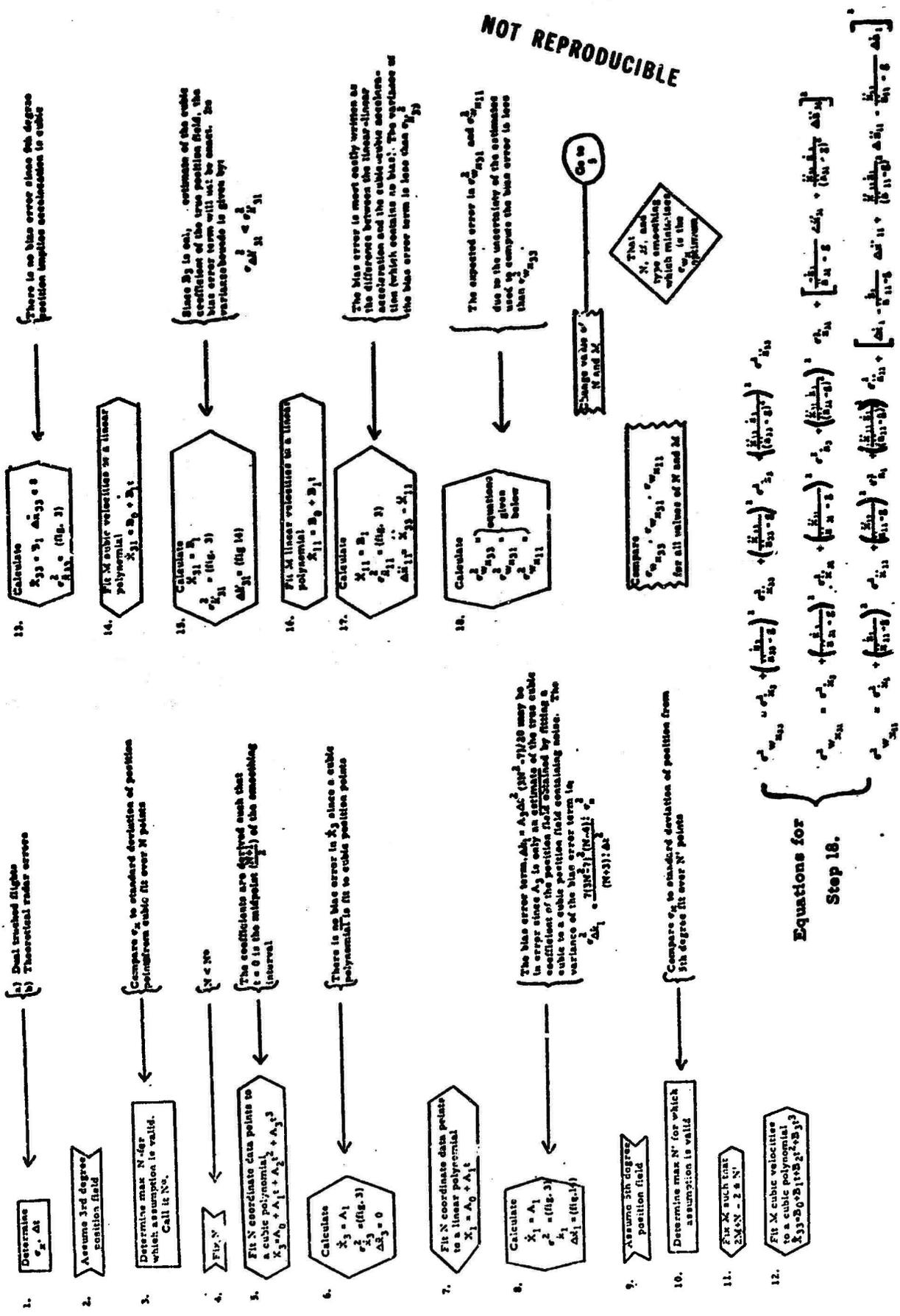
Figure 15: Schematic for Calculating Total Error in Winds

35

be made concerning the path of the sphere. Step two is to assume that the true position path of the sensor is a third degree polynomial. Step three is to determine the maximum number of points (N) for which this assumption is valid. This number can be determined by comparing the theoretical or dual track noise error (σ_x) to the standard deviation of the position data from the cubic fit over N data points. If the cubic assumption is valid for N data points, then the noise error should approximate the standard deviation of the position points from the cubic fit. N in turn is increased until the standard deviation of the position points from the cubic fit significantly exceeds σ_x. The smallest value of N for which the cubic assumption is found valid over all segments of the flight is called N*. Step four is to choose some N less than or equal to N* for an initial velocity smoothing interval. Step five is to fit a cubic polynomial to the N position data points. The coefficients of the cubic fit should be given with respect to t = o as the midpoint of the smoothing interval in order to utilize the bias error formulas of Figure 19. Thus, the velocity at the midpoint is the coefficient A_1 (step 6). Since the cubic polynomial was fit to assumed cubic position points, no bias error will result in the computed velocity A_1. The error in the cubic velocity due to radar noise (σ_{w_3}) is calculated by the noise error formulas in Figure 3.

The noise and bias errors are next calculated for linear velocity smoothing by steps 7 and 8. Step 7: A linear polynomial is fitted to the cubic position data points. In this case there is both a noise and a bias error associated with the linear velocity. Step 8: The noise error is computed from the linear noise error formula (Figure 3). The bias error is estimated from the formula

$$\Delta \dot{x}_1 = A_3 \Delta_t^2 (3N^2 - 7)/20 \qquad (\text{Figure 14}) \text{ where } A_3 \text{ is the estimate of the true cubic}$$

coefficient of the position field determined by fitting a cubic polynomial to the assumed cubic position data which is contaminated by radar noise. Due to the noise in the data, the A_3 used to calculate the bias error is not the true A_3 of the position field. Therefore there will be an error in the calculation of the bias error. However, the variance of the error will be less than the cubic noise error term (Comment Step 8). Consequently, even though the bias error calculated is only an estimate of the true bias error, bounds can be placed on the accuracy of the estimate. Furthermore, when an actual flight is analyzed and a large number of calculations of A_3 have been made the calculated values of A_3 will have as their mean the true A_3 so that the calculated bias error will be centered about the true bias error and a judgement can be made concerning its magnitude.

For the sake of acceleration error calculations, the position field is now assumed to be of degree 5. Step 10 is to determine the maximum number of points for which a fifth degree polynomial assumption holds. Call this number N'. N' is found by the same technique used to find N* (Refer to step 3). M, the number of data points used to compute acceleration, is now chosen so that 2M + N-2 is less than or equal to N' (Step 11). The number 2M + N-2 is the number of position points that influence an acceleration calculation when M points are used for acceleration calculations and N points for velocity. Position assumed quintic

over N' points implies velocity is quartic over N' points. Fitting quartic
velocity by a cubic polynomial will result in no bias error (the first derivative
of a cubic polynomial fit coincides with the first derivative of a quartic poly-
nomial fit when evaluated at the midpoint of the interval). Step 12: A cubic
polynomial is fitted to the velocity points obtained from the cubic fits of position.
No bias error is present   in this cubic-cubic acceleration (B_1) since the
velocity points fitted were free of bias (Step 13). The noise error for the cubic-
cubic acceleration is calculated from the noise error formulas. Next, acceleration
bias using cubic-linear smoothing is determined. Step 14: A linear polynomial
is fitted to the cubic velocity points (i. e. , velocities obtained by cubic fits to
position). The bias error for the cubic-linear acceleration is given by

$B_3 \Delta t_1^2 (3M^2-7)/20$, where B_3 is the estimate of the true cubic coefficient obtained
by fitting a cubic polynomial to noisy quartic velocity points and Δt_1 is the time
spacing between velocity points, (step 15). Analagous to the velocity case there
will be an error in the calculation of the bias error, since the calculated B_3 is
only an estimate of the true cubic coefficient. The bounds for the variance of
the bias estimate can be shown to be less than $\sigma^2_{x_{33}}$. The noise error for cubic-
linear acceleration is calculated from Figure 3. Step 16: A linear polynomial
is fitted to the velocities obtained by the linear fits of position data. The noise
error in this linear-linear acceleration is given by Figure 3. The most easily
accessible means of calculating the bias error for the linear-linear acceleration
is to difference the cubic-cubic acceleration from the linear-linear acceleration
(step 17). Since the cubic-cubic acceleration contains no bias, its difference
from the linear-linear acceleration will estimate the bias. The error variance
bounds of the estimate of the bias can be shown to be less than $\sigma^2_{x_{33}}$. Having
calculated the noise and bias errors for linear-linear, cubic-cubic, and cubic-
linear velocity and acceleration measurements, a substitution for these values
into Equation 18 yields the total wind error for each type double smoothing (step 18).
A comparison between the three total wind errors for the three types of smoothing
determines that type smoothing which produces the minimum total error for the
particular N and M chosen. By changing the values of N and M the procedure
can be repeated and further comparisons made. The optimum double smoothing
technique is that combination of degree polynomials (cubic-cubic, cubic-linear,
linear-linear) and smoothing intervals (N and M) that gives the minimum total
wind error. Plots of the total wind error for each type double smoothing, and
for N-M values of 51-35, 53-11, and 31-11 are presented as Figures 16-18. These
are merely three illustrations of some of the possible combinations. Figures 19-20
present the total wind error for quadratic and quartic single fit smoothing. The
total error plots for single fit smoothing are determined by a procedure similar
to that discussed for double smoothing. The noise and bias error formulas for
single fit smoothing are also given in Figures 3 and 14. After analyzing plots
of the types illustrated in Figures 16-20 for all feasible combinations of N and M,
it was determined that the 51-35 cubic-cubic provides optimum wind reduction.
With this type smoothing, the total wind error (which consists only of noise
error) remains less than 2 m/sec to 85 km and 10 m/sec to nearly 100 km. Even

37
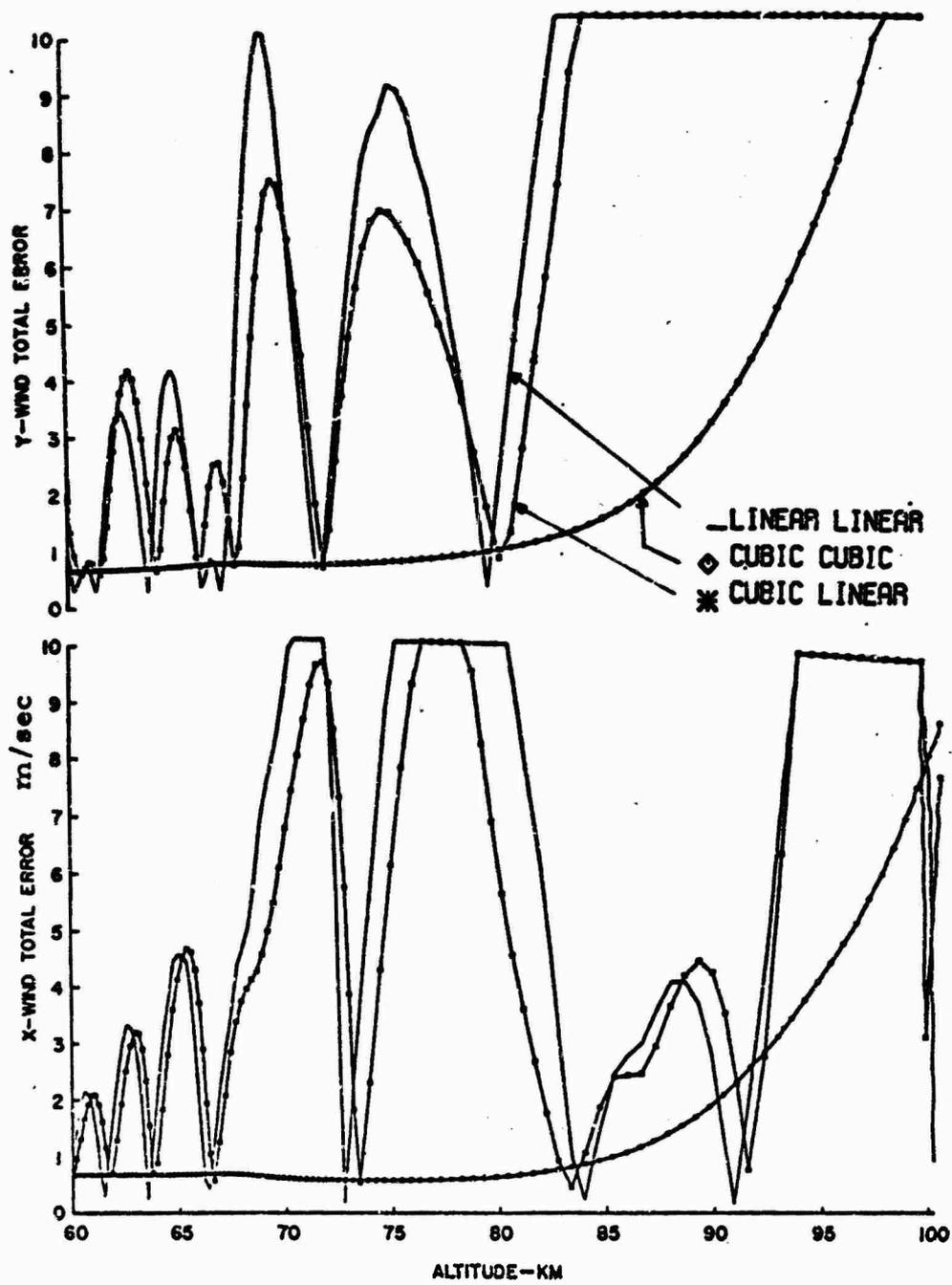
Figure 16: Total Error in X Wind and Y Wind for 51-35 Smoothing of Viper Dart 13
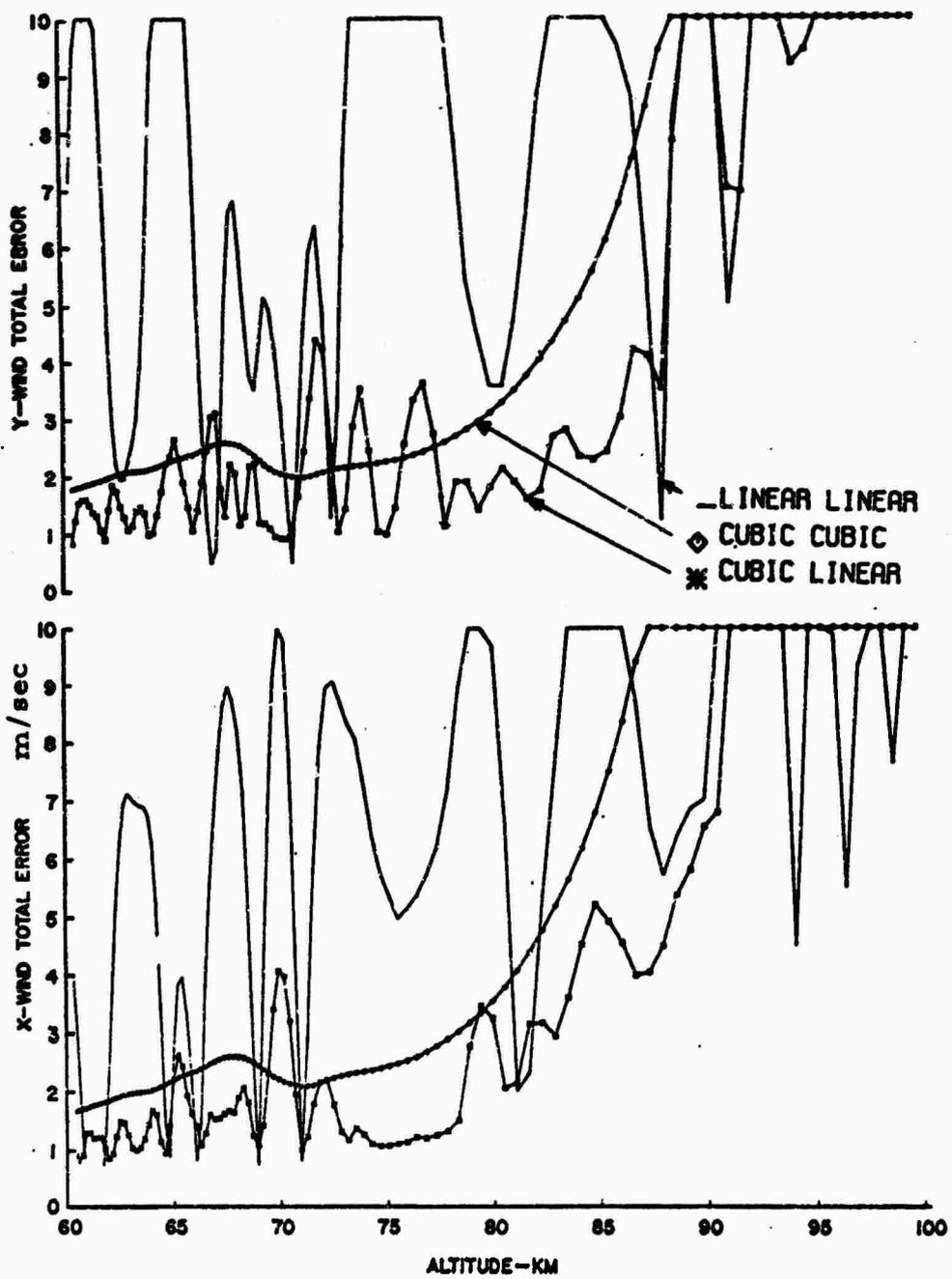
Figure 17: Total Error in X Wind and Y Wind for 53-11 Smoothing of Viper Dart 13

39
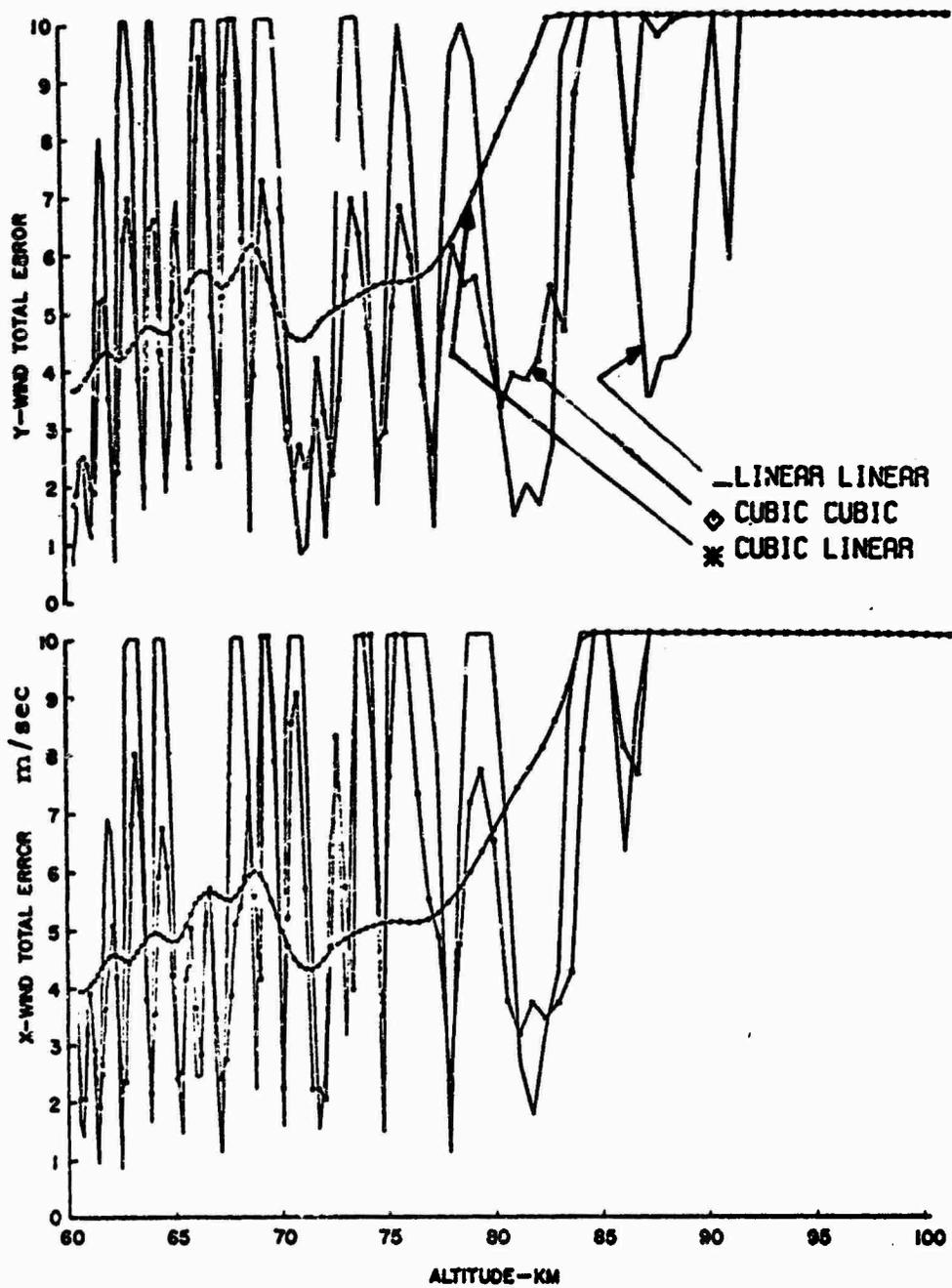
Figure 18: Total Error in X Wind and Y Wind for 31-11 Smoothing of Viper Dart 13

40
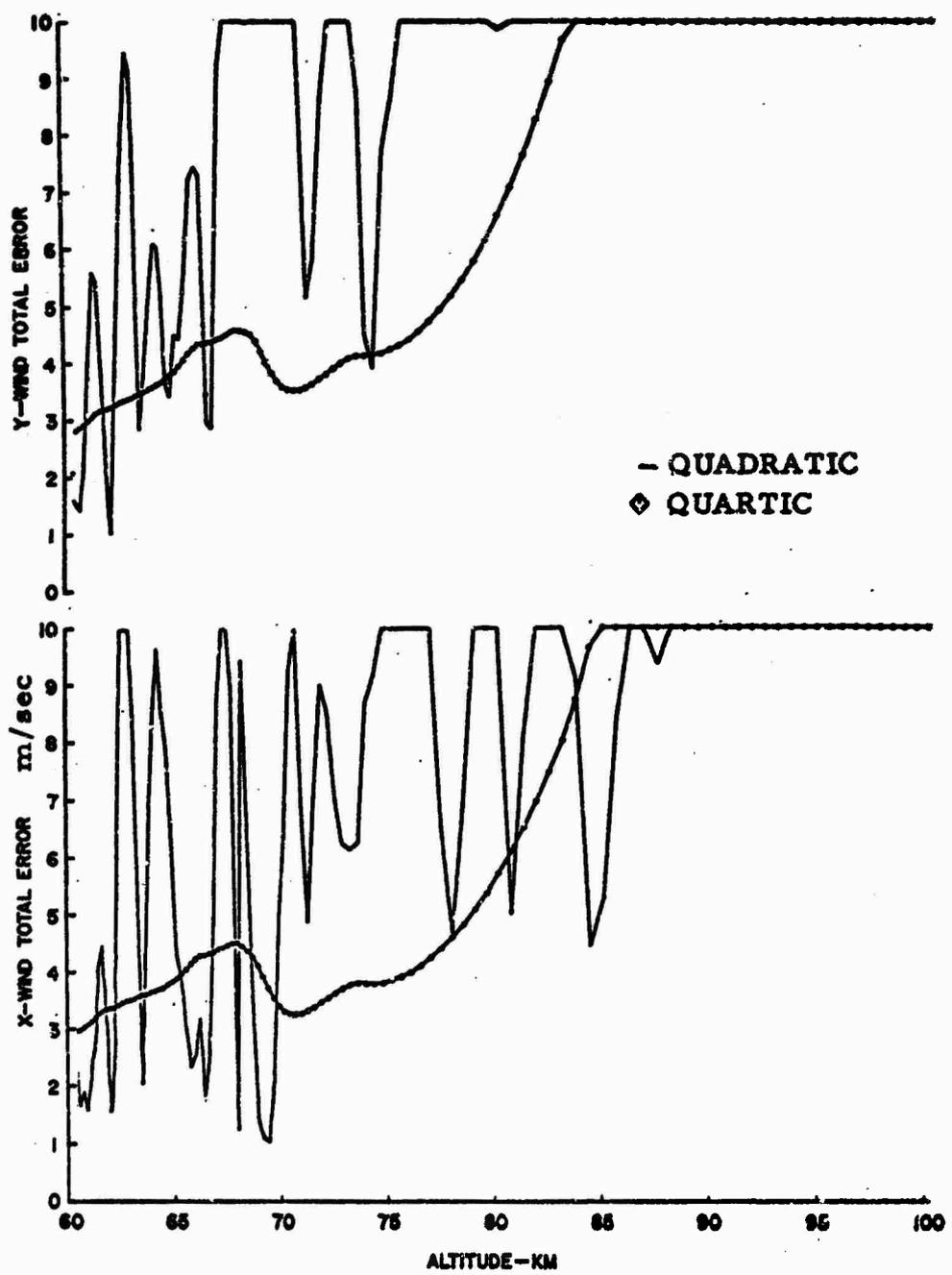
Figure 19: Total Error in X Wind and Y Wind for 31 Point Smoothing of Viper Dart 13

41
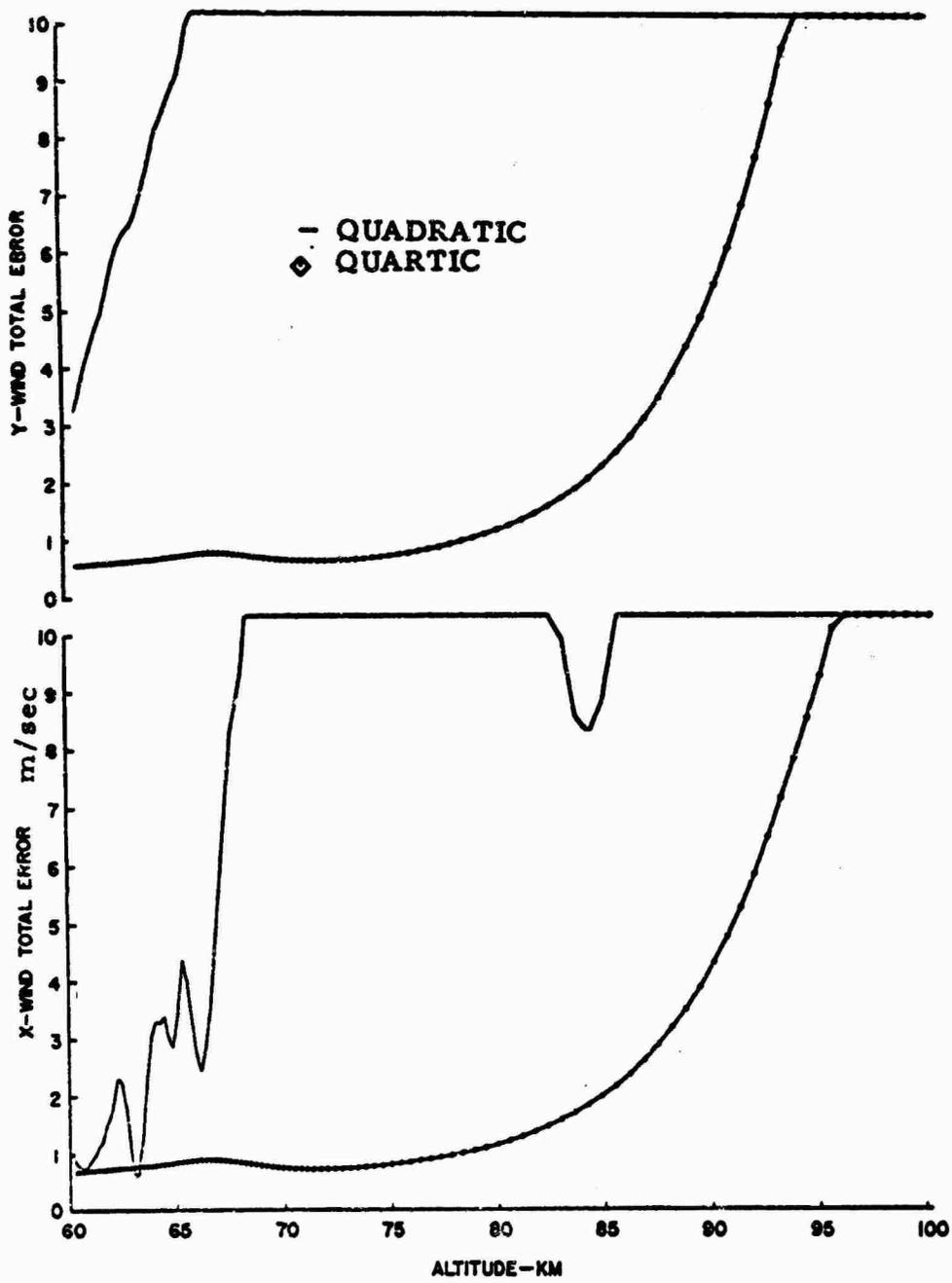
Figure 20: Total Error in X Wind and Y Wind for 99 Point Smoothing of Viper Dart 13

42

with optimum smoothing, the amount of detail that can be observed at the very high altitudes is limited because of the large altitude layer used in the smoothing. The frequency response curves (Figure 21) indicate the detail that can be observed. Plotted in the figure is the ratio of the amplitude of a sinusoidal wind after passing through the smoothing filter to the true amplitude of the original wind. Each curve gives the ratio versus wavelength at a specific altitude. For example, at 80 km the amplitude of a 10 km wave in the wind profile would appear in the reduced data to have 1/4 its actual amplitude. A 20 km wave would retain 65% of its amplitude in the reduced data. As seen from the figure, at altitudes in excess of 70 kilometers, wavelengths less than 10 km are largely destroyed, so that only a mean wind profile can be ascertained. Below 70 km, wavelengths of 5 km and less will appear in the reduced data.

3.4 Summary of Wind Errors Using Optimum Smoothing

The 51-35 cubic-cubic smoothing technique in X, Y, and Z was found to be the optimum for measuring wind between 70 and 100 km. Using this smoothing, winds can be measured to at least an accuracy of 2 m/sec to 85 km and 10 m/sec to 95 km. Above 70 km, however, fine details in the wind profile are lost so that only details with vertical structure in excess of 10 km are retained by the smoothing technique. Below 70 km, fine scale structure with vertical wavelengths of 2 to 5 km can be observed in the reduced data.

Steady State Wind Error (M/Sec)
Altitude (Km)

	100	95	90	85	80	75	70	65	60	55	50	40	30
Noise error in wind component	13	6	4	1	1	1	1	less than 1 m/sec					
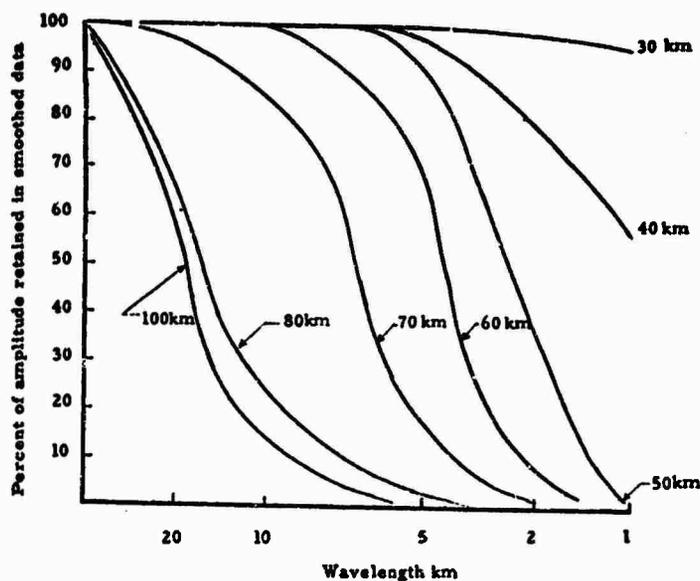
Figure 21: Steady State Wind Error and Frequency
Response for 51-35 Cubic-Cubic Smoothing

43

3.5 Wind Validity

It is interesting to observe that a collapsed sphere cannot accurately measure density but can accurately determine wind. The reason being the following: The equation used to compute density is indirectly proportional to the drag coefficient. When a sphere collapses its drag coefficient changes drastically. The drag coefficient tables available are for spheres only and, thus, cannot be used for density determination when a sphere loses its spherical shape. On the other hand, the simplified equation (not containing buoyancy and coriolis terms) used to compute wind does not depend upon the drag coefficient of the sphere and hence, can be evaluated even when the sphere is in a collapsed condition. A slight effect of sphere collapse on wind determination does occur, however, through the buoyancy term which requires a value for density. The insignificance of the buoyancy force above 30 km discards this as a possible source of wind error. Thus, wind accuracy can be maintained for a sphere in collapsed as well as inflated condition.

4. PRESSURE

The equation used for Pressure Computation is

$$P_i = P_{i-1} + \int_{Z_{i-1}}^{Z_i} \rho g \, dz \quad . \tag{19}$$

In order to use Equation 19, an initial pressure (P_o) is required. This pressure is computed from the gas law

$$P_o = T_o \, \rho_o \, \frac{R}{M_a}$$

where T_o is an estimate of the initial temperature generally taken from the 1962 Standard Atmosphere or a Supplemental Atmosphere, ρ_o is computed from the density equation (1) by using T_o to evaluate the initial Mach and Reynolds numbers, R is the universal gas constant and M is the molecular weight of air. The integration of Equation 19 is accomplished by the formula:

$$\int_{Z_{i-1}}^{Z_i} \rho g \, dz = g \text{ Antilog} \left(\frac{\text{Log} (\rho_i) - \text{Log} (\rho_{i-1})}{2} \right) (Z_i - Z_{i-1}) .$$

4.1 Pressure Error Equation

In order to simplify the derivation of the error equation for pressure, linear integration using the trapazoidal rule is assumed, i.e.,

$$\int_{Z_{i-1}}^{Z_i} \rho g \, dz = g \, \frac{(\rho_i + \rho_{i-1})}{2} (Z_i - Z_{i-1}).$$

44

Thus

$$P_i = P_{i-1} + \frac{g}{2} (\rho_i + \rho_{i-1}) (Z_i - Z_{i-1}).$$

The error in P_i in terms of density errors is

$$\epsilon_{P_i} = P_{i-1} + \epsilon_{P_{i-1}} + \frac{g}{2} (\rho_i + \epsilon_{\rho_i} + \rho_{i-1} + \epsilon_{\rho_{i-1}}) (Z_i - Z_{i-1}) - P_{i-1} - \frac{g}{2} (\rho_i + \rho_{i-1}) (Z_i - Z_{i-1})$$

or, by simplifying,

$$\epsilon_{F_i} = \epsilon_{P_o} + \frac{g}{2} \left[\epsilon_{\rho_o} (Z_1 - Z_o) + \sum_{n=1}^{i-1} \epsilon_{\rho_n} (Z_{n+1} - Z_{n-1}) + \epsilon_{\rho_i} (Z_i - Z_{i-1}) \right]. \quad (20)$$

Two sources of error are apparent in equation 20: a) the error in pressure due to the error in the initial computation of pressure (from the initial estimate of temperature) and b) the error in pressure due to the integration of density errors. Both noise and bias errors are present in density. These errors will effect pressure differently.

4.1.1 Pressure Errors Resulting from Error in Initial Pressure

As seen from Equation 20, the error in pressure at any point (P_i) of the flight due to the error in initial pressure is constant. The percent error in pressure due to the initial pressure error decreases as the flight progresses since

$$\frac{\epsilon_{P_o}}{P_i}$$

becomes very small after a few kilometers. For a 10% error in the initial estimate of temperature and a 73 km sphere apogee. Engler (Ref. 1) has shown that after 6 to 7 km of flight the resulting error in pressure has diminished to less than 1%. For a 125 km apogee, theoretical trajectories have been computed using initial temperatures of $T_o = T_{"62"}$, and $T_o = .9T_{"62"}$, and $T_o = 1.1T_{"62"}$ at 100 km. These results agree with Engler's and are presented in Table 8.

45

TABLE 8

Percent Error in Pressure
Resulting from a 10% Error in the Initial Temperature

ALTITUDE ~ KM

	100	95	90	85	80	75	70	65	60	55	50	45	35	30
$\frac{\Delta p}{p}$ (100)	6	1.4	.6	.1	LESS THAN 0.1%									

4.1.2 Pressure Errors Resulting from Noise Errors in Density

Assuming the errors in each density data point (ϵ_{ρ_i}) are independent with mean 0 and standard deviation σ_{ρ_i} the pressure error variance at a point P_i is given as

$$\sigma_{P_i}^2 = \frac{g^2}{4}\left[\sigma_{\rho_o}^2 (Z_i - Z_o)^2 + \sum_{n=1}^{i-1}\sigma_{\rho_n}^2 (Z_{n+1} - Z_{n-1})^2 + \sigma_{\rho_i}^2 (Z_i - Z_{i-1})^2\right]. \quad (21)$$

Equation 21 has been evaluated for the expected noise error profile in density for the expanding 19-21 linear-cubic smoothing. See Table 4 for pertinent values of $\frac{\sigma_\rho}{\rho}$ (100). The results are presented in terms of percent pressure error in Table 9.

TABLE 9

Percent Error in Pressure
Resulting from Noise Error in Density--125 Km Apogee

ALTITUDE ~ KM

	100	95	90	85	80	75	70	65	60	55	50	45	40	35	30
$\frac{\sigma_\rho}{\rho}$ (100)	8.0	3.5	1.5	1.0	0.7	0.8	1.5	2.0	2.0	2.0	2.0	2.0	2.0	2.0	2.0
$\frac{\sigma_P}{P}$ (100)	1.0	1.2	0.7	0.4	0.2	0.2	0.2	0.2	0.2	0.2	0.2	C.2	0.1	0.1	0.1

4.1.3 Pressure Errors Resulting from Bias Errors in Density

Bias errors arise in density because of bias introduced by the smoothing function (and perhaps bias errors in drag coefficient). For the expanding 19-21 linear-cubic smoothing the bias is given for 125 km apogee in Figure 5. Assuming this bias profile, the resulting pressure error at any point P_i can be evaluated as

46

$$\Delta P_i = \frac{g}{2}\left[\Delta \rho_0 \,(Z_i - Z_0) + \sum_{n=1}^{i-1} \Delta \rho_n \,(Z_{n+1} - Z_{n-1}) + \Delta \rho_i \,(Z_i - Z_{i-1}) \right]. \tag{22}$$

where $\Delta \rho_i$ is the signed ($\pm$) bias in density at the ith point. The percent error in pressure $\dfrac{\Delta P_i}{P_i}$ resulting from the evaluation of Equation 22 is presented in Table 10. See Table 4 for pertinent values of $\dfrac{\Delta \rho}{\rho}$ (100).

TABLE 10

Percent Error in Pressure
Resulting from Bias Error in Density--125 Km Apogee

	ALTITUDE ~ KM														
	100	95	90	85	80	75	70	65	60	55	50	45	40	35	30
$\frac{\Delta \rho}{\rho}$ (100)	+2.0	+3.5	+4.0	+3.0	-1.5	-1.0	-1.0	0	0	0	0	0	0	0	0
$\frac{\Delta P}{P}$ (100)	+2.0	+2.4	+2.3	+3.1	+1.5	-0.2	-0.4	-0.2	-0.1	-0.1	0	0	0	0	0

4.1.4 Constant Percent Bias in Density

It is interesting to observe the effect that a constant percent bias in density has on pressure accuracy. Assume $\dfrac{\Delta \rho_i}{\rho_i} = K$ a constant. Then from Equation 19

$$\Delta P_i = \frac{T_0 R}{M_a}\, \rho_0 \left(1 + \frac{\Delta \rho_0}{\rho_0}\right) + g \int_{Z_0}^{Z_i} \left(1 + \frac{\Delta \rho}{\rho}\right) dz - \frac{T_0 R}{M_a} \rho_0 - g \int_{Z_0}^{Z_i} \rho \, dz$$

$$= K \left(P_0 + g \int_{Z_0}^{Z_i} \rho \, dz \right) = K P_i \tag{23}$$

thus

$$\frac{\Delta P_i}{P_i} = K.$$

Hence a constant percent bias in density (or for that matter in drag coefficient) produces the same percent bias in pressure.

4.2 Summary of Pressure Errors

Pressure errors result from the error in the initial estimate of temperature, past and present noise errors in density, and past and present bias errors in density. Figure 22 shows the estimated magnitude of the resulting pressure errors for a 125 km apogee using the expanding 19-21 lin-cub smoothing on density. A 10% error in the initial estimate of temperature is shown to diminish to less

47

than a 1% error in pressure after 7 km of flight. The pressure error from the noise in density is less than 2% above 90 km and less than 1% below 90 km. The pressure bias introduced by the smoothing induced bias in density is 2-3% above 82 km and decreases to less than 1% below 78 km. A constant percent bias in density produces the same constant percent bias in pressure
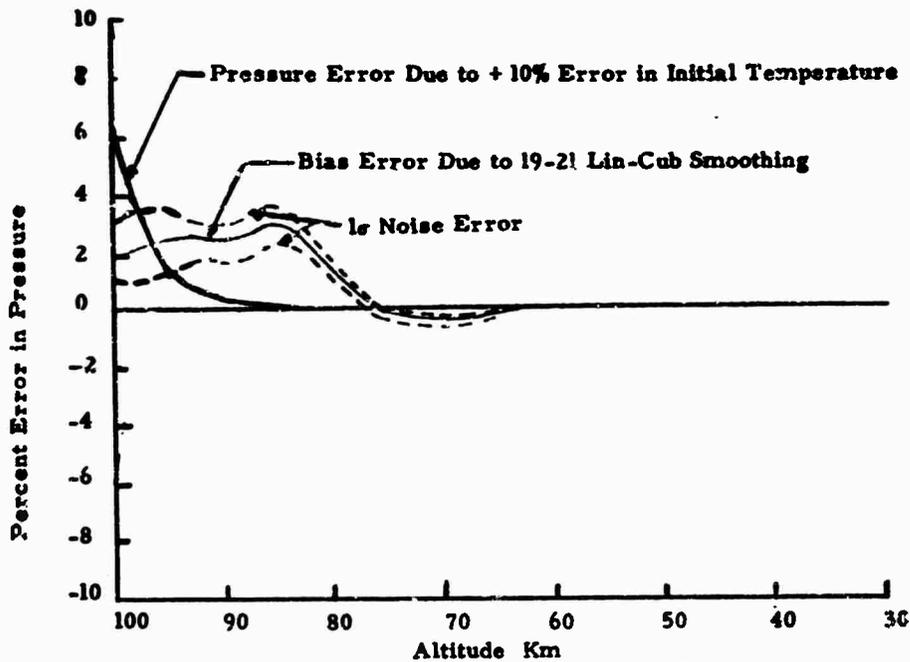
Figure 22: Pressure Errors for Sphere with 125 Km Apogee

5.   TEMPERATURE

Temperature is computed from the pressure and density using the gas law. Temperature errors result from errors in density and pressure. In addition, above 90 km temperature errors may also result from a change in the molecular weight of air.

5.1   Temperature Error Equation

The temperature increment resulting from error increments in pressure and density is approximated by

$$dT = \frac{\partial T}{\partial P} \; dP + \frac{\partial T}{\partial \rho} \; d\rho \qquad (24)$$

or

$$\frac{dT}{T} = \frac{dP}{P} - \frac{d\rho}{\rho}$$

48

The effect of density and pressure errors on temperature depends upon the type of errors in density and pressure. Noise and bias errors occur in density. The effect of each of these type errors on pressure accuracy has been described in section 4. By combining each type density error with the resultant error it produces in pressure, and substituting into Equation 24, a temperature error profile is generated. In addition to density errors that produce pressure errors, the error in the initial temperature also results in pressure and temperature errors.

5.1.1 Temperature Errors Resulting from Error in the Initial Pressure

The error in the initial estimate of temperature produces a pressure error and also a density error since the Mach and Reynolds number and thus C_D depend on temperature. The combined effect of this pressure and density error is given in Table 11.

TABLE 11

Percent Error in Temperature
Resulting from a +10% Error in the Initial Temperature

ALTITUDE ~KM

		100	95	90	85	<85	
$\frac{\Delta p}{P}$ (100)		6.0	1.4	.6	.1	Less than 0.1%	From Table 8
$\frac{\Delta \rho}{\rho}$ (100)		-4.0	-.8	-.3	-.1	Less than 0.1%	From Table 2
$\frac{\Delta T}{T}$ (100)		10.0	2.2	.9	.2	Less than 0.2%	

5.1.2 Temperature Errors Resulting from Noise Errors in Density

Assuming the ith pressure and ith density errors to be independent, (which is not completely correct but they are essentially independent since the ith pressure error, after a few data points, depends primarily on the previous density errors and only to a small degree on the ith density error), the percent error variance in temperature is

$$\left(\frac{\sigma_T}{T} \right)^2 = \left(\frac{\sigma_P}{P} \right)^2 + \left(\frac{\sigma_\rho}{\rho} \right)^2 . \qquad (25)$$

The evaluation of Equation 25 using the noise error density profile for the 19-21 smoothing and the pressure error profile it produces is presented as Table 12 for a sphere apogee of 125 Km.

49

TABLE 12

Percent Error in Temperature
Resulting from Noise Errors in Density and Pressure--125 Km Apogee

ALTITUDE ~ KM

	100	95	90	85	80	75	70	65	60	55	50	45	40	35	30	
$\frac{\sigma p}{p}$ (100)	8.0	3.5	1.5	1.0	0.7	6.8	1.5	2.0	2.0	2.0	2.0	2.0	2.0	2.0	2.0	From Table 4
$\frac{\sigma_{\rho}}{\rho}$ (100)	1.9	1.2	0.8	0.4	0.1	0.2	0.2	0.2	0.2	0.2	0.2	0.2	0.1	5.1	0.1	From Table 9
$\frac{\sigma T}{T}$ (100)	8.1	3.7	1.7	1.1	0.7	0.8	1.5	2.0	2.0	2.0	2.0	2.0	2.0	2.0	2.0	

5.1.3 Temperature Errors Resulting from Bias Errors in Density

The bias errors in density introduced by the 19-21 smoothing and the resulting pressure errors are given in Table 10. A substitution of these values into Equation 24 yields the resulting bias in temperature. (See Table 13).

TABLE 13

Percent Error in Temperature
Resulting from Bias Errors in Density and Pressure--125 Km Apogee

ALTITUDE ~ KM

	100	95	90	85	80	75	70	65	60	55	50	45	40	35	30	
$\frac{\Delta \rho}{\rho}$ (100)	+2.0	+3.5	+4.0	+3.0	-1.5	-1.0	-1.0	0	0	0	0	0	0	0	0	From Table 10
$\frac{\Delta p}{p}$ (100)	+2.0	+2.4	+2.3	+3.1	+1.5	-0.2	-0.4	-0.2	-0.1	-0.1	0	0	0	0	0	
$\frac{\Delta T}{T}$ (100)	+0.0	-1.1	-1.7	+0.1	3.0	+0.8	+0.6	-0.2	-0.1	-0.1	0	0	0	0	0	

5.1.4 Constant Percent Bias in Density

It was shown in section 4 that a constant percent bias in density yielded the same percent bias in pressure. Hence, from Equation 24 it follows directly that no temperature error is introduced by a constant percent error in density.

5.2 Summary of Temperature Errors

Temperature errors are the result of errors in density and pressure and, above 90 km, may also be the result of a change in the molecular weight of air. Figure 23 shows the estimated temperature errors resulting from density and pressure errors for a sphere with apogee 125 km. A 10% error in the initial estimate of temperature is shown to diminish to less than a 1% error in temperature after 10 km of flight. The noise error in temperature resulting from the noise in density is a maximum of 3.7% at 95 km (approximately 8 deg), decreasing to less than 2% (approximately 4 deg) by 90 km and remaining at 2% or less

for the remainder of the flight. The temperature bias produced by the 19-21 smoothing varies between ± 2% (approximately 4 deg) from 100 to 75 km and is less than 1/2% (approximately 1 deg) below 75 km. A constant percent bias in density produces no error in temperature.
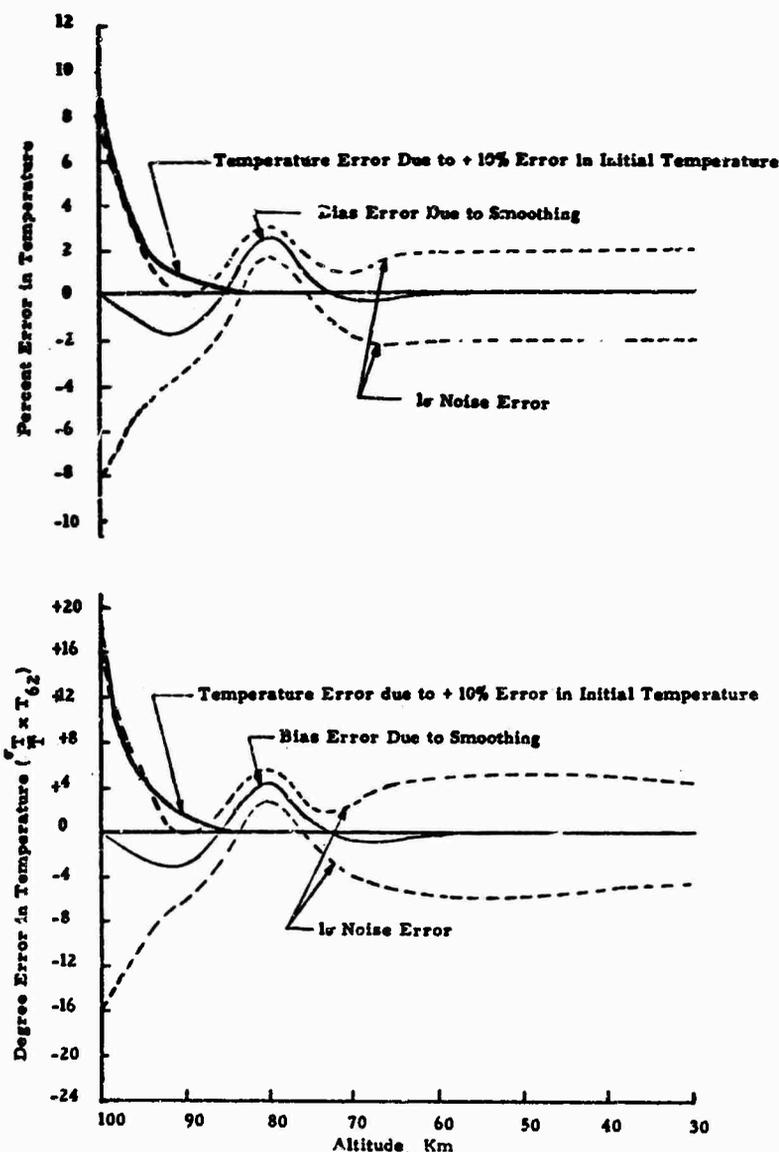
Figure 23: Temperature Errors for sphere with 125 Km apogee.

6. DESCRIPTION OF HIGH ALTITUDE ROBIN PROGRAM

This section summarizes the mechanics of the computer program, wirtten to implement the techniques derived in sections 2-5. The program title is, "May, 1970 AFCRL High Altitude ROBIN Program." A users manual (Ref. 12) which describes the program and describes how to interpret the output data is available through the Vertical Sounding Techniques Branch (CRER) of the Air Force Cambridge Research Laboratories. The basic flow of the program, order of computation, iteration procedures, etc., are akin to those explained in Reference 1.

6.1   Editing

Input to the ROBIN Program is time and X, Y, Z position coordinates
which have been obtained by a transformation of the radar observed slant range,
elevation angle and azimuth angle. Prior to performing any computation on the
position coordinates an editing procedure is inaugurated to remove any spurious
data that may have resulted from a radar malfunction. The editing begins when
the ascent part of the rocket trajectory exceeds 150,000 ft. The procedure
consists of comparing the first difference between consecutive position coordinates
with a pre-established tolerance. If the difference exceeds the tolerance, the
second of the two points is considered bad. The succeeding point (third point)
is then differenced from the first point and compared to twice the tolerance.
If the third point is accepted, a linear interpolation between the first and third
points replaces the bad second point. If the third point fails the tolerance, the
procedure is repeated using the fourth, fifth, etc. data point until either
another good point is found or 20 consecutive bad points (2 seconds of data) have
been determined. If 20 consecutive bad points are found, or alternately, if
2 seconds of missing data is found the program is restarted. The tolerance
used for the X and Y components is 150 ft. This implies that the maximum
allowable velocity obtained by finite difference between two consecutive 0.1
second data points is 1500 ft/sec. Since vertical velocities often exceed 2500
ft/sec at high altitudes, two tolerances are used for testing the Z coordinate.
The Z tolerance below 200,000 ft is 200 ft, and above 200,000 ft is 360 ft.

The editing procedure, though not overly sophisticated, performs very
capably with typical ROBIN flights. Experience has shown that the radar track
requires considerable editing on the upleg section of the rocket trajectory, and
again at the very low altitudes, below 30 km, of the balloon trajectory. The
usable segment of data, between 30 km and 125 km, for computing meteorological
parameters requires minimal, and sometimes no editing.

6.2   Smoothing

The program is designed to accept FPS-16 Radar Data at 0.1 second
increments after it has been transformed to rectangular (X, Y, Z) coordinates.
The program averages 5 of the 0.1 second data points to arrive at 1/2 second
data points which are statistically independent. These 1/2 second spaced
rectangular position coordinates become the input data for the smoothing
procedure.

6.2.1   Density

Above 60 km the vertical velocity and acceleration required for input
to the density equation is computed by 19-21 linear cubic smoothing. That is
19 vertical position coordinates (1/2 second spaced) are fitted by a linear poly-
nomial and the slope taken as the vertical velocity. A slide of two data points
after each fit results in a series of velocities spaced one second apart in time.
21 of these velocities are fitted by a cubic polynomial and the derivative at the

52

midpoint of the interval taken as the acceleration. A slide of one velocity point after each fit of velocity results in acceleration time spacing of one second. The horizontal velocities and accelerations required for the density equation are computed by 51-35 cubic-cubic smoothing. Below 60 km the velocity smoothing interval is expanded in such a way so as to maintain an approximate 2% error in density. This is accomplished by expanding the smoothing interval by 4 points each 50 seconds. That is, at time 60 km + 50 seconds, 23-21 lin-cub smoothing is initiated ; at time 60 km + 100 seconds, 27-21 smoothing, etc., until 51-21 smoothing is reached. At this point (approximately 35 km) the 51-21 linear-cubic smoothing is retained for the remainder of the flight.

6.2.2 Winds

All three rectangular coordinates, vertical as well as horizontal, used in the wind equation are computed by 51-35 cubic-cubic smoothing.

6.3 Calculation of Meteorological Parameters

The derivation of the equations used to calculate wind, density, temperature, and pressure using the passive sphere technique is well substantiated in Reference 1. All forces acting upon the sphere are included in the equation with the exception of the forces acting upon the apparent mass of the sphere. It can easily be shown that the apparent mass of the sphere can be neglected without affecting measurement accuracy. A flow diagram of the procedures used to calculate the meteorological parameters as excerpted from Reference 1 is given in Figure 24.
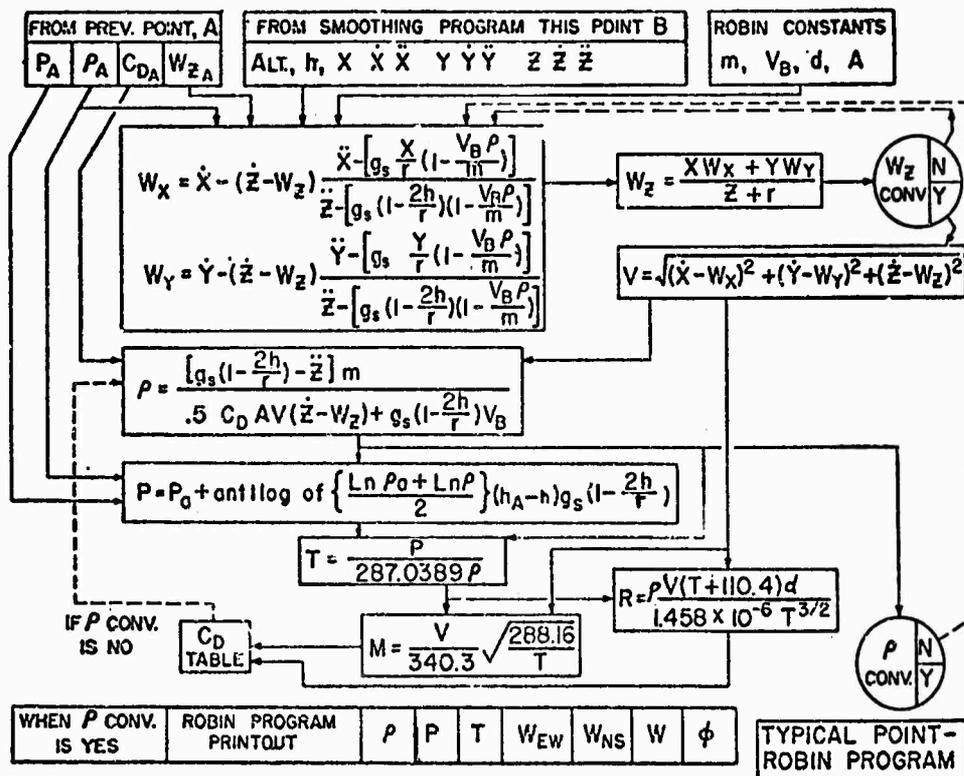
Figure 24: Procedural Diagram for Calculation of Meteorological Parameters

53

6.4   Determination of Density Validity

The validity of density data is determined by two checks: the time of fall check and the density gradient check (λ check).

6.4.1   Time of Fall Check

The time of fall check is the primary test for sphere collapse. It is used between 80 km and 30 km. To use the time of fall test above 55 km sphere apogee must be first calculated. Having determined the sphere apogee, the actual time of fall of the sphere between 80 and 70 km, between 70 and 60 km, 60 and 55 km, etc., is compared with that expected for a sphere falling from the determined apogee, through an atmosphere of 0.8 $\rho_{"62"}$ and 1.2 $\rho_{"62"}$.

If the actual time of fall is not within the range of that expected, sphere collapse is indicated. The printout reads "time of fall test between xx and xx km indicates sphere collapse."

6.4.2   Density Gradient Check (λ check)

The density gradient check is used below 60 km and overlaps the time of fall test between 60 and 30 km. It is the secondary sphere collapse check. The density gradient $\left(\frac{1}{\rho} \frac{d\rho}{dz} \right)$ is estimated below 60 km by calculating λ as defined by Equation 8. If λ does not fall within the range of

$$.00014 - \sqrt{(.00005)^2 + \left(\frac{.08484}{\Delta z} \right)^2} \leq \lambda \leq .00014 + \sqrt{(.00005)^2 + \left(\frac{.08484}{\Delta z} \right)^2}$$

sphere collapse is indicated and the printout reads "density gradient exceeds nominal value." It is possible that a large vertical wind may at times, trip the λ check. Thus, the λ check should be interpreted in conjunction with the time of fall test.

6.5   Measurement Accuracy

Included in the calculation of each parameter (density, wind, temperature, and pressure) is a calculation of the estimated noise error in each parameter. The estimate is made using the formulas: Density noise error terms of Equation 6; Winds, Equation 16; Pressure, Equation 21; Temperature, Equation 25. The position error is determined by assuming r.m.s. errors of 0.1 mil in azimuth and elevation and 4.5 yards in slant range. The other types error present (bias, C_D error, etc.) are not included in the computer printout. For the magnitude of these errors "the reader" is referred to Figures 5, 16, and 23, and Table 1.

54

A frequency response table for density and wind is printed for various escape altitudes at the end of the program (Figure 25). This serves as a means of determining the amount of detail observable in the wind and density output.

6.6 Program Options and Output

The program contains options for the type of output desired by the user. Option 1: the program allows for the output to be printed in either of two forms; a) data can be printed at constant time increments of one second, or b) the data can be printed to include constant altitude of 200 meters. The constant altitude printout is determined by linear interpolation of the constant time data. Figures 26 and 27 show a sample of each type output. Option 2: the program allows for a plot of the output data on a Cal-comp plotter. The temperature, density ratio, pressure ratio, and wind components can be plotted as a function of altitude. Figure 28 shows the output data that serves as the input to the plotting program. Sample plots from the Cal-comp plotter can be observed in Figures 29, 30, 32, 33, 34, 35, 39, and 40.

7 OPTIMUM WIND AND DENSITY REDUCTION OF THREE OPERATIONAL FLIGHTS

A series of three Viper Dart flights were launched at Eglin Air Force Base on 18 February 1968 at 18:00, 19:00 and 20:00 zulu. Each flight was tracked by two FPS-16 radars. The flights are identified as Viper Dart 11, 12 and 13 and the radars as radar 23 and radar 27. The flights were reduced using the May 1970 High Altitude ROBIN Program.

7.1 Density Accuracy

Figures 29 and 30 show the density ratio ($\dfrac{\rho}{\rho_{"62"}}$) for each track of each flight. For each of the flights, there is excellent agreement between radar 23 and radar 27. Figure 31 shows the percent noise error in density obtained from the printout of the computer program*. If the 1σ error estimate is valid, approximately 2/3 of the actual errors (density differences from two radar tracks should be within the 1σ estimate. Figure 31 appears to substantiate this contention, especially below 95 km. It is interesting, however to observe the variation in density between flights one hour apart in time, particularly in the 62-54 km region. The cause of these differences is not known. Possible causes are:

a) An actual fluctuation in density between the launch times of the flights.

---

* The bias errors and the error due to the initial guess of temperature are essentially the same in both radar tracks. As a result,differencing densities, pressures, temperatures or winds does not determine the magnitude of these errors.

RATIC CF APPLITUCE OF SMCCTMED LENSITY LAVE TC APPLITLCE OF CRIGINAL
WAVE AS A FUNCTION CF ALTITLDE AND WAVELENGTH.
(ALTITLDE AND WAVELENGTH PEASLMEC IN KILCPETERS.)

ALTITLDE

```
       X 100  X  90  X  80  X  70  X  60  P  50  X  40  X  30  X
       XXXXXXXXXXXXXXXXXXXXXXXXXXXXXXXXXXXXXXXXXXXXXXXXXXXXXXXXXXXXX
 M     X       X       X       X       X       X       X       X       X
 A   1 X 0.01 X 0.01 X 0.01 X 0.01 X 0.01 X 0.22 X 0.42 X 0.75 X
 V     X       X       X       X       X       X       X       X       X
 E   2 X 0.01 X 0.01 X 0.01 X 0.04 X 0.22 X 0.52 X 0.80 X 0.90 X
 L     X       X       X       X       X       X       X       X       X
 E   5 X 0.01 X 0.02 X 0.03 X 0.47 X 0.84 X 0.90 X 0.96 X 0.99 X
 N     X       X       X       X       X       X       X       X       X
 G  10 X 0.47 X 0.51 X 0.55 X 0.72 X 0.97 X 0.58 X 0.59 X 0.99 X
 T     X       X       X       X       X       X       X       X       X
 H  20 X 0.54 X 0.95 X 0.56 X 0.58 X 0.55 X 0.59 X 0.59 X 0.99 X
```

NOT REPRODUCIBLE

RATIC CF AMPLITLDE OF SPUCTMEC SIALSCICAL WIAC TC APPLITLCE OF
CRIGINAL WINC AS A FUNCTION CF ALTITLCE ANC WAVELENGTH.
(ALTITLCE ANC WAVELENGTH PEASLREG IN KILCPETERS.)

ALTITLDE

```
       X 100  X  90  X  80  X  70  X  60  X  50  X  40  X  30  X
       XXXXXXXXXXXXXXXXXXXXXXXXXXXXXXXXXXXXXXXXXXXXXXXXXXXXXXXXXXXXX
 M     X       X       X       X       X       X       X       X       X
 A   1 X 0.01 X 0.01 X 0.01 X 0.01 X 0.01 X 0.02 X 0.57 X 0.96 X
 V     X       X       X       X       X       X       X       X       X
 E   2 X 0.01 X 0.01 X 0.01 X 0.03 X 0.10 X 0.40 X 0.76 X 0.99 X
 L     X       X       X       X       X       X       X       X       X
 E   5 X 0.02 X 0.03 X 0.06 X 0.12 X 0.70 X 0.58 X 0.55 X 0.99 X
 N     X       X       X       X       X       X       X       X       X
 G  10 X 0.1  X 0.17 X 0.24 X 0.85 X 0.97 X 0.59 X 0.99 X 0.99 X
 T     X       X       X       X       X       X       X       X       X
 H  20 X 0.56 X 0.63 X 0.66 X 0.50 X 0.92 X 0.59 X 0.55 X 0.99 X
```

Figure 25: Program Output - Frequency Response of Density and Wind

PATRICK VE-02C3

	XV-VEL	XV-ACC	Z-VEL	Z-ACC
# PTS. FIT	51	35	19 *	21
DEGREE FIT	3	3	3	3

ID LAIT	ALT	GS	RG	PWSL	ZB	AMS DIA	INT
0 8 6	28.25	-9.780373	6312898.7	0.	0.	0.1177	1.00000 0

TIME ZLLL	ALT METERS	EWINE P/S	NWINC N/S	SPEEC KNOTS	DIR CEG	PRESS MB	T K	DENSITY GR/M3	Z VEL M/S	Z ACC P/S2	MACH	REYNL	CC	DENS 0C000	PRES PERCENT	TEMP C0000	EW M/S	NW N/S
12.49.20	124158								-316.19	-9.29								
12.49.21	123862								-325.46	-9.29								
12.49.22	123556								-334.72	-9.29								
12.49.23	123219								-343.60	-9.29								
12.49.24	122874								-353.26	-9.30								

PALLCCA AFOGEE = 129 KM.

TIME	ALT								Z VEL	Z ACC								
12.49.25	122520								-362.64	-9.29								
12.49.26	122155								-371.91	-9.28								
12.49.27	121784								-381.21	-9.28								
12.49.28	121404								-390.47	-9.28								
12.49.29	121012								-399.66	-9.28								
12.49.30	120637								-408.95	-9.28								
12.49.31	120200								-418.40	-9.28								
12.49.32	119782								-427.53	-9.27								
12.49.33	119354								-436.85	-9.26								
12.49.34	118917								-445.59	-9.27								
12.49.35	118467								-455.32	-9.27								
12.49.36	118013								-464.63	-9.26								
12.49.37	117545								-473.95	-9.27								
12.49.38	117073								-483.21	-9.27								
12.49.39	116591								-492.33	-9.26								
12.49.40	116096								-501.69	-9.26								
12.49.41	115593								-510.56	-9.25								
12.49.42	115081								-520.24	-9.23								
12.49.43	114562								-529.48	-9.20								
12.49.44	114031								-538.65	-9.18								
12.49.45	113450								-547.77	-9.16								
12.49.46	112944								-556.54	-9.14								
12.49.47	112385								-566.07	-9.12								
12.49.48	111819								-575.18	-9.11								
12.49.49	111244								-584.21	-9.11								
12.49.50	110659								-593.38	-9.10								
12.49.51	110066								-602.28	-9.10								
12.49.52	109462								-611.47	-9.10								
12.49.53	108850								-620.51	-9.08								
12.49.54	108229								-629.69	-9.05								
12.49.55	107601								-638.70	-9.00								
12.49.56	106961								-647.85	-8.95								
12.49.57	106313								-656.72	-8.88								
12.49.58	105654								-665.54	-8.80								
12.49.59	104990								-674.20	-8.70								
12.50.-0	104311								-682.68	-8.57								
12.50. 1	103633								-691.29	-8.44								
12.50. 2	102940								-699.54	-8.31								
12.50. 3	102244								-707.86	-8.15								
12.50. 4	101532	47.35	-91.84	200.71	332	0.0002	217	0.0004	-715.90	-7.92	2.55	19	2.266	5.7	0.3	5.7	12.9	11.0
12.50. 5	100814	53.66	-53.41	192.66	327	0.0003	202	0.0004	-723.52	-7.69	2.66	25	2.127	5.1	0.7	5.1	11.6	10.0
12.50. 6	100094	59.33	-74.05	164.33	321	0.0003	191	0.0005	-731.45	-7.45	2.75	31	2.002	4.6	0.8	4.6	10.5	9.2
12.50. 7	99360	64.59	-63.08	175.93	314	0.0003	189	0.0006	-738.66	-7.19	2.79	37	1.937	4.1	0.9	4.2	9.5	8.4
12.50. 8	98621	70.40	-50.82	168.66	305	0.0004	188	0.0007	-745.63	-6.90	2.82	43	1.879	3.7	1.0	3.8	8.6	7.7
12.50. 9	97877	75.29	-37.95	163.78	296	0.0004	187	0.0009	-752.40	-6.56	2.85	50	1.829	3.3	1.0	3.5	7.8	7.1
12.50.10	97126	78.92	-24.56	160.56	287	0.0005	188	0.0009	-759.05	-6.17	2.87	56	1.800	3.0	0.9	3.1	7.1	6.4
12.50.11	96366	80.57	-11.32	159.81	277	0.0006	190	0.0010	-764.85	-5.75	2.88	64	1.771	2.7	0.9	2.8	6.4	5.9
12.50.12	95602	80.42	1.25	156.23	269	0.0006	193	0.0012	-769.37	-5.30	2.88	72	1.741	2.4	0.9	2.6	5.7	5.3
12.50.13	94831	77.08	12.25	151.61	260	0.0007	192	0.0013	-774.49	-4.75	2.91	83	1.700	2.2	0.8	2.3	5.0	4.7
12.50.14	94057	72.09	20.91	145.90	253	0.0008	192	0.0015	-780.14	-4.11	2.94	96	1.653	1.9	0.8	2.1	4.5	4.2
12.50.15	93277	65.39	27.09	137.49	247	0.0010	193	0.0017	-783.55	-3.44	2.95	110	1.620	1.7	0.7	1.9	3.9	3.7
12.50.16	92503	57.19	30.72	126.06	241	0.0011	195	0.0019	-786.91	-2.72	2.96	124	1.592	1.6	0.6	1.7	3.4	3.3
12.50.17	91726	48.13	32.39	112.70	236	0.0012	197	0.0022	-788.92	-1.95	2.95	138	1.564	1.4	0.6	1.5	3.0	2.9
12.50.18	90900	38.57	32.03	97.38	230	0.0014	200	0.0025	-790.05	-1.09	2.94	155	1.533	1.3	0.6	1.4	2.6	2.5
12.50.19	90129	29.26	30.20	81.68	224	0.0016	198	0.0028	-790.56	-0.11	2.96	179	1.499	1.2	0.5	1.3	2.3	2.2
12.50.20	89351	20.53	27.24	66.26	217	0.0018	194	0.0033	-790.22	1.06	3.00	214	1.434	1.1	0.5	1.2	2.0	2.0
12.50.21	88561	12.40	23.45	51.58	207	0.0021	187	0.0039	-788.02	2.46	3.05	262	1.376	0.9	0.4	1.0	1.8	1.7
12.50.22	87775	5.02	19.21	38.57	194	0.0024	177	0.0049	-783.65	4.15	3.11	331	1.307	0.8	0.4	0.9	1.6	1.6
12.50.23	86995	-1.39	14.73	28.83	174	0.0028	171	0.0058	-780.29	6.09	3.16	411	1.251	0.8	0.4	0.8	1.4	1.4
12.50.24	86214	-6.82	10.21	23.85	146	0.0033	165	0.0069	-774.55	8.28	3.18	503	1.203	0.7	0.3	0.8	1.3	1.3
12.50.25	85445	-1.47	3.69	24.56	116	0.0039	161	0.0083	-766.46	10.73	3.19	617	1.162	0.6	0.3	0.7	1.2	1.2
12.50.26	84691	-15.32	1.48	29.89	95	0.0045	157	0.0100	-755.51	13.29	3.18	742	1.127	0.6	0.3	0.6	1.1	1.1
12.50.27	83925	-18.51	-2.45	36.26	82	0.0053	155	0.0119	-741.00	15.86	3.14	877	1.097	0.5	0.2	0.6	1.0	1.1
12.50.28	83185	-21.03	-5.98	42.51	74	0.0062	154	0.0142	-723.35	18.33	3.07	1016	1.075	0.5	0.2	0.6	1.0	1.0
12.50.29	82472	-22.50	-9.01	47.60	68	0.0073	155	0.0162	-703.44	20.57	2.97	1133	1.059	0.5	0.2	0.6	0.9	1.0
12.50.30	81772	-24.05	-11.76	52.01	63	0.0084	157	0.0186	-680.65	22.47	2.86	1244	1.051	0.5	0.2	0.5	0.9	0.9

* Expanding to 51 points

Figure 26: Program Output - One Second Data; Option 1a

57

	XY-VEL	XY-ACC	Z-VEL	Z-ACC														
* PTS. F17	51	35	19*	21														
DEGREE F17	3	3	1	3														
ID UNIT	ALA	CS		RG	MMSL	28	AMS DIA	INT										

21749 8 6 32.40 -9.791104 6370695.9 1209.0 0. 0.1222 1.00000 1

TIME ZULU	ALT METERS	EWIND M/S	NWIND M/S	SPEED KNOTS	DIR DEG	PRESS MB	T K	DENSITY GR/M3	Z VEL M/S	Z ACC M/S2	MACH	REYNL	CD	****R.P.S. NOISE ERROR 1**** DENS PRES TEMP *****PERCENT*****			EW M/S	NW M/S
0. 3.11	79775	-35.54	-17.54	76.98	63	0.0137	185	0.0256	-274.50	-1.33	1.11	621	1.234	0.0	0.0	0.0	0.5	0.9
	79600	-33.47	-19.29	75.12	59	0.0141	183	0.0268	-275.04	-1.00	1.12	641	1.191	0.0	0.0	0.0	0.5	0.9
0. 3.12	79514	-32.46	-20.14	74.21	58	0.0143	181	0.0275	-275.31	-0.83	1.12	600	1.184	0.0	0.0	0.0	0.5	0.9

BALLOON APOGEE = 85 KM.

TIME ZULU	ALT METERS	EWIND M/S	NWIND M/S	SPEED KNOTS	DIR DEG	PRESS MB	T K	DENSITY GR/M3	Z VEL M/S	Z ACC M/S2	MACH	REYNL	CD	DENS	PRES	TEMP	EW M/S	NW M/S
	79400	-31.79	-21.23	73.53	55	0.0146	178	0.0295	-275.37	-0.58	1.13	710	1.172	0.7	0.0	0.7	0.5	0.8
0. 3.13	79253	-29.78	-22.64	72.67	52	0.0150	174	0.0300	-275.44	-0.26	1.14	768	1.155	0.7	0.1	0.7	0.5	0.8
	79200	-29.10	-23.04	72.16	50	0.0152	173	0.0306	-275.34	-0.14	1.15	789	1.150	0.7	0.1	0.7	0.5	0.8
	79000	-26.53	-24.57	70.25	46	0.0158	167	0.0328	-274.96	0.32	1.16	867	1.130	0.7	0.1	0.7	0.5	0.8
9. 3.14	78991	-26.42	-24.64	70.17	46	0.0158	167	0.0129	-274.95	0.34	1.16	970	1.129	0.7	0.1	0.7	0.5	0.8
	78800	-23.14	-25.32	67.71	41	0.0165	163	0.0351	-274.57	0.80	1.17	950	1.112	0.7	0.1	0.7	0.5	0.8
9. 3.15	78728	-22.19	-26.26	66.79	40	0.0167	161	0.0360	-274.44	0.93	1.18	979	1.105	0.7	0.1	0.7	0.5	0.8
	78600	-20.35	-26.85	65.55	36	0.0171	160	0.0372	-274.70	1.28	1.18	1020	1.099	0.7	0.1	0.7	0.5	0.8
9. 3.16	78466	-18.44	-27.47	64.26	33	0.0176	159	0.0385	-274.97	1.60	1.18	1061	1.093	0.7	0.1	0.7	0.4	0.8
	78400	-17.45	-27.84	63.92	31	0.0179	158	0.0393	-274.67	1.76	1.19	1087	1.089	0.7	0.1	0.7	0.4	0.7
0. 3.17	78204	-14.53	-28.94	62.90	26	0.0186	155	0.0416	-273.81	2.21	1.19	1164	1.078	0.6	0.1	0.6	0.4	0.7
	78200	-14.46	-28.96	62.88	25	0.0186	155	0.0417	-273.77	2.22	1.19	1166	1.077	0.6	0.1	0.6	0.4	0.7
	78000	-11.34	-29.93	62.27	20	0.0195	153	0.0443	-272.03	2.65	1.19	1250	1.066	0.6	0.1	0.6	0.4	0.7
0. 3.18	77944	-10.49	-30.20	62.10	19	0.0197	152	0.0451	-271.54	2.77	1.19	3273	1.065	0.6	0.1	0.6	0.4	0.7
	77800	-7.50	-30.73	61.67	13	0.0203	150	0.0470	-269.43	3.00	1.19	1332	1.054	0.6	0.1	0.6	0.4	0.7
0. 3.19	77686	-5.12	-31.15	61.33	9	0.0209	149	0.0487	-267.74	3.18	1.19	1379	1.047	0.6	0.1	0.6	0.4	0.7
	77600	-3.05	-31.15	61.06	123	0.0213	149	0.0497	-266.58	3.27	1.18	1403	1.042	0.6	0.1	0.6	0.4	0.7
0. 3.20	77426	1.15	-31.13	60.52	357	0.0221	148	0.0519	-264.22	3.45	1.17	1452	1.034	0.6	0.1	0.6	0.4	0.7
	77400	1.73	-31.10	60.59	355	0.0222	148	0.0522	-263.65	3.47	1.17	1461	1.032	0.6	0.1	0.6	0.4	0.7
	77200	6.00	-30.85	61.15	349	0.0233	147	0.0550	-259.41	3.60	1.15	1527	1.022	0.6	0.1	0.6	0.4	0.7
0. 3.21	77171	6.62	-30.82	61.23	347	0.0234	147	0.0555	-258.79	3.62	1.15	1536	1.020	0.6	0.1	0.6	0.4	0.7
	77000	9.53	-30.74	62.63	342	0.0243	147	0.0576	-255.93	3.66	1.14	1575	1.009	0.6	0.1	0.6	0.4	0.7
0. 3.22	76916	10.94	-30.70	63.31	340	0.0248	147	0.0587	-254.62	3.68	1.13	1593	1.003	0.6	0.1	0.6	0.4	0.7
	76800	12.75	-30.53	64.38	316	0.0255	147	0.0601	-252.75	3.68	1.12	1615	0.995	0.6	0.1	0.6	0.4	0.7
0. 3.23	76664	14.84	-30.34	65.62	333	0.0263	147	0.0615	-250.58	3.68	1.11	1640	0.986	0.6	0.1	0.6	0.4	0.7
	76600	15.85	-30.23	66.37	331	0.0266	148	0.0626	-249.61	3.67	1.10	1650	0.981	0.6	0.1	0.6	0.4	0.7
0. 3.24	76415	18.72	-29.89	68.51	327	0.0278	149	0.0644	-246.87	3.63	1.08	1679	0.967	0.6	0.1	0.7	0.4	0.6
	76400	18.97	-29.92	68.68	326	0.0279	149	0.0650	-246.70	3.62	1.08	1679	0.965	0.6	0.1	0.7	0.4	0.6
	76200	22.14	-28.91	70.78	321	0.0271	151	0.0667	-244.57	3.50	1.06	1677	0.950	0.7	0.1	0.7	0.4	0.6
0. 3.25	76169	22.64	-28.76	71.10	321	0.0293	152	0.0670	-244.24	3.46	1.06	1677	0.948	0.7	0.1	0.7	0.4	0.6
	76000	25.53	-28.09	73.81	316	0.0304	154	0.0684	-242.49	3.12	1.04	1671	0.931	0.7	0.1	0.7	0.4	0.6
0. 3.26	75923	26.84	-27.77	75.05	315	0.0309	155	0.0691	-241.69	3.25	1.03	1668	0.924	0.7	0.1	0.7	0.4	0.6
	75800	28.65	-26.80	76.30	312	0.0317	157	0.0703	-240.56	3.15	1.02	1675	0.912	0.7	0.1	0.7	0.4	0.6
0. 3.27	75680	30.41	-25.84	77.51	310	0.0325	158	0.0715	-239.42	3.05	1.01	1681	0.901	0.7	0.1	0.7	0.4	0.6
	75600	31.24	-25.29	78.12	308	0.0131	158	0.0726	-238.64	2.99	1.00	1693	0.891	0.7	0.1	0.7	0.4	0.6
0. 3.28	75441	32.87	-24.22	79.31	306	0.0342	159	0.0746	-237.12	2.80	0.99	1716	0.871	0.7	0.1	0.7	0.4	0.6
	75400	33.26	-23.99	79.67	305	0.0345	159	0.0753	-236.57	2.85	0.99	1731	0.865	0.7	0.1	0.7	0.4	0.6
0. 3.29	75204	35.12	-22.84	81.38	303	0.0360	159	0.0791	-234.00	2.74	0.98	1803	0.838	0.7	0.1	0.7	0.4	0.6
	75200	35.15	-22.81	81.40	302	0.0360	158	0.0791	-231.94	2.74	0.98	1804	0.838	0.7	0.1	0.7	0.4	0.6
	75000	36.45	-21.67	82.38	300	0.0375	156	0.0834	-230.96	2.64	0.97	1890	0.813	0.7	0.1	0.7	0.4	0.6
9. 3.30	74970	36.55	-21.49	82.53	300	0.0378	156	0.0841	-230.51	2.63	0.97	1903	0.810	0.7	0.1	0.7	0.4	0.6
	74800	37.31	-20.58	82.78	298	0.0392	154	0.0882	-227.97	2.58	0.96	1990	0.792	0.7	0.1	0.7	0.4	0.6
0. 3.31	74738	37.55	-20.25	82.87	298	0.0397	154	0.0897	-227.06	2.56	0.96	2023	0.785	0.7	0.1	0.7	0.4	0.6

DRAG VALUE NOT GIVEN — 0.99 2592

DRAG VALUE NOT GIVEN — 0.96 2527

* Expanding to 51 points

Figure 27: Program Output - Constant Altitude (interpolation); Option 1b

58

| ALTITUDE	DENS RAT	PRES RAT	TEMP	EAST WIND	NORTH WIND
95800.	1.03614	1.05121	200.	-22.76	15.19
95600.	1.02511	1.04919	201.	-19.49	18.09
95400.	1.01559	1.04839	203.	-14.23	20.99
95200.	1.00386	1.04809	204.	-9.59	22.13
95000.	0.99322	1.04991	206.	-4.91	23.15
94800.	0.97647	1.04414	208.	-0.25	24.15
94600.	0.95727	1.03585	211.	4.03	24.34
94400.	0.93561	1.03683	213.	9.30	24.54
94200.	0.92405	1.03492	215.	12.26	24.75
94000.	0.91273	1.03311	219.	14.53	24.98
93800.	0.99595	1.02595	219.	16.80	25.21
93600.	0.98138	1.02011	221.	19.03	25.34
93400.	0.97089	1.01512	222.	20.98	24.90
93200.	0.86172	1.01132	223.	22.53	24.46
93000.	0.85325	1.00856	224.	24.84	23.86
92800.	0.83609	0.99986	225.	26.45	22.06
92600.	0.82063	0.99261	227.	28.07	20.27
92400.	0.90715	0.98667	229.	29.68	18.46
92200.	0.90306	0.98172	228.	31.08	16.24
92000.	0.90004	0.97789	229.	32.49	14.01
91800.	0.79221	0.96863	227.	33.84	11.82
91600.	0.79031	0.96128	225.	34.65	9.92
91400.	0.78565	0.95525	223.	35.47	8.02
91200.	0.79015	0.95044	221.	36.28	6.12
91000.	0.79184	0.94747	219.	36.49	4.86
90800.	0.78802	0.93901	218.	36.70	3.59
90600.	0.78562	0.93201	216.	36.92	2.33
90400.	0.78112	0.92676	215.	36.69	1.43
90200.	0.77750	0.92276	215.	36.39	0.56
90000.	0.77459	0.91998	214.	36.10	-0.31
89800.	0.76564	0.91196	214.	35.66	-1.21
89600.	0.76528	0.90552	213.	35.16	-2.13
89400.	0.76202	0.90038	213.	34.67	-3.04
89200.	0.75563	0.89651	213.	34.18	-3.86
89000.	0.75811	0.89377	212.	33.70	-4.64
88800.	0.75251	0.88621	212.	33.21	-5.41
88600.	0.75205	0.88031	211.	32.42	-5.99
88400.	0.75725	0.87596	209.	31.90	-6.33
88200.	0.76348	0.87278	206.	31.19	-6.65
88000.	0.77146	0.87103	204.	30.48	-6.98
87800.	0.77699	0.86533	201.	29.81	-7.20
87600.	0.78352	0.86097	198.	29.13	-7.41
87400.	0.79142	0.85801	195.	28.46	-7.62
87200.	0.80093	0.85720	193.	27.84	-7.82
87000.	0.81154	0.85743	190.	27.23	-8.01
86800.	0.81797	0.85305	189.	26.40	-8.20
86600.	0.83207	0.85146	184.	25.51	-7.98
86400.	0.84760	0.85105	181.	24.43	-7.75
86200.	0.86455	0.85176	178.	23.35	-7.54
86000.	0.87282	0.85455	175.	21.96	-7.15
85800.	0.87690	0.85287	175.	20.52	-6.72
85600.	0.98132	0.85249	174.	19.09	-6.29
85400.	0.98702	0.85370	173.	17.70	-5.88
85200.	0.99392	0.85617	173.	16.55	-5.48
85000.	0.90197	0.85969	172.	15.31	-5.09
84800.	0.90515	0.85875	171.	14.15	-4.65
84600.	0.90569	0.85939	170.	13.09	-4.23
84400.	0.91553	0.86175	169.	12.02	-3.79
84200.	0.92229	0.86433	169.	11.02	-3.34
84000.	0.92543	0.86874	169.	10.16	-2.86
83800.	0.93149	0.86844	168.	9.29	-2.37

Figure 28: Computer Output of Data for Plotting
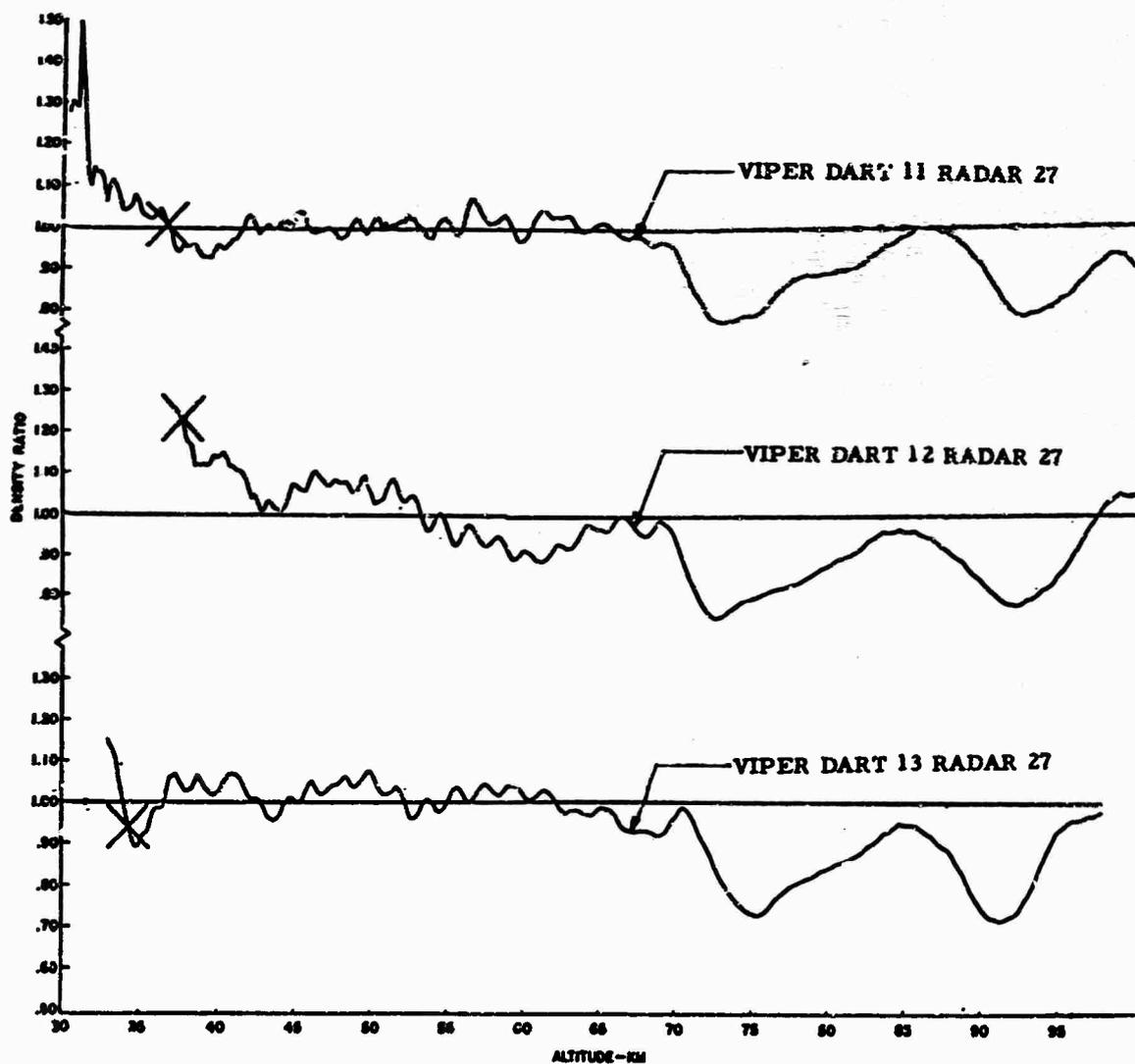
Figure 29: Density Ratio from Viper Darts 11, 12, and 13; Radar 27

b) Spacial variations in density between the paths of three spheres.

c) Inaccuracies of the drag coefficients being experienced at different altitudes for the three spheres.

d) A change in the vertical motions of the atmosphere.

60

These discrepancies in density, one hour apart in time, are not due to the inability of the radar to accurately track the spheres. Comparison of densities from the two tracks of the same sphere clearly rule out this cause. Nor are the density discrepancies thought to be a result of a sphere collapse or elongation. Both sphere collapse checks indicate the spheres were still inflated to at least 40 km.
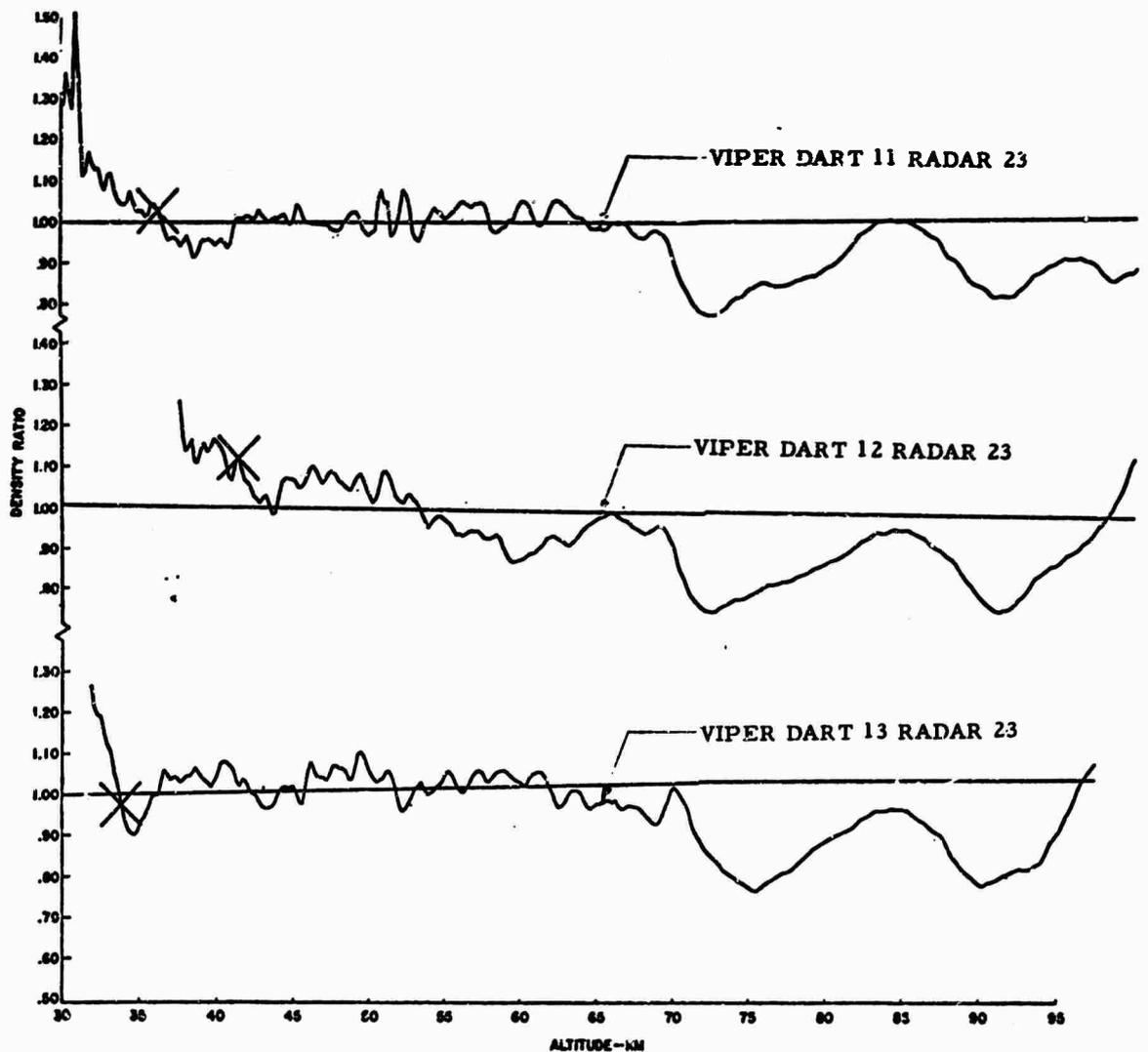

Figure 30: Density Ratio from Viper Darts 11, 12, and 13: Radar 23
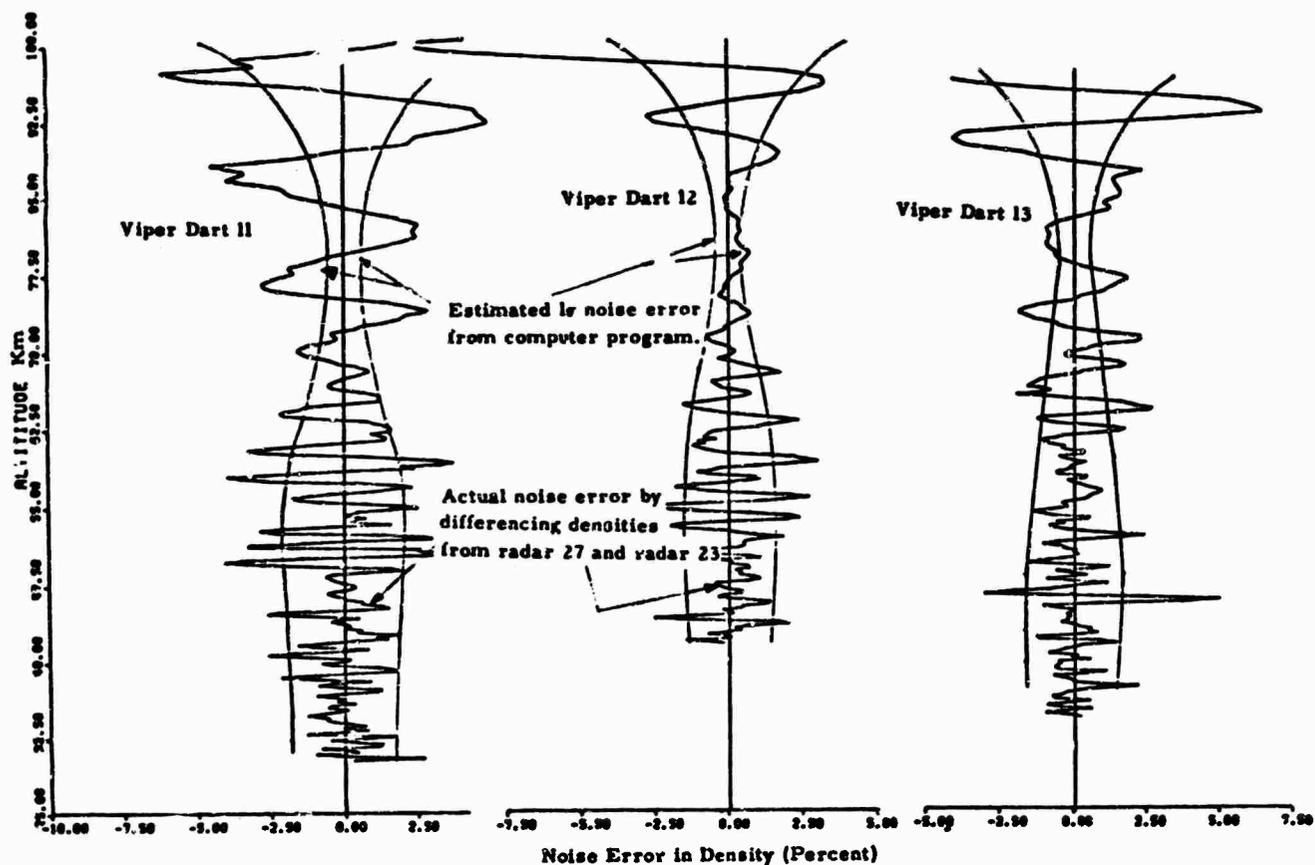
Figure 31: Comparison of Estimated to Actual Density Errors:
Viper Darts 11, 12, and 13

7.2 Wind Accuracy

Figures 32-35 are plots of the W_x (East Wind) and W_y (North Wind) wind components for each of the three flights. Above 85 km Viper Darts 12 and 13 show large differences between winds from radar 23 and radar 27. To determine if the differences were within the bounds of that estimate, plots were made comparing the actual noise errors to the estimated 1σ errors. Figures 36 and 37 show the noise error in winds obtained by differencing the winds from the two tracks compared to that estimated by the computer program output. Both the W_x and W_y component errors from Viper Dart 11 show the expected agreement. Viper Darts 12 and 13 show good agreement in general only below 85 km. The cause of this decrease in agreement, which is beyond what is predicted from the total error plots for 51-35 cubic-cubic smoothing (Figure 16) has been investigated. The following results have been obtained.

62

The tracks of radar 23 from both Viper Dart 12 and Viper Dart 13 flights showed large oscillation in horizontal position which did not appear in the tracks of radar 27 from the same flights (see Figure 38). Previous experience with FPS-16 tracking data, indicates the cause of the oscillation in the track from radar 23 is probably a low servo band width setting. The fact that radar 27 produces a smooth non-oscillating track indicates the oscillations as seen in the track of radar 23 are not real. Further investigation of the effect of the servo on tracking of passive spheres is in order. In comparing the wind profile from the flights one hour apart, changes in the wind field are seen. These changes, especially below 80 km appear to be real variations in the wind field, since they are observed by both radars.
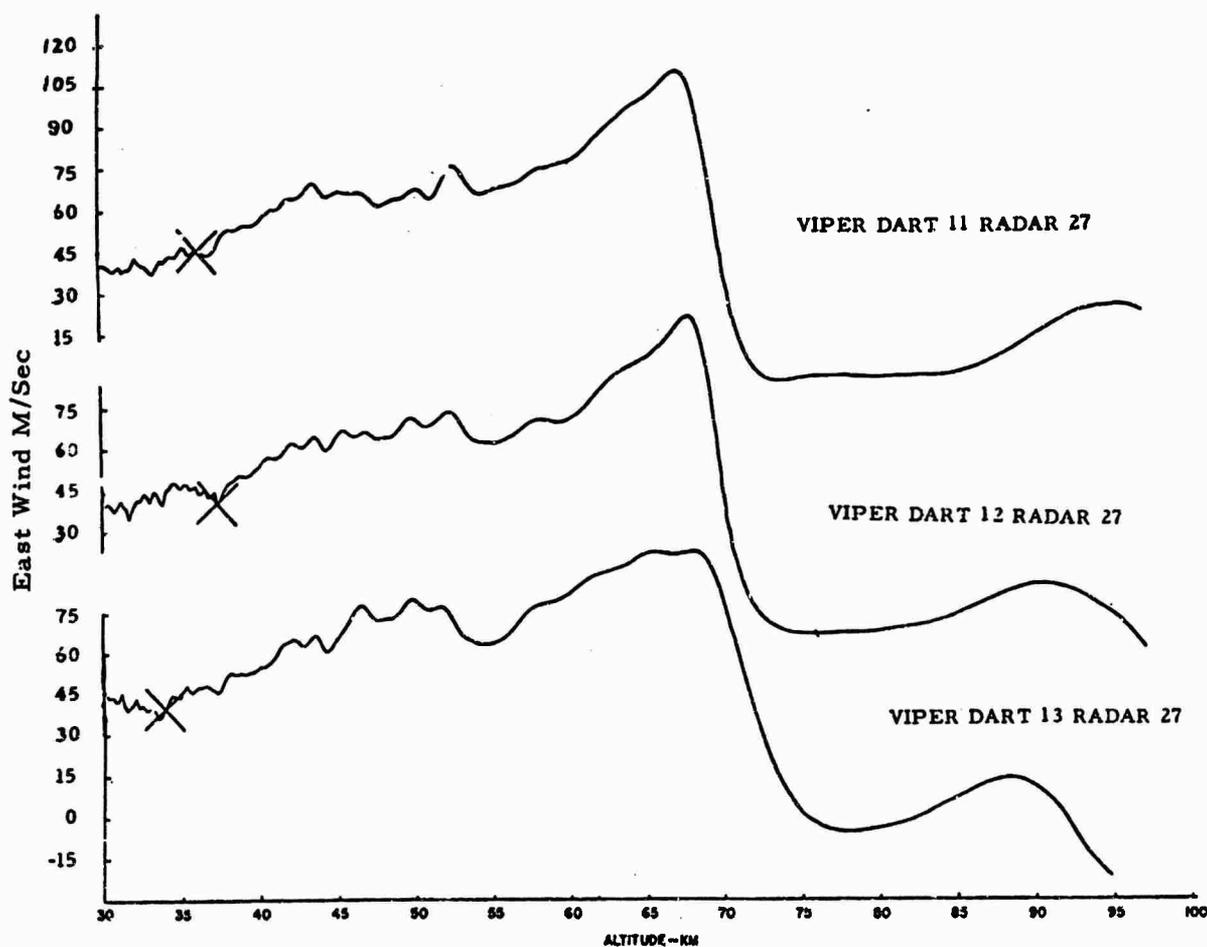

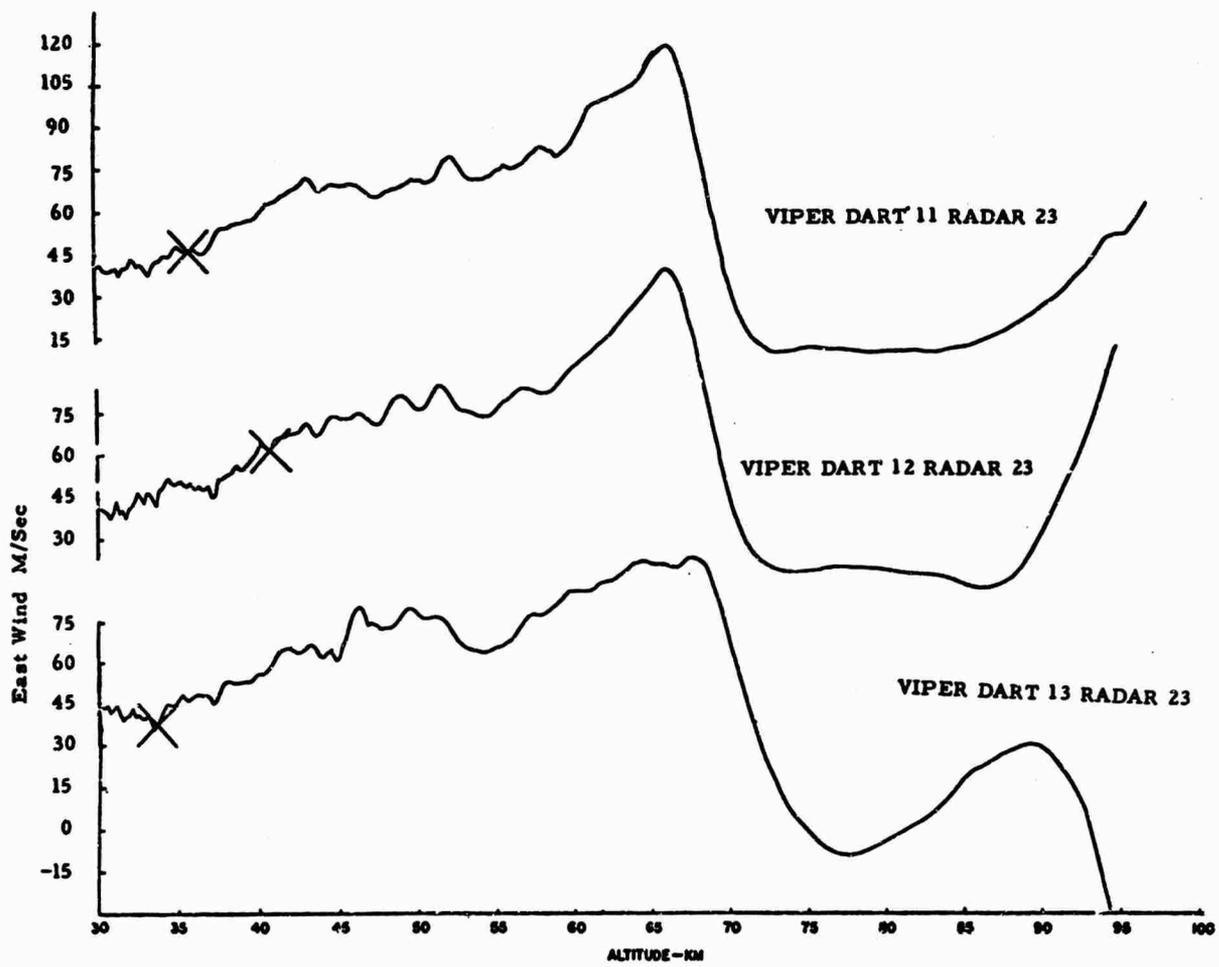Figure 32: East Wind from Viper Darts 11, 12, and 13: Radar 27

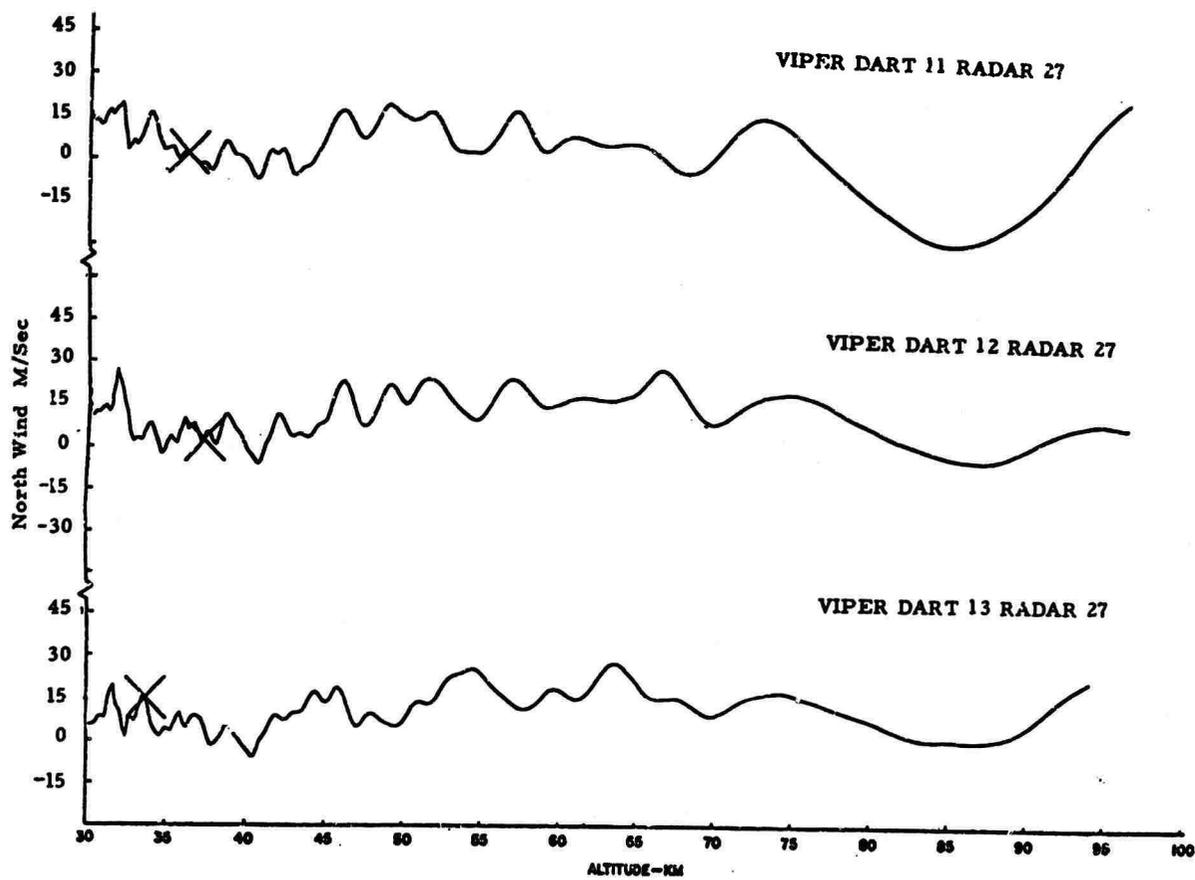Figure 33: East Wind from Viper Darts 11, 12, and 13: Radar 23

64

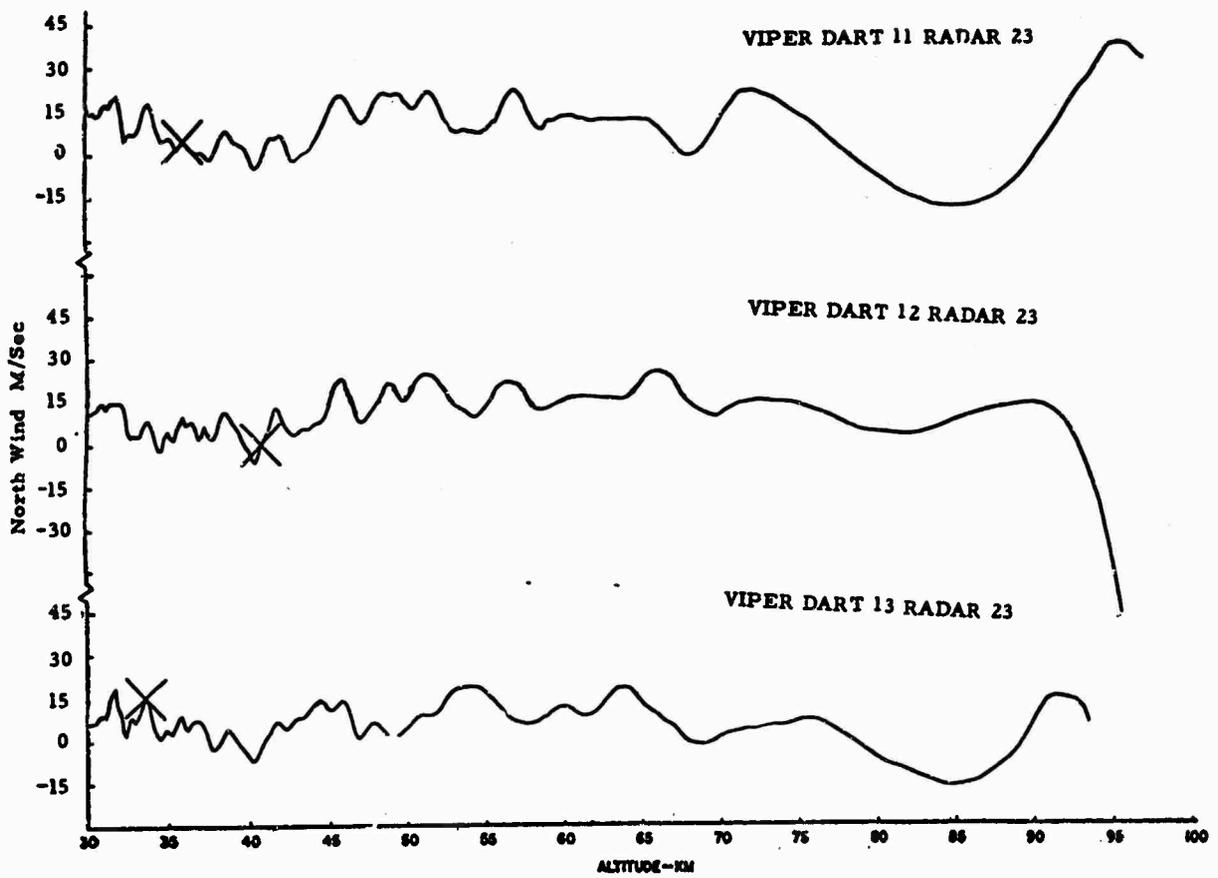Figure 34: North Wind from Viper Darts 11, 12, and 13; Radar 27

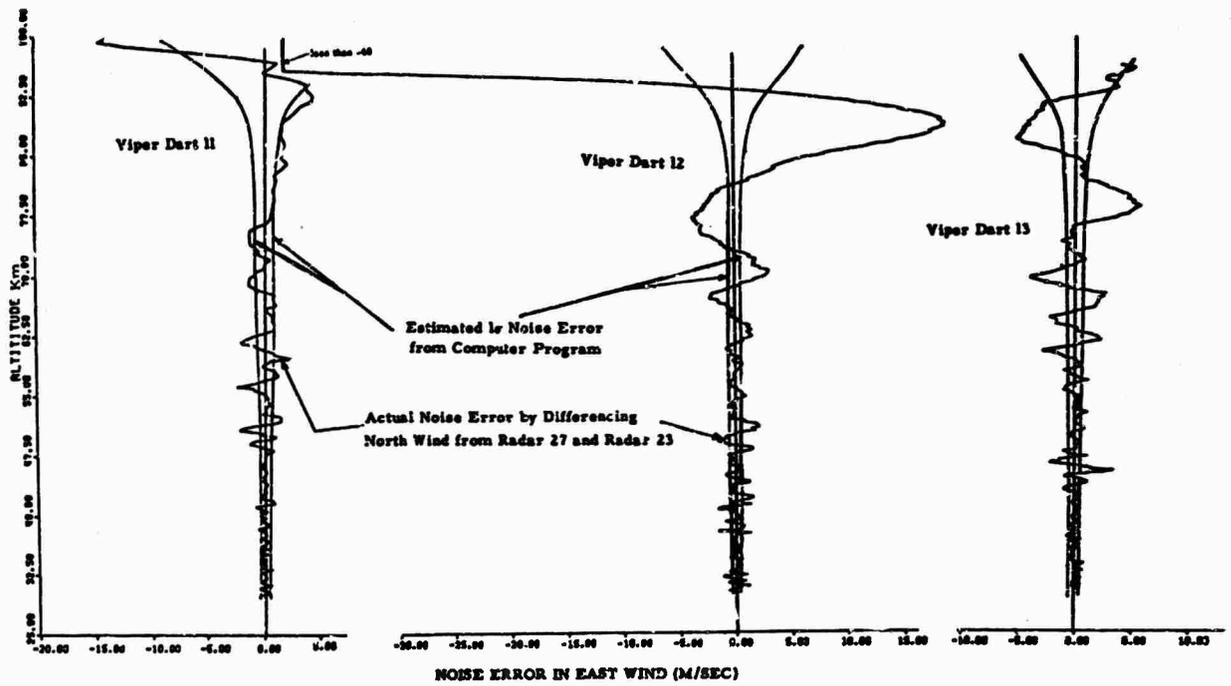**Figure 35:** North Wind from Viper Darts 11, 12 and 13: Radar 23

66

Figure 36: Comparison of Estimated to Actual East Wind Errors;
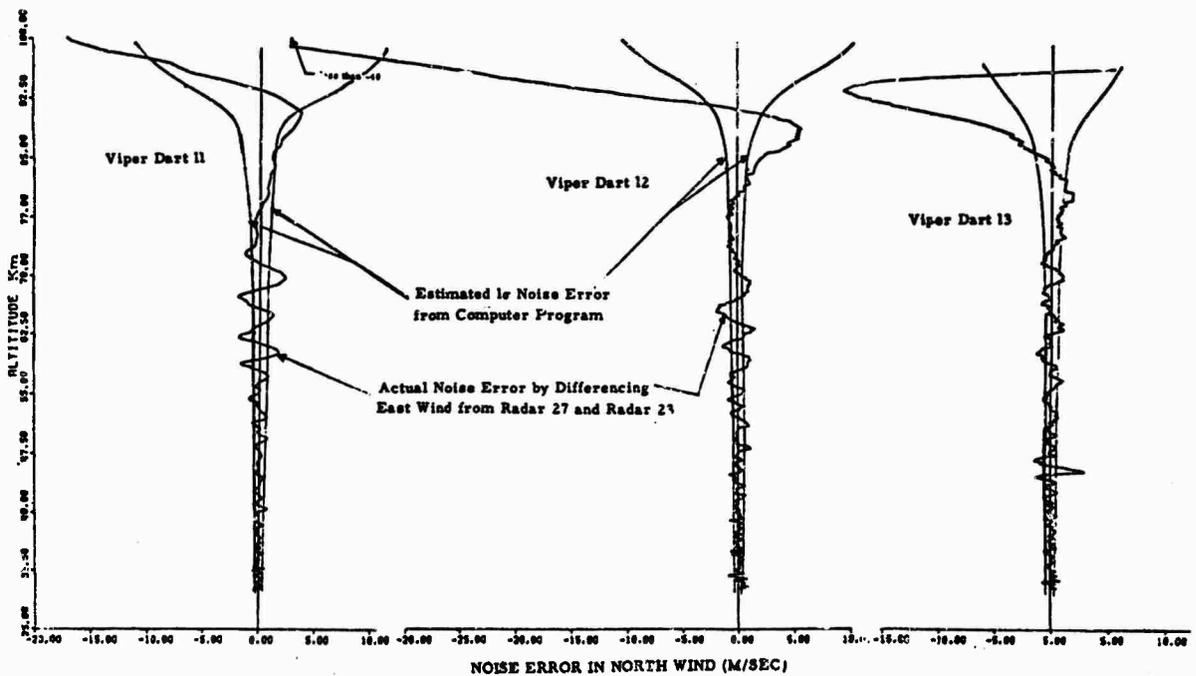Viper Darts 11, 12, and 13

Figure 37: Comparison of Estimated to Actual North Wind Errors;
Viper Darts 11, 12, and 13.

67
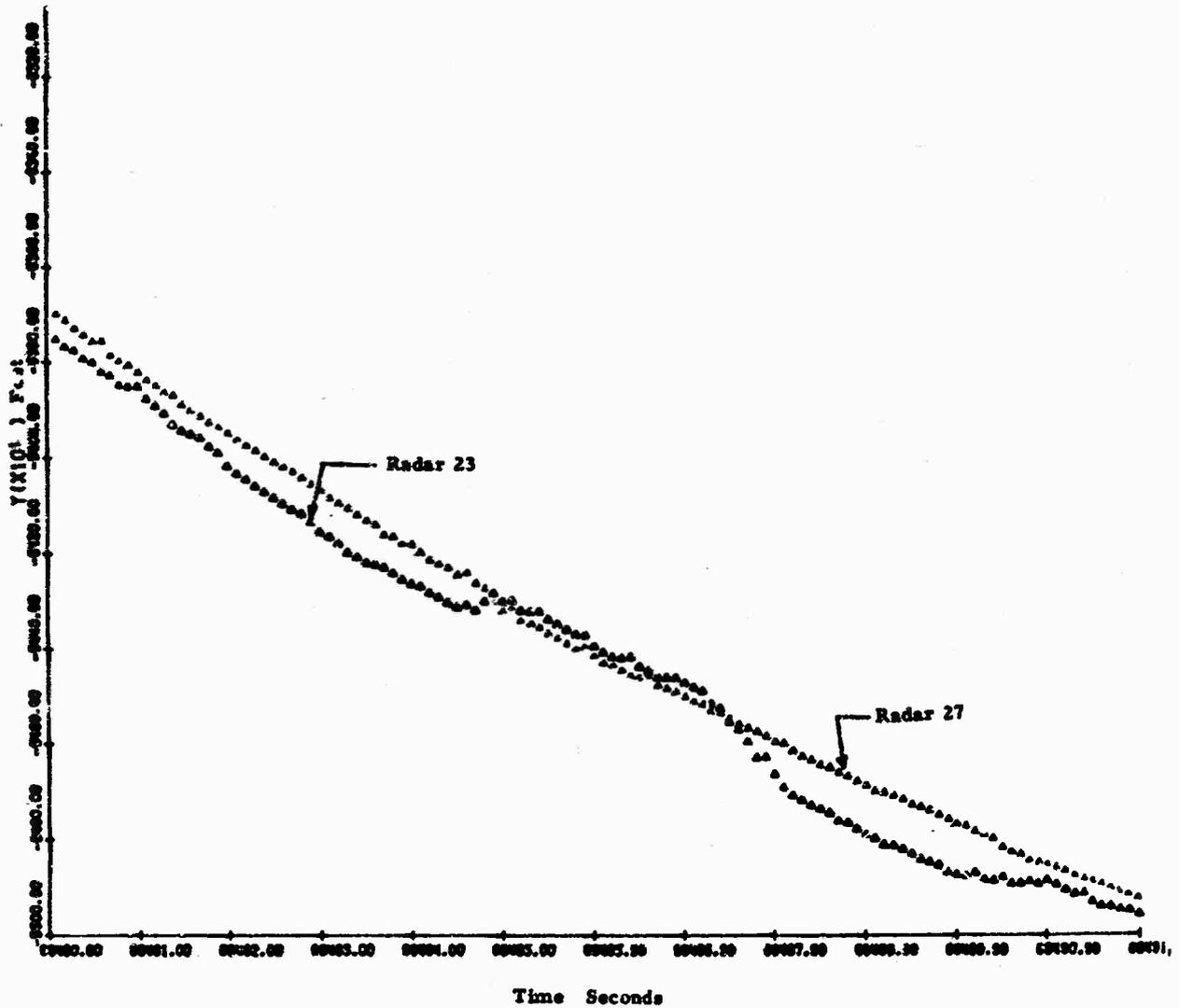
Figure 38: Comparison of Y positions from Radar 27 and Radar 23; Viper Dart 12

7.3 Pressure Accuracy

Figures 39 and 40 show the pressures obtained by each radar for the three flights. The actual noise error in pressure (by differencing the pressure from the two tracks of the same flight) is compared to the estimated 1σ noise error in pressure obtained from the High Altitude ROBIN Program output in Figure 41. The agreement between the actual and the estimated errors is good below 90 km. Above 90 km pressure errors are larger than that estimated. This is apparently the result of the low servo band width setting of radar 23.
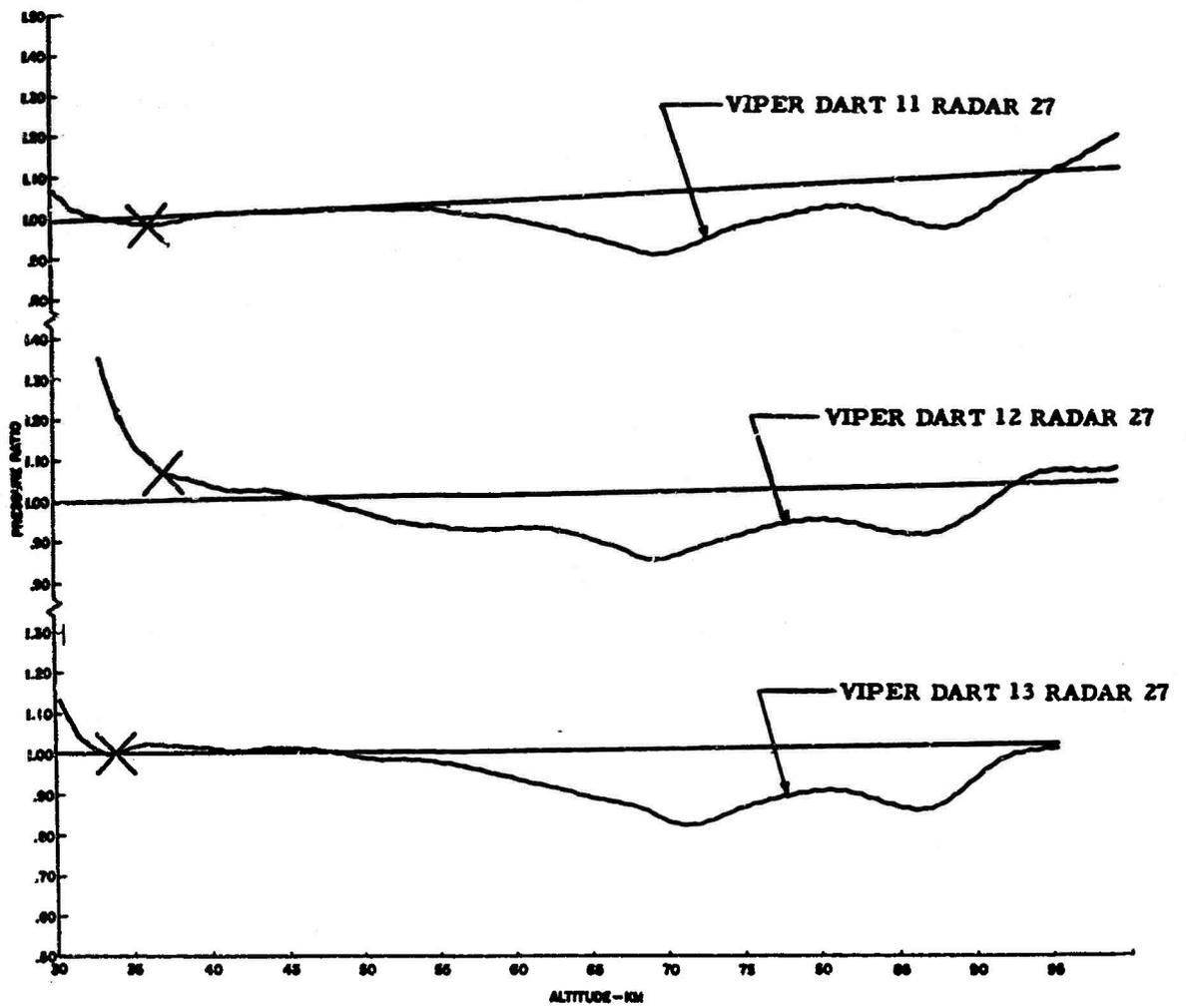
Figure 39: Pressure Ratio from Viper Darts 11, 12 and 13; Radar 27
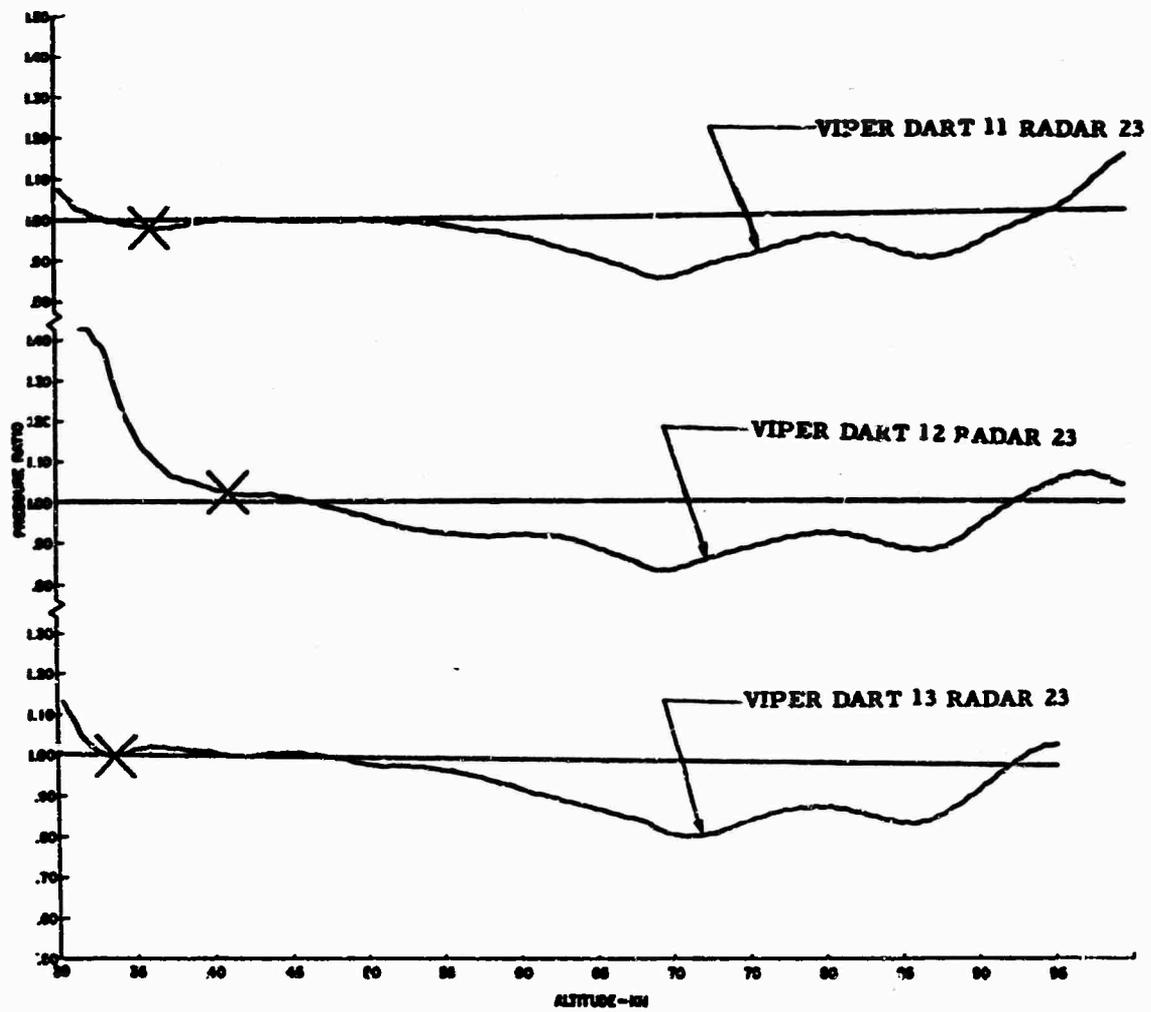
Figure 40: Pressure Ratio from Viper Darts 11, 12, and 13: Radar 23

70
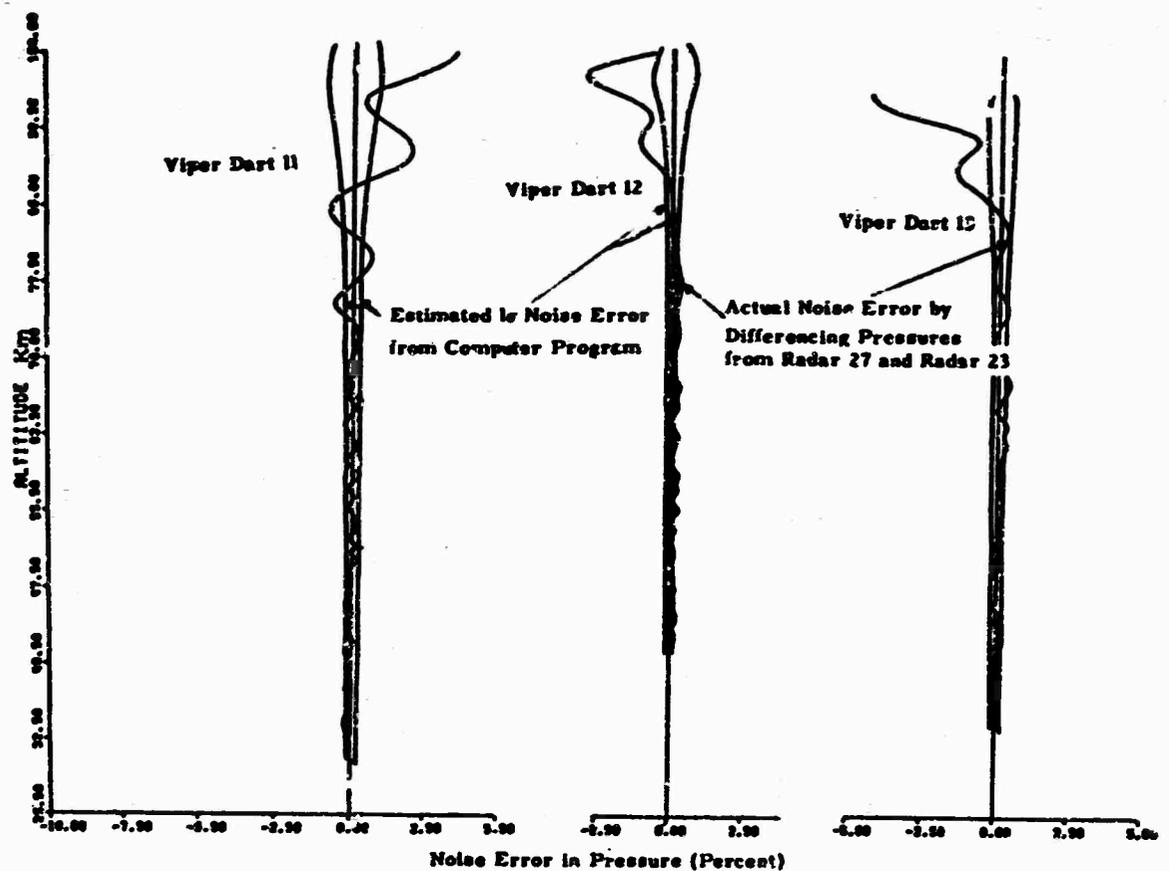
Figure 41: Comparison of Estimated to Actual Pressure Errors; Viper
Viper Darts 11, 12,and 13.

7.4   Temperature Accuracy

The temperature profiles for flights Viper Dart 11 -13 are presented
in Figures 42 and 43.   By differencing the temperatures from two tracks of
the same flight the noise error in temperature is computed.   Figure 44 shows
the actual noise error in temperature for each flight and the estimated 1σ noise
error. For each of the three flights, the agreement is very good except above
90 km.   The disagreement above 90 km results from the somewhat larger than
anticipated density and temperature errors above 90km.

71

Figure 42: Temperature from Viper Darts 11, 12, and 13; Radar 27

72

Figure 43: Temperature from Viper Darts 11, 12, and 13; Radar 23

73

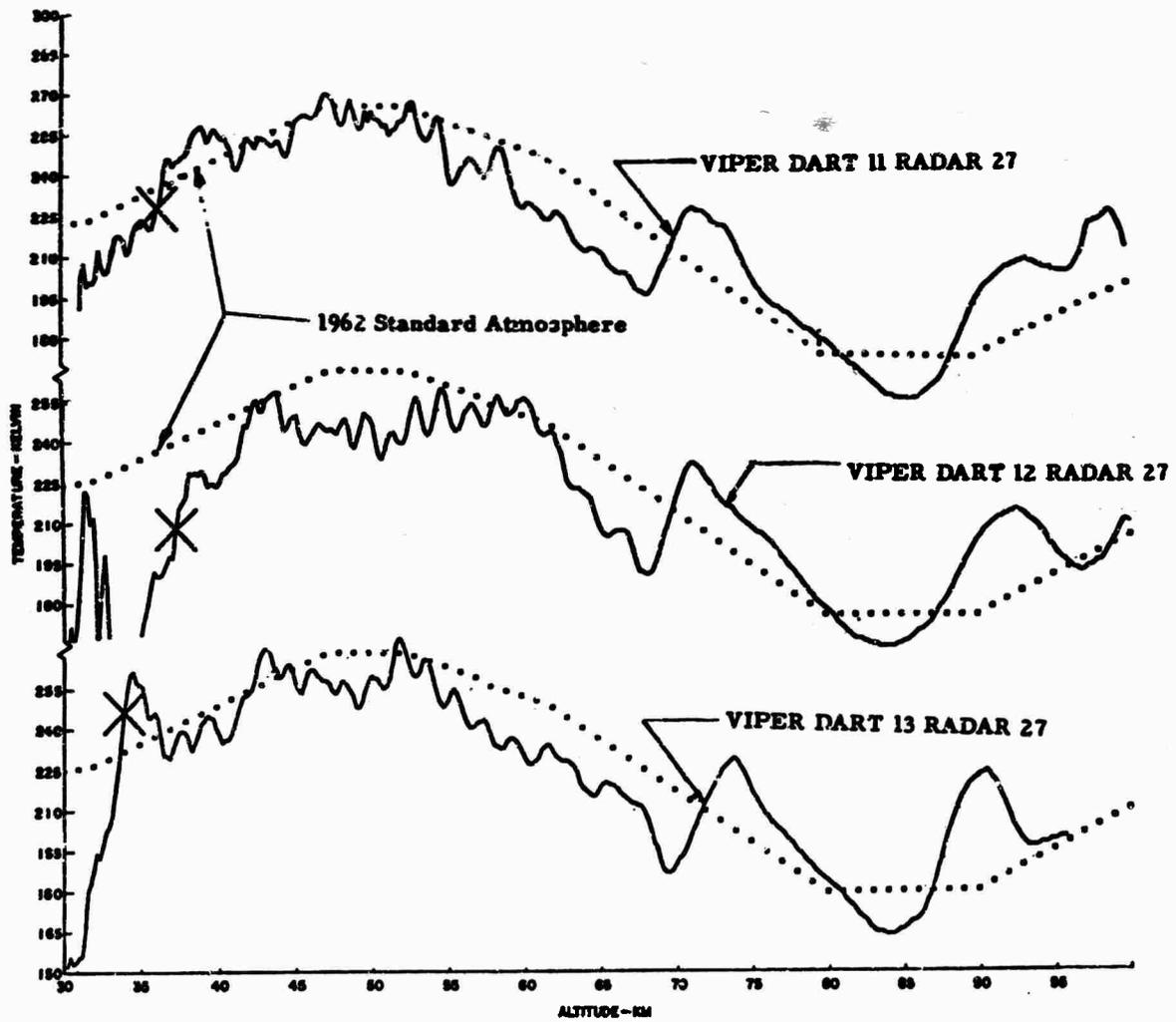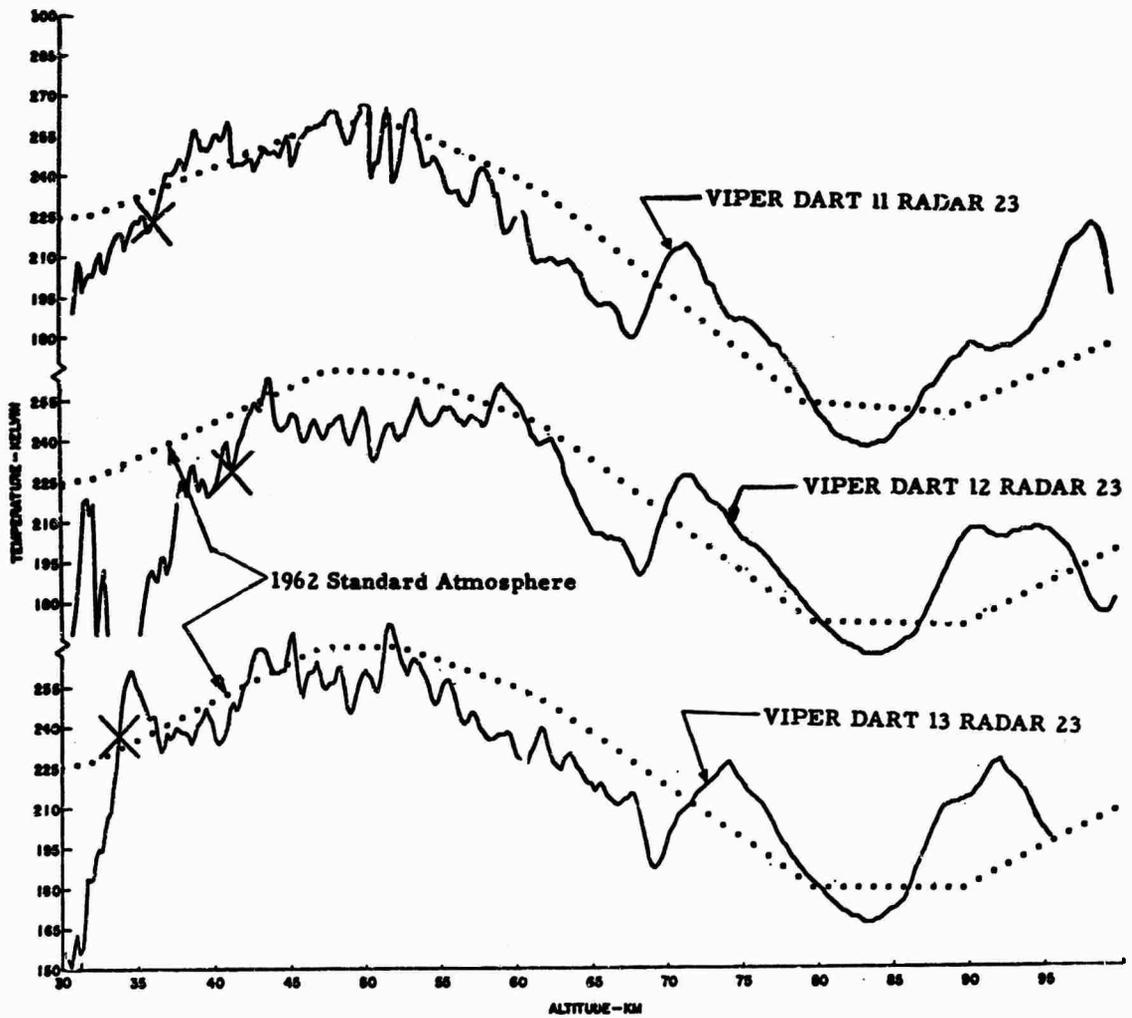NOISE ERROR IN TEMPERATURE (DEGREES)
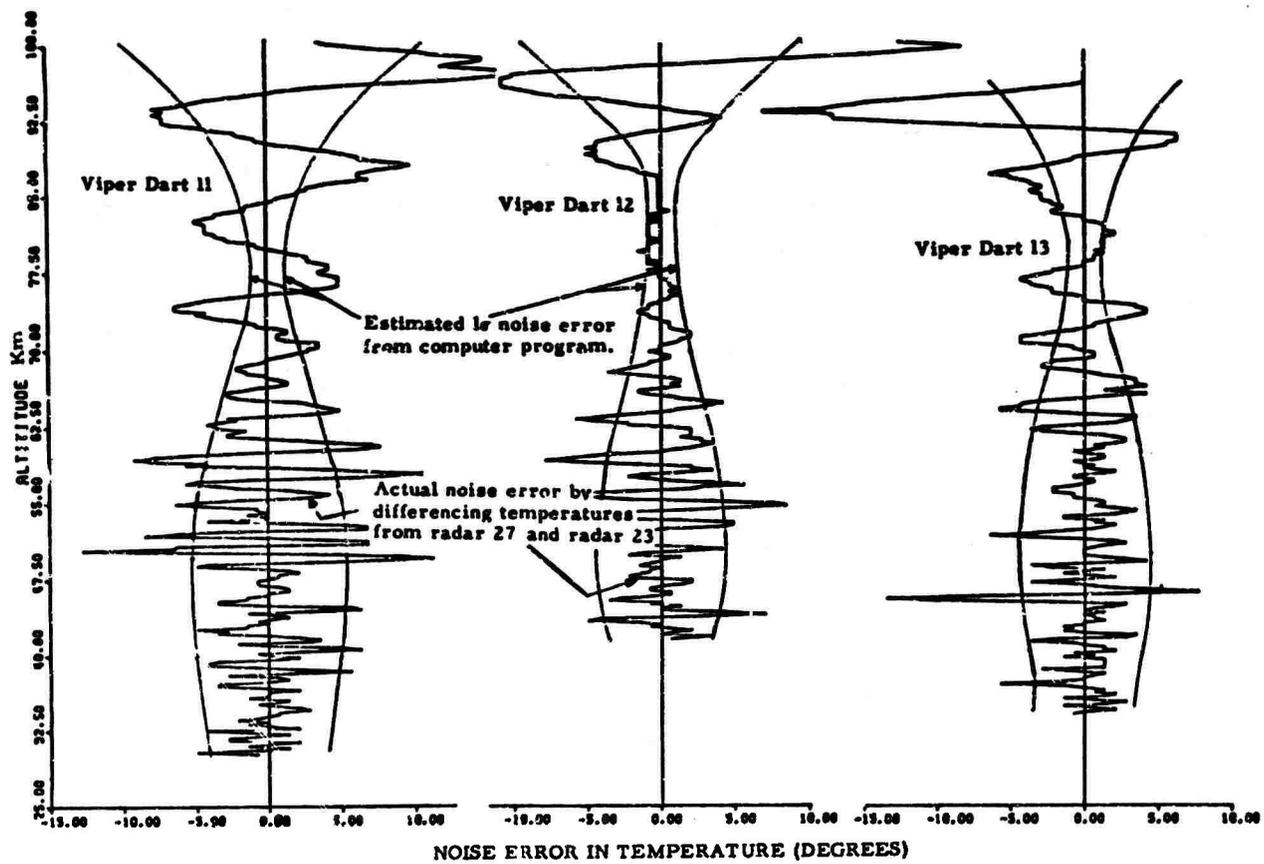
Figure 44: Comparison of Estimated to Actual Temperature Errors

7.5   Conclusions

A series of three Viper Dart flights launched one hour apart has been reduced, using the May 1970 AFCRL ROBIN Program. The density noise error for these flights was consistent with that predicted for the expanding 19-21 linear-cubic smoothing over the entire altitude span(30-100 km). Observed differences in density between the flights one hour apart cannot be attributed to smoothing error, since the two tracks of each sphere show remarkable consistency. Wind accuracy for the three flights was commensurate with that predicted for the 51-35 cubic-cubic in general only below 85 km. Viper Dart 11, however, showed good agreement over the entire range from 30 to 100 km. The decrease in accuracy above 85 km for Viper Dart 12 and 13 is believed to be caused by a low servo band width setting on radar 23. Horizontal position plots from radar 23 show oscillations not found in the track of radar 27. These oscillations are often observed in sphere tracking at a low servo band width. They do not appear predominate in vertical position plots (Z,t) indicating perhaps a low servo band in azimuth for radar 23. Further investigation of this problem is necessary. As in the case of density, the one hour apart flights often show large changes in the structure of the wind field below 80 km, sometimes as large as 15 m/sec. Since both radar tracks (for each sphere) observe the same wind detail (below 80 km) this variation in wind structure is believed to be real. Temperature and pressure accuracy was in good agreement with that estimated to altitudes of 90 km. Above 90 km the low servo band width setting of radar 23 is believed to increase the errors in excess of that estimated.

8. SUMMARY OF DENSITY, WINDS, PRESSURE AND TEMPERATURE ERRORS

For the convenience of the reader this section summarizes the expected errors in wind and thermodynamic computations from the ROBIN System using the May 1970 AFCRL ROBIN Program. Table 14 shows the error estimates for each of the meteorological parameters and the source of these errors. All errors listed in Table 14 are point errors in the sense that they are the estimated errors in a data point at the specified altitude. In the case of pressure and temperature, which are computed from an integration of density, the point errors reflect the effect of the errors in previous data points. For each of the meteorological parameters the noise error is the error in that parameter which results from the noise in the radar coordinates. The bias error is that error resulting from any bias introduced by the smoothing process. The error in density resulting from errors in the Drag Coefficient are difficult to assess due to the inconsistent results obtained by different experimenters. Those C_D errors quoted in Table 14 are the UDRI's best estimate, with the information available, and is subject to revision if warrented upon the completion of work in progress at AEDC. The error in density from a X m/sec vertical wind is obtained by multiplying the error from a 1 m/sec vertical wind (given in Table 14) by X. To compute the effect of C_D errors on pressure and temperature the direction (+ or -) of the C_D error as well as its magnitude must be known. Since this is not known the effect of the C_D errors on these parameters cannot be determined. To compute the effect of vertical winds on pressure and temperature a vertical wind profile vs altitude must be assumed. Since little is known of the structure of vertical winds in the atmosphere a representative profile is not available. The noise error in winds can be thought of as the error in the mean wind profile. An estimate of the bias error in wind is not given because it depends upon the wind field itself. For a given wave structure of the wind field the distortion of any frequency resulting from the smoothing process is given by the frequency response. Table 15 shows the frequency response for both wind and density data.

TABLE 14

SUMMARY OF DENSITY, PRESSURE, TEMPERATURE, AND WIND ERRORS

	Altitude (Km)	100	95	90	85	80	75	70	65	60	55	50	40	30
DENSITY ERRORS (Percent)	Noise Error	8	3.5	1.5	1	0.7	0.8	1.5	2	2	2	2	2	2
	Bias Error	+2	+3.5	+4	+3	-1.5	-3	-1	less than 1/2%					
	Error due to 10% error in T_o	4	0.8				less than 1/2%							
	Error from C_D	13	8	6	3	1	2	6	4	3	2	2	2	2
	Error from 1 m/sec vertical wind — wavelength (Km) 2	.01	.01	.01	.01	.01	.02	.03	.18	.3	.7	1	4	9
	5	.01	.01	.01	.01	.01	.2	.4	.7	1.6	1.5	2.0	5.0	10.0
	10	.2	.2	.2	.2	.2	.4	.6	.8	1.0	1.5	2.0	5.0	10.0
PRESSURE ERRORS (Percent)	Noise Error	1	1.2	0.7			less than 1/2%							
	Bias Error	+2	+2.4	+2.3	+3.1	+1.5	less than 1/2%							
	Error due to 10% error in T_o	6	1.4	0.6			less than 1/2%							
	Error due to C_D error and vertical winds	Cannot be determined												
TEMPERATURE ERRORS (Percent)	Noise Error	8.1	3.7	1.7	1.1	0.7	0.8	1.5	2	2	2	2	2	2
	Bias Error	0	-1.1	-1.7	+0.1	+3	+0.8	+0.6	less than 1/2%					
	Error due to 10% error in T_o	10	2.2	0.9	less than 1/2%									
	Error due to C_D error and vertical winds	Cannot be determined												
WIND ERRORS (M/SEC)	Noise Error	13	6	4	1	1	1	1	less than 1 m/sec					

Table 15

Frequency Response of Wind and Density

125 Km Apogee

RATIC CF APPLITUCE OF SMOOTHED CENSITY WAVE TC APPLITLCE OF CRIGINAL
WAVE AS A FUNCTICN CF ALTITUDE AND WAVELENGTH.
(ALTITLDE AND WAVELENGTH PEASUREC IN KILCPETEKS.)

ALTITLOE

		100	90	80	70	60	50	40	30
W	1	0.01	C.C1	C.C1	C.C1	C.C1	C.22	C.42	C.75
A	2	0.01	C.C1	C.C1	C.C4	C.22	0.52	C.8C	C.90
V E L E N G T H	5	0.01	C.C2	C.03	C.47	C.84	C.50	0.96	C.99
	10	0.47	C.51	0.55	C.72	C.97	C.58	C.59	C.99
	20	0.54	C.95	0.56	C.53	C.55	C.59	0.55	C.99

RATIC CF AMPLITLDE OF SMUCTHEC SINUSOICAL WIND TO APPLITUCE OF
ORIGINAL WINC AS A FUNCTION OF ALTITUDE ANC WAVELENGTH.
(ALTITUCE ANC WAVELENGTH PEASURED IN KILCPETERS.)

ALTITLDE

		100	90	80	70	60	50	40	30
W	1	0.01	C.C1	C.01	C.C1	C.01	C.C2	0.57	C.96
A	2	C.01	C.01	C.C1	C.C3	C.1C	C.40	0.76	C.99
V E L E N G T H	5	C.C2	C.C2	C.C6	C.13	C.7C	0.58	C.55	C.99
	10	0.14	C.17	C.24	C.25	C.97	C.59	0.99	C.99
	20	C.56	C.63	C.66	C.5C	C.98	0.59	C.55	C.99

78

REFERENCES

1. Engler, Nicholas A., 1965, Development of Methods to Determine Winds, Density, Pressure, and Temperature from the Robin Falling Balloon, University of Dayton Research Institute, AFCRL-65-448.

2. Engler, Nicholas A., 1967, Report on High Altitude Robin Flights, October 1966, University of Dayton Research Institute, AFCRL-67-0433.

3. Aroesty, Jerome, 1962, Sphere Drag in a Low Density Supersonic Flow, University of California Institute of Engineering Research, HE-150-192.

4. Ashkenas, Harold, Sphere Drag at Low Reynolds Numbers and Supersonic Speeds (Mach 1-5), J. P. L. Research Summary, 36-12, Vol. 1 pp 93-96.

5. Heinrich, H. G., Niccum, R. J., and Haak, E. L., The Drag Coefficient of a Sphere Corresponding to a "One Meter Robin Sphere" Descending from 260,000 ft. Altitude, G. T. Schjeldahl Company, Northfield, Minnesota, 1963.

6. Heinrich, Niccum, Haak, Jamison, and George, 1965, Modification of the Robin Meteorological Balloon, Vol. II Drag Evaluation, University of Minnesota, AFCRL-65-734 (II).

7. Goin, K. L. and Lawrence, W. R., 1968, Subsonic Drag of Spheres at Reynolds Numbers from 200 to 10,000. AIAA Journal, May 1968, Vol. 6, No. 5.

8. Luers, James K., 1968, Estimation of Errors in Density and Temperature Measured by the High Altitude Robin Sphere, Proceedings of the Third National Conference on Aerospace Meteorology, May 1968.

9. Potter, J. Leith., and Miller, John T., 1968, Consideration of Simulation Parameters for Blunt Thick Bodies in Rarefied High-Speed Flows, Arnold Engineering Development Center, AEDC TR-68-242.

10. Luers, James K., and Engler, Nicholas, 1967, On Optimum Methods for Obtaining Wind Data from Balloon Sensors, Journal of Applied Meteorology, October 1967, pp 816-823.

11.   Bollermann, Bruce and Walker, Robert L., 31 January 1970, Design
        Development and Flight Test of the Viper Dart ROBIN Meteo-
        rological Rocket System; Design Improvement, AFCRL 70-0150.

12.   Luers, James, 1970, May 1970 High Altitude ROBIN Program; Users
        Manual, University of Dayton Research Institute, UDRI-TM-70-02.

APPENDIX A

DERIVATION OF THE DENSITY ERROR EQUATION

Consider density as given by the equation:

$$\rho = \frac{2m(\ddot{Z} - g)}{C_D AV(\dot{Z} - W_z)}.$$

Assuming errors in density as a function of errors in C_D, W_z, $\dot{Z}$, $\ddot{Z}$, V the error increment in density is approximated by:

$$\Delta\rho = \frac{\partial\rho}{\partial C_D}\Delta C_D + \frac{\partial\rho}{\partial V}\Delta V + \frac{\partial\rho}{\partial\dot{Z}}\Delta\dot{Z} + \frac{\partial\rho}{\partial\ddot{Z}}\Delta\ddot{Z} + \frac{\partial\rho}{\partial W_z}\Delta w_z.$$

Density Error due to Drag Coefficient

Assuming that drag coefficient errors are independent of the other errors, the percent change in density resulting from a C_D error of ϵ_{C_D} is given by

$$\frac{\epsilon_\rho}{\rho} = -\frac{\epsilon_{C_D}}{C_D}.$$

If each error in C_D is independent, and with normal distribution and zero mean, the percent error variance in density resulting from the C_D error distribution is given by

$$\left(\frac{\sigma_\rho}{\rho}\right)^2 = \left(\frac{\sigma_{C_D}}{C_D}\right)^2$$

A-1

Density Error Due to Errors in V.

The increment of error in density for horizontal velocity errors of $\epsilon_{\dot{x}}$ and $\epsilon_{\dot{y}}$ and horizontal wind errors of ϵ_{w_x} and ϵ_{w_y} is given by

$$\epsilon_\rho = \frac{\partial \rho}{\partial V} \epsilon_v = \frac{\partial \rho}{\partial \dot{X}} \epsilon_{\dot{x}} + \frac{\partial \rho}{\partial \dot{Y}} \epsilon_{\dot{y}} + \frac{\partial \rho}{\partial W_x} \epsilon_{w_x} + \frac{\partial \rho}{\partial W_y} \epsilon_{w_y}.$$

the percent error increment is:

$$\frac{\epsilon_\rho}{\rho} = -\frac{\dot{X} - W_x}{V^2} \epsilon_{\dot{x}} - \frac{\dot{Y} - W_y}{V^2} \epsilon_{\dot{y}} + \frac{\dot{X} - W_x}{V^2} \epsilon_{w_x} + \frac{\dot{Y} - W_y}{V^2} \epsilon_{w_y} \qquad (1A)$$

Since the errors in $\dot{X}$ and $\dot{Y}$ are much smaller than the errors in W_x and W_y, the primary contribution to Eq. 1A comes from the last two terms. Hence, Eq. 1A can be approxima. by

$$\frac{\epsilon_\rho}{\rho} = \frac{\dot{X} - W_x}{V^2} \epsilon_{w_x} + \frac{\dot{Y} - W_y}{V^2} \epsilon_{w_y}.$$

Assuming normally distributed and independent errors in W_x and W_y the percent error variance in density becomes

$$\left(\frac{\sigma_\rho}{\rho}\right)^2 = \left[\frac{\dot{X} - W_x}{V^2}\right]^2 \sigma_{w_x}^2 + \left[\frac{\dot{Y} - W_y}{V^2}\right]^2 \sigma_{w_y}^2.$$

The assumptions $\epsilon_{\dot{x}} << \epsilon_{w_x}$ and $\epsilon_{\dot{y}} << \epsilon_{w_y}$ are not critical in the derivation

of an error equation. Even if the assumptions introduced a 10% error in the

error equation, the results would be satisfactory for our purpose. The impor-

tant criterion is to measure the meteorological parameters as accurately as

possible and to have an estimate of their errors. If the estimate is off by 10%, it

is of little consequence.

Density Error Due to Vertical Velocity and Acceleration Errors

The error increment in density resulting from vertical velocity and

acceleration errors of $\epsilon_{\dot{z}}$ and $\epsilon_{\ddot{z}}$ is given by

$$\epsilon_\rho = \frac{\partial \rho}{\partial \dot{Z}} \epsilon_{\dot{z}} + \frac{\partial \rho}{\partial \ddot{Z}} \epsilon_{\ddot{z}} \qquad (2A)$$

Velocity and acceleration are computed by smoothing vertical position coordinates.

The smoothed velocity and acceleration contain noise error due to radar noise

and bais error introduced by the smoothing process. Interpreting Eq. 2A in

terms of noise error in velocity $(\epsilon_{\dot{z}})$ and acceleration $(\epsilon_{\ddot{z}})$ the percent noise

error variation in density is given by

$$\frac{\epsilon_\rho}{\rho} = - \frac{V^2 + (\dot{Z} - W_z)^2}{V^2 (\dot{Z} - W_z)} \epsilon_{\dot{z}} + \frac{1}{\ddot{Z} - g} \epsilon_{\ddot{z}} \qquad (3A)$$

By assuming independent and normally distributed errors in velocity and

acceleration and observing that $W_z << \dot{Z}$ and $V \approx \dot{Z}$ Equation 3A simplifies to

$$\left(\frac{\sigma_\rho}{\rho} \right)^2 = \left(\frac{2\sigma_{\dot{z}}}{\dot{Z}} \right)^2 + \left(\frac{\sigma_{\ddot{z}}}{\ddot{Z} - g} \right)^2 \quad .$$

A-3

The squared bias error in density introduced by bias velocity and acceleration errors is given by

$$\left(\frac{\Delta\rho}{\rho}\right)^2 = \left(\frac{2\Delta\dot{z}}{\dot{Z}} + \frac{\Delta\ddot{z}}{\ddot{Z} - g}\right)^2.$$

where $\Delta\rho$ represent the bias error in the parameter ρ, and $\Delta\dot{z}$ and $\Delta\ddot{z}$ the bias in $\dot{Z}$ and $\ddot{Z}$. The total percent error in density is defined as

$$\left(\frac{\sigma_\rho}{\rho}\right)^2_{total} = \left(\frac{\sigma_\rho}{\rho}\right)^2_{noise} + \left(\frac{\Delta\rho}{\rho}\right)^2_{bias}$$

or

$$\left(\frac{\sigma_\rho}{\rho}\right)^2 = \left(\frac{2\sigma_{\dot{z}}}{\dot{Z}}\right)^2 + \left(\frac{\sigma_{\ddot{z}}}{\ddot{Z} - g}\right)^2 + \left[\frac{2\Delta z}{\dot{Z}} + \frac{\Delta\ddot{z}}{\ddot{Z} - g}\right]^2.$$

Density Error Due to Vertical Winds

The percent variation in density resulting from a vertical wind error of Δw_z is, to a first order approximation

$$\frac{\Delta\rho}{\rho} = \frac{V^2 + (\dot{Z} - W_z)^2}{V^2(\dot{Z} - W_z)} \Delta w_z. \tag{4A}$$

Since $W_z << \dot{Z}$ and $V \approx \dot{Z}$, the squared percent error in density for a vertical wind error of Δw_z is

$$\left(\frac{\Delta\rho}{\rho}\right)^2 = \left(\frac{2\Delta w_z}{\dot{Z}}\right)^2.$$

A-4

APPENDIX B

DERIVATION OF THE NOISE ERROR FORMULAS

a) Velocity

Let $\hat{X}(i)$ be the radar-observed data point at time $t = i$, $X(i)$ the true value of the data point at $t = i$ and $\epsilon(i)$ the error in the observed data point; thus

$$\hat{X}(i) = X(i) + \epsilon(i).$$

If N equally time spaced data points are fitted by least squares to a polynomial of degree k, then the smoothed velocity at the midpoint of the interval ($\frac{N+1}{2}$ th point) is given in terms of Legendre Polynomials as

$$\dot{X}\left(\frac{N+1}{2}\right) = A_1 P_1'\left(\frac{N+1}{2}\right) + A_2 P_2'\left(\frac{N+1}{2}\right) + \ldots A_k P_k'\left(\frac{N+1}{2}\right)$$

where

$$A_k = \frac{\sum\limits_{i=1}^{N} P_k(i)\,\hat{X}(i)}{\Delta t \sum\limits_{i=1}^{N} P_k^2(i)} \quad,$$

$$P_0(i) = 1,$$

$$P_1(i) = i - \frac{N+1}{2},$$

$$P_{k+1}(i) = P_1 P_k - \frac{k(N^2 - k^2)}{4(4k^2 - 1)} P_{k-1},$$

Δt = time spacing between data points,

N = Number of data points used in smoothing,

B-1

$$k = \text{Degree of smoothing Polynomial}$$

$$P_k^{'}(i) = \text{First derivative with respect to i of } P_k(i).$$

Substitution of $X(i) + \epsilon(i)$ for $\hat{X}(i)$ in each A_k gives

$$\dot{X}\left(\frac{N+1}{2}\right) = \frac{\displaystyle\sum_{i=1}^{N} P_1(i)\left[X(i) + \epsilon(i)\right]}{\Delta t \displaystyle\sum_{i=1}^{N} P_1^2(i)} P_1^{'}\left(\frac{N+1}{2}\right) + \ldots + \frac{\displaystyle\sum_{i=1}^{N} P_k(i)\left[X(i) + \epsilon(i)\right]}{\Delta t \displaystyle\sum_{i=1}^{N} P_k^2(i)} P_k^{'}\left(\frac{N+1}{2}\right).$$

Rearranging in terms of $\epsilon(i)$ yields

$$\dot{X}\left(\frac{N+1}{2}\right) = \sum_{i=1}^{N} \left\{ \frac{P_1(i) P_1^{'}\left(\frac{N+1}{2}\right)}{\Delta t \displaystyle\sum_{i=1}^{N} P_1^2(i)} + \ldots + \frac{P_k(i) P_k^{'}\left(\frac{N+1}{2}\right)}{\Delta t \displaystyle\sum_{i=1}^{N} P_k^2(i)} \right\} \left[X(i) + \epsilon(i)\right].$$

Assuming that the distribution of each $\epsilon(i)$ is normal with mean 0 and variance σ_x^2 and that $\text{cov}(\epsilon(i), \epsilon(j)) = 0$ for $i \neq j$ the error variance of the smoothed velocity is

$$\sigma_{\dot{x}}^2\left(\frac{N+1}{2}\right) = \sum_{i=1}^{N} \left\{ \frac{P_1(i) P_1^{'}\left(\frac{N+1}{2}\right)}{\Delta t \displaystyle\sum_{i=1}^{N} P_1^2(i)} + \ldots + \frac{P_k(i) P_k^{'}\left(\frac{N+1}{2}\right)}{\Delta t \displaystyle\sum_{i=1}^{N} P_k^2(i)} \right\}^2 \sigma_x^2.$$

B-2

Since $\sum\limits_{i=1}^{N} P_j(i) P_k(i) = 0$ for $j \neq k$ the above equation simplifies to

$$\sigma^2_{\dot{x}(\frac{N+1}{2})} = \left\{ \frac{\left[P'_1(\frac{N+1}{2})\right]^2}{\sum\limits_{i=1}^{N} P_1^2(i)} + \ldots + \frac{\left[P'_k(\frac{N+1}{2})\right]^2}{\sum\limits_{i=1}^{N} P_k^2(i)} \right\} \frac{\sigma^2_x}{\Delta t^2} . \quad (1B)$$

It can easily be shown that for even k

$$P'_{k(even)}(\frac{N+1}{2}) = 0.$$

Hence equation (1B) simplifies to

$$\sigma^2_{\dot{x}(\frac{N+1}{2})} = \left\{ \frac{\left[P'_1(\frac{N+1}{2})\right]^2}{\sum\limits_{i=1}^{N} P_1^2(i)} + \frac{\left[P'_3(\frac{N+1}{2})\right]^2}{\sum\limits_{i=1}^{N} P_3^2(i)} + \frac{\left[P'_5(\frac{N+1}{2})\right]^2}{\sum\limits_{i=1}^{N} P_5^2(i)} + \ldots \right\} \frac{\sigma^2_x}{\Delta t^2} . \quad (2B)$$

The terms in parenthesis on the right side of the above equation can be written as a function of N. (See reference 10). The expressions for the first two terms are

$$\frac{\left[P'_1(\frac{N+1}{2})\right]^2}{\sum\limits_{i=1}^{N} P_1^2(i)} = \frac{12}{N(N^2-1)} \quad (3B)$$

and

$$\frac{\left[P_3' \left(\frac{N+1}{2}\right)\right]^2}{\sum\limits_{i=1}^{N} P_3^2(i)} = \frac{7(3N^2 - 7)^2 (N-4)!}{(N+3)!} \qquad (4B)$$

By substitution of 3B and 4B into 2B, the noise error in velocity is determined for polynomial smoothing of degrees 1 through 4. Note that since

$P_2' \left(\frac{N+1}{2}\right) = P_4' \left(\frac{N+1}{2}\right) = 0$ both the velocity obtained from a second or forth degree polynomial, and the noise error in this velocity are identical to that obtained from a first or third degree polynomical respectively.

Acceleration

The noise error in acceleration for double polynomial smoothing is obtained by two applications of the appropriate velocity noise error formulas.

For accelerations that are obtained as the second derivative of the least squares fit of a pclynomial of degree k over N data points, the noise error formulas are derived as follows: The smoothed acceleration at the midpoint of the interval is given by:

$$\ddot{X}\left(\frac{N+1}{2}\right) = A_2 P_2'' \left(\frac{N+1}{2}\right) + A_3 P_3'' \left(\frac{N+1}{2}\right) + \ldots + A_k P_k'' \left(\frac{N+1}{2}\right) \qquad (5B)$$

where P_k'' is the second derivative of P_k. By writing $\hat{X}(i) = X(i) + \epsilon(i)$ and rearranging, Equation 5B becomes

B-4

$$\ddot{X}\left(\frac{N+1}{2}\right) = \sum_{i=1}^{N}\left\{\frac{P_2(i)\,P_2''\left(\frac{N+1}{2}\right)}{\Delta t^2 \sum\limits_{i=1}^{N} P_2^{\,2}(i)} + \ldots + \frac{P_k(i)\,P_k''\left(\frac{N+1}{2}\right)}{\Delta t^2 \sum\limits_{i=1}^{N} P_k^{\,2}(i)}\right\}[X(i) + \epsilon(i)],$$

The error variance of the smoothed acceleration is

$$\sigma_{\ddot{x}}^{2}\left(\frac{N+1}{2}\right) = \left\{\frac{\left[P_2''\left(\frac{N+1}{2}\right)\right]^2}{\sum\limits_{i=1}^{N} P_2^{\,2}(i)} + \ldots + \frac{\left[P_k''\left(\frac{N+1}{2}\right)\right]^2}{\sum\limits_{i=1}^{N} P_k^{\,2}(i)}\right\}\frac{\sigma_x^2}{\Delta t^4}. \qquad (6B)$$

It can be shown that for odd k

$$P_{k(odd)}''\left(\frac{N+1}{2}\right) = 0.$$

This Equation (6B) simplifies to

$$\sigma_{\ddot{x}}^{2}\left(\frac{N+1}{2}\right) = \left\{\frac{\left[P_2''\left(\frac{N+1}{2}\right)\right]^2}{\sum\limits_{i=1}^{N} P_2^{\,2}(i)} + \frac{\left[P_4''\left(\frac{N+1}{2}\right)\right]^2}{\sum\limits_{i=1}^{N} P_4^{\,2}(i)} + \ldots\right\}\frac{\sigma_x^2}{\Delta t^4}. \qquad (7B)$$

The first two terms in parenthesis when written in terms of N are

$$\frac{\left[P_2''\left(\frac{N+1}{2}\right)\right]^2}{\sum\limits_{i=1}^{N} P_2^{\,2}(i)} = \frac{720}{N^5 - 5N^3 + 4N} \qquad (8B)$$

B-5

and

$$\frac{\left[P_4''\left(\frac{N+1}{2}\right)\right]^2}{\sum\limits_{i=1}^{N} P_4^2(i)} = \frac{44100\,(3N^2 - 13)^2}{49N\,(N^2 - 1)(N^6 - 29N^4 + 244N^2 - 576)}. \qquad (9B)$$

A substitution of Equations(8B) and (9B) into (7B) will yield the noise error

formulas for acceleration obtained as the second derivative of a Quadratic

and Quartic Polynomial fit.

APPENDIX C

BIAS ERROR FORMULAS

Velocity

Assume true position is given by a k th degree polynomial that is

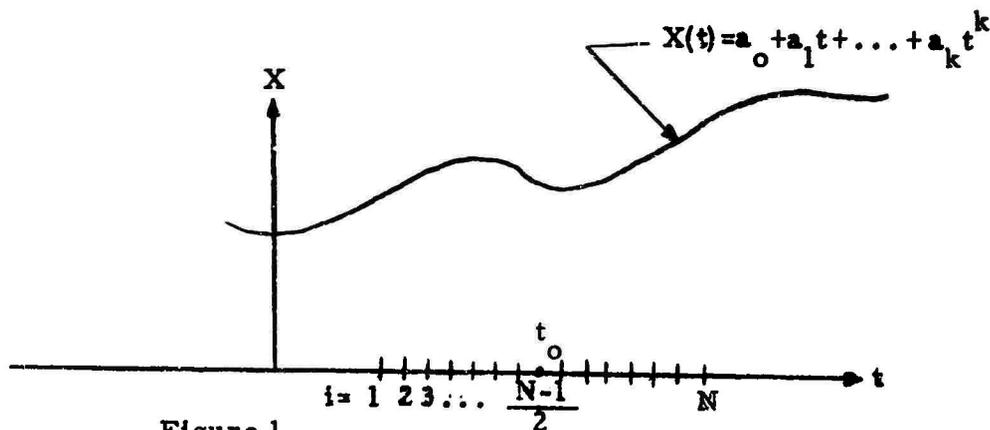$$X(t) = a_o + a_1 t + a_2 t^2 + \ldots + a_k t^k.$$

Initially we will derive the bias error for velocity obtained as the first derivative of a linear polynomial fit to the true position.

Velocity from Linear Polynomial Fit

Let N (odd) be the number of position points used in the fit. Let t_o correspond to the time at the midpoint ($\frac{N+1}{2}$th point) of the smoothing interval.

(See figure 1)

Figure 1

(Note that the values of the coefficients depend on the coordinate system. If the coefficients of the k th degree position field are given with respect to the coordinate system with origin at t_o then we have $t_o = 0$.) The relationship between t and numbering of the data points by i=1, 2, ... N is

$$t = t_o - (\frac{N+1}{2}) \Delta t + i\Delta t.$$

In terms of Legendre Polynomials the velocity at the midpoint of the smoothing interval, for linear smoothing is

$$\dot{X}(\frac{N+1}{2}) = \frac{\sum\limits_{i=1}^{N} P_1(i) X(i)}{\Delta t \sum\limits_{i=1}^{N} P_1^2(i)} P_1'(\frac{N+1}{2}).$$

or by substitution for x(i)

$$\dot{X}(\frac{N+1}{2}) = \frac{P_1'(\frac{N+1}{2})}{\Delta t \sum\limits_{i=1}^{N} P_1^2(i)} \left\{ a_0 \sum\limits_{i=1}^{N} P_1(i) + a_1 \sum\limits_{i=1}^{N} P_1(i) t + \ldots + a_k \sum\limits_{i=1}^{N} P_1(i) t^k \right\} \quad (1C)$$

where

$X(i)$ = true position at time $t = t_0 - (\frac{N+1}{2}) \Delta t + i \Delta t,$

$P_1(i) = i - \frac{N+1}{2},$

$\dot{P}_1(i) = 1.$

Since $t = t_0 - (\frac{N+1}{2}) \Delta t + i \Delta t$ for convenience t can be written as

$$t = t_0 + P_1(i) \Delta t \quad (2C)$$

C-2

Substituting (2C) into (1C) yields

$$\dot{X}\left(\frac{N+1}{2}\right) = \frac{1}{\Delta t \sum\limits_{i=1}^{N} P_1^2(i)} \left[a_o \sum\limits_{i=1}^{N} P_1(i) + a_1 \sum\limits_{i=1}^{N} P_1(i)(t_o + P_1(i)\Delta t) + \dots + a_k \sum\limits_{i=1}^{N} P_1(i)(t_o + P_1(i)\Delta t)^k \right]$$

The terms inside brackets in Equation (3C) are evaluated by use of the following identities characteristic of Legendre Polynomials:

$$\sum\limits_{i=1}^{N} P_1(i) = 0$$

$$\sum\limits_{i=1}^{N} P_1^4(i) = \sum\limits_{i=1}^{N} P_1(i)\left[P_3(i) + \frac{3N^2-7}{20} P_1(i) \right] = \frac{3N^2-7}{20} \sum\limits_{i=1}^{N} P_1^2(i)$$

$$\sum\limits_{i=1}^{N} P_1^3(i) = 0$$

The first few terms of Equation (3C) in brackets then become

$$a_o \sum\limits_{i=1}^{N} P_1(i) = 0,$$

C-3

$$a_1 \sum_{i=1}^{N} P_1(i) \{t_o + P_1(i) \Delta t\} = a_1 \left[\sum_{i=1}^{N} P_1(i) t_o + \sum_{i=1}^{N} P_1^2(i) \Delta t \right] = a_1 \Delta t \sum_{i=1}^{N} P_1^2(i),$$

$$a_2 \sum_{i=1}^{N} P_1(i) (t_o + P_1(i) \Delta t)^2 = a_2 \left[t_o^2 \sum_{i=1}^{N} P_1(i) + 2t_o \Delta t \sum_{i=1}^{N} P_1^2(i) + \Delta t^2 \sum_{i=1}^{N} P_1^3(i) \right] = 2a_2 t_o \Delta t \sum_{i=1}^{N} P_1^2(i),$$

$$a_3 \sum_{i=1}^{N} P_1(i) (t_o + P_1(i) \Delta t)^3 = a_3 \left[3t_o^2 \Delta t \sum_{i=1}^{N} P_1^2(i) + \Delta t^3 \sum_{i=1}^{N} P_1^4(i) \right],$$

$$a_4 \sum_{i=1}^{N} P_1(i) (t_o + P_1(i) \Delta t)^4 = a_4 \left[4t_o^3 \Delta t \sum_{i=1}^{N} P_1^2(i) + 4t_o \Delta t^3 \sum_{i=1}^{N} P_1^4(i) \right].$$

Substituting these terms into (3C) gives

$$\dot{x}\left(\frac{N+1}{2}\right) = a_1 + 2a_2 t_o + 3a_3 t_o^2 + a_3 \Delta t^2 \left(\frac{3N^2 - 7}{20}\right) + 4a_4 t_o^3 + 4a_4 t_o \Delta t^2 \left(\frac{3N^2 - 7}{20}\right) + \ldots$$

The true velocity at the midpoint is

$$\dot{x}(t_o) = a_1 + 2a_2 t_o + 3a_3 t_o^2 + 4a_4 t_o^3 + \ldots$$

Thus, the bias error in velocity (defined as the difference between the true and fitted velocities) is given for linear velocity smoothing by

$$\Delta \dot{x} = a_3 \Delta t^2 \left(\frac{3N^2 - 7}{20}\right) + 4a_4 t_o \Delta t^2 \left(\frac{3N^2 - 7}{20}\right) + \ldots \qquad (4C)$$

C-4

If the coefficients a_o, a_1... are those associated with the coordinate system with origin at t_o (i.e., $t_o = 0$) (4C) simplifies to

$$\Delta \dot{X} = a_3 \Delta t^2 \left(\frac{3N^2 - 7}{20} \right) + \text{terms in } a_5, a_7, \ldots$$

VELOCITY FROM CUBIC POLYNOMIAL FIT

The cubic velocity fit of a kth degree position field is given by

$$\dot{X}\left(\frac{N+1}{2}\right) = \frac{\sum_{i=1}^{N} P_1(i) \, X(i)}{\Delta t \sum_{i=1}^{N} P_1^2(i)} P_1'\left(\frac{N+1}{2}\right) + \frac{\sum_{i=1}^{N} P_3(i) \, X(i)}{\Delta t \sum_{i=1}^{N} P_3^2(i)} P_3'\left(\frac{N+1}{2}\right) \quad (5C)$$

where

$$X(i) = a_o + a_1 (t_o + P_1 \Delta t) + \ldots + a_k (t_o + P_1 \Delta t)^k$$

$$P_3'(i) = \frac{7 - 3N^2}{20}$$

Recalling that the first term of Equation (5C) was evaluated above, Equation (5C) can be rewritten as

$$\dot{X}\left(\frac{N+1}{2}\right) = a_1 + 2a_2 t_o + 3a_3 t_o^2 + a_3 \Delta t^2 \left(\frac{3N^2-7}{20}\right) + 4a_4 t_o^3 + 4a_4 t_o \Delta t^2 \left(\frac{3N^2-7}{20}\right) + \ldots -$$

$$- \frac{\frac{3N^2-7}{20}}{\Delta t \sum_{i=1}^{N} P_3^2(i)} \left[a_o \sum_{i=1}^{N} P_3(i) + \ldots + a_k \sum_{i=1}^{N} P_3(i) (t_o + P_1(i) \Delta t)^k \right] \cdot \quad (6C)$$

C-5

The following identities are useful in evaluating the terms in brackets.

$$\sum_{i=1}^{N} P_3(i) = 0$$

$$\sum_{i=1}^{N} P_3(i) P_1(i) = 0 ,$$

$$\sum_{i=1}^{N} P_1^5(i) = \sum_{i=1}^{N} P_1^7(i) = 0$$

$$P_3(i) = P_1^3(i) + \frac{7-3N^2}{20} P_1(i).$$

Using these identities the terms in brackets of Equation (6C) become

$$a_0 \sum_{i=1}^{N} P_3(i) = 0,$$

$$a_1 \sum_{i=1}^{N} P_3(i) (t_o + P_1(i) \Delta t) = 0,$$

$$a_2 \sum_{i=1}^{N} P_3(i) (t_o + P_1(i) \Delta t)^2 = 0,$$

C-6

$$a_3 \sum_{i=1}^{N} P_3(i) \left(t_o + P_1(i) \Delta t\right)^3 = a_3 \Delta t^3 \sum_{i=1}^{N} P_3^2(i),$$

$$a_4 \sum_{i=1}^{N} P_3(i) \left(t_o + P_1(i) \Delta t\right)^4 = 4 a_4 t_o \Delta t^3 \sum_{i=1}^{N} P_3^2(i),$$

Substituting into (6C) yields

$$\dot{X}\left(\frac{N+1}{2}\right) = a_1 + 2a_2 t_o + 3a_3 t_o^2 + 4a_4 t_o \Delta t^2 + \ldots$$

The bias error in velocity for the cubic fit is

$$\Delta \dot{x} = \text{terms in } a_5, a_6,$$

If the coefficients a_o, a_1, . . . are associated with the coordinate system with origin $t_o = 0$ the bias error formula simplifies to

$$\Delta \dot{x} = \text{terms in } a_5, a_7, \ldots$$

If velocity is obtained by a second or fourth degree polynomial fit, then this bias in velocity is the same as that for a linear or cubic fit respectively. This follows because the slope of a linear and quadratic fit are identical at the midpoint of the interval. Similarly, the slope of a cubic and quartic fit are identical at the midpoint of the interval.

C-7

Acceleration from second derivative of quadratic fit

The acceleration obtained from second derivative of quadratic fit is calculated as

$$\ddot{X}\left(\frac{N+1}{2}\right) = \frac{\displaystyle\sum_{i=1}^{N} P_2(i)X(i)}{\Delta t^2 \displaystyle\sum_{i=1}^{N} P_2^{\,2}(i)}\; P_2^{\,\prime\prime}\left(\frac{N+1}{2}\right) \qquad (7C)$$

where

$$P_2^{\,\prime\prime}\left(\frac{N+i}{2}\right) = 2.$$

By writing the position as a kth degree polynomial and substituting into (7C) gives

$$\ddot{X}\left(\frac{N+1}{2}\right) = \frac{2}{\Delta t^2 \displaystyle\sum_{i=1}^{N} P_2^{\,2}(i)}\left\{ a_o \sum_{i=1}^{N} P_2(i) + a_1 \sum_{i=1}^{N} P_2(i)(t_o + P_1(i)\,\Delta t) + \ldots + a_k \sum_{i=1}^{N} P_2(i)(t_o + P_1(i)\,\Delta t)^k\right\} \quad (8C)$$

By using the identities

$$\sum_{i=1}^{N} P_2(i) = 0$$

$$\sum_{i=1}^{N} P_2(i)\,P_1^{\,2}(i) = \sum_{i=1}^{N} P_2^{\,2}(i),$$

C-8

$$\sum_{i=1}^{N} P_2(i) P_1^3(i) = \sum_{i=1}^{N} P_2(i) P_1^5(i) = 0$$

$$\sum_{i=1}^{N} P_2(i) P_1^4(i) = \frac{3N^2-13}{14} \sum_{i=1}^{N} P_2^2(i)$$

equation (8C) reduces to

$$\ddot{X}\left(\frac{N+1}{2}\right) = 2a_2 + 6a_3 t_o + 12a_4 t_o^2 + 2a_4 \Delta t^2\left(\frac{3N^2-13}{14}\right) + 20a_5 t_o^3 + 10a_5 t_o \Delta t^2\left(\frac{3N^2-13}{14}\right) + \ldots$$

The bias in acceleration is

$$\Delta \ddot{x} = 2a_4 \Delta t^2\left(\frac{3N^2-13}{14}\right) + 10a_5 t_o \Delta t^2\left(\frac{3N^2-13}{14}\right) + \ldots \qquad (9C)$$

If the origin of the coordinate system is $t_o = 0$ then Equation (9C) simplifies to

$$\Delta \ddot{x} = 2a_4 \Delta t^2\left(\frac{3N^2-13}{14}\right) + \text{terms in } a_6, a_8, \ldots$$

The derivation of the bias error for the second derivative of a quartic fit of a kth degree polynomial is derived in a manner similar to the above derivation. The first term of the bias error expression will contain a_6 and t_o. If the origin of the coordinate system is $t_o = 0$ then the bias error formula will consist of terms that contain only the even coefficients a_6, a_8, ...

DOCUMENT CONTROL DATA - R & D

(Security classification of title, body of abstract and indexing annotation must be entered when the overall report is classified)

1. ORIGINATING ACTIVITY *(Corporate author)*	2a. REPORT SECURITY CLASSIFICATION
University of Dayton Research Institute Dayton, Ohio 45409	**UNCLASSIFIED**
	2b. GROUP

3. REPORT TITLE

A METHOD OF COMPUTING WINDS, DENSITY, TEMPERATURE, PRESSURE, AND THEIR ASSOCIATED ERRORS FROM THE HIGH ALTITUDE ROBIN SPHERE USING AN OPTIMUM FILTER.

4. DESCRIPTIVE NOTES *(Type of report and inclusive dates)*

Scientific   Final, January 1967-December 1969 / approved 15 July 1970

5. AUTHOR(S) *(First name, middle initial, last name)*

James K. Luers

6. REPORT DATE	7a. TOTAL NO. OF PAGES	7b. NO. OF REFS
July 1970	80	12

8a. CONTRACT OR GRANT NO.	9a. ORIGINATOR'S REPORT NUMBER(S)
F 1962867C0102 b. PROJECT NO., Work Unit Nos. 6682-02-01, 6670-03-01 c. DOD Element: 65701F, 62101F DOD Subelement: 676682, 681300	
d.	9b. OTHER REPORT NO(S) *(Any other numbers that may be assigned this report)* AFCRL-70-0366

10. DISTRIBUTION STATEMENT

This document has been approved for public release and sale; its distribution if unlimited.

11. SUPPLEMENTARY NOTES	12. SPONSORING MILITARY ACTIVITY
TECH., OTHER	Air Force Cambridge Research Laboratories (CRE) L. G. Hanscom Field, Bedford, Mass 01730

13. ABSTRACT

Optimum reduction techniques have been determined and a computer program written to measure density, winds, temperature and pressure from the passive ROBIN Sphere in the 30-100 km region of atmosphere. The program extends the maximum altitude of the 1965 ROBIN Program from 70-100 km. Output from the computer program also includes the estimated noise errors in density, winds, temperature, and pressure, the frequency response of density and winds as function of altitude, and Cal-comp plots of the meteorological parameters.

The smoothing techniques used in the program were determined so as to minimize the sum of the random and bias errors in density and winds. A separate smoothing function was determined for density and for wind calculations. The density smoothing function expands below 60 km in order to maintain a constant 2% noise error in density.

All possible sources of error in the meteorological parameters are discussed. For the first time error equations have been derived for temperature and pressure errors. Error estimates are made for random errors, bias errors, and errors resulting from the initial estimate of temperature.

DD FORM 1473
1 NOV 65

14 KEY WORDS	LINK A		LINK B		LINK C	
	ROLE	WT	ROLE	WT	ROLE	WT
Passive Sphere						
Wind						
Density						
Polynomial Smoothing						
Temperature						
Pressure						